

GENE EXPRESSION AND LIPID ACCUMULATION IN GREEN MICROALGA
Chlamydomonas reinhardtii (137c) UNDER SALT STRESS CONDITION



A Thesis Submitted in Partial Fulfillment of the Requirements
for the Degree of Master of Science in Microbiology and Microbial Technology
Department of Microbiology
Faculty of Science
Chulalongkorn University
Academic Year 2018
Copyright of Chulalongkorn University

การแสดงออกของยีนและการสะสมไขมันในจุลสาหร่ายสีเขียว
Chlamydomonas reinhardtii (137c) ภายใต้ภาวะเครียดจากเกลือ



วิทยานิพนธ์นี้เป็นส่วนหนึ่งของการศึกษาตามหลักสูตรปริญญาวิทยาศาสตรมหาบัณฑิต
สาขาวิชาจุลชีววิทยาและเทคโนโลยีจีโนมิกส์ ภาควิชาจุลชีววิทยา
คณะวิทยาศาสตร์ จุฬาลงกรณ์มหาวิทยาลัย
ปีการศึกษา 2561
ลิขสิทธิ์ของจุฬาลงกรณ์มหาวิทยาลัย

ธนาภา อธิกิจ : การแสดงออกของยีนและการสะสมไขมันในจุลสาหร่ายสีเขียว

Chlamydomonas reinhardtii (137c) ภายใต้ภาวะเครียดจากเกลือ. (

GENE EXPRESSION AND LIPID ACCUMULATION IN GREEN MICROALGA

Chlamydomonas reinhardtii (137c) UNDER SALT STRESS CONDITION) อ.ที่ปรึกษาหลัก : รศ. ดร.

รุ่งอรุณ วาติถิ สิริศรัทธา

ไบโอดีเซลเป็นพลังงานทางเลือกชนิดหนึ่งที่สำคัญในการลดปัญหาการปลดปล่อยก๊าซคาร์บอนไดออกไซด์ซึ่งเป็นสาเหตุสำคัญของการเกิดภาวะโลกร้อน ชีวมวลของจุลสาหร่ายจัดเป็นแหล่งผลิตเชื้อเพลิงชีวภาพรุ่นที่สาม หนึ่งในยุทธวิธีการเพิ่มผลิตซึ่งเป็นสารตั้งต้นในการผลิตไบโอดีเซลสามารถทำได้โดยการเลี้ยงจุลสาหร่ายภายใต้ภาวะเครียดต่างๆ ความเข้มข้นเกลือสูงเป็นภาวะหนึ่งที่มีประสิทธิภาพในการเพิ่มการสะสมลิพิด งานวิจัยนี้ได้ศึกษาผลของเกลือต่อการสะสมลิพิดในจุลสาหร่ายสีเขียว *Chlamydomonas reinhardtii* (137c) ผลการศึกษาแสดงให้เห็นว่า การเพิ่มความเข้มข้นของ NaCl KCl และ LiCl ส่งผลให้ปริมาณกรดไขมันอิ่มตัวเพิ่มขึ้น 1.8 1.2 และ 1.1 เท่าตามลำดับเมื่อเทียบกับภาวะควบคุม ขณะที่กรดไขมันไม่อิ่มตัวที่มีพันธะคู่หลายตำแหน่งมีปริมาณลดน้อยลงอย่างมีนัยสำคัญทางสถิติ ผลของ NaCl ต่อการแสดงออกของยีนที่เกี่ยวข้องกับวิถีชีวสังเคราะห์ลิพิดจำนวน 7 ยีน พบว่า ยีนที่เกี่ยวข้องกับกระบวนการสังเคราะห์กรดไขมันมีการแสดงออกเพิ่มมากขึ้นอย่างมีนัยสำคัญ โดย *PDH2 MAT* และ *KAS2* แสดงออกเพิ่มขึ้น 1.83 ± 0.20 1.82 ± 0.06 และ 1.70 ± 0.05 เท่าเมื่อเทียบกับภาวะปกติ งานวิจัยนี้สนใจศึกษาการแสดงออกของยีน *ChMAT* ในไมเซลล์ไซยาโนแบคทีเรียน้ำจืด *Synechococcus elongatus* PCC 7942 รวมถึงการเพิ่มการแสดงออกของยีน *SynMAT* พบว่าการแสดงออกของ *ChMAT* ตรวจสอบเฉพาะในระดับการถอดรหัสแต่ไม่สามารถแสดงออกในระดับโปรตีน สำหรับเซลล์ที่แสดงออกเกินของ *SynMAT* ตรวจสอบการแสดงออกของยีนและโปรตีนได้อย่างชัดเจน ภายใต้ระยะการเจริญที่ต่างกันของเซลล์ ระดับการแสดงออกของยีน *SynMAT* และโปรตีนไม่มีความแตกต่างกัน สำหรับการศึกษาค้นคว้าของจุลสาหร่าย *SynMAT* และ *SynLACS* มีการแสดงออกลดน้อยลง ใน *SynMAT/7942* องค์ประกอบของกรดไขมันมีการปรับเปลี่ยน โดยจากการวิเคราะห์ FAMES บ่งชี้ว่า การเพิ่มการแสดงออกของ *SynMAT* ใน *S. elongatus* PCC 7942 ส่งผลให้กรดไขมันอิ่มตัวมีปริมาณเพิ่มขึ้น ขณะที่กรดไขมันไม่อิ่มตัวที่มีพันธะคู่ตำแหน่งเดียวมีปริมาณลดลงเมื่อเทียบกับเซลล์ควบคุม และยังพบว่าส่งผลต่อสัดส่วนของ C16 และ C18 เป็นหลัก งานวิจัยนี้อาจเป็นการศึกษาเบื้องต้นในการพัฒนาวิธีการเพิ่มการสะสมลิพิดในจุลสาหร่ายหรือในไซยาโนแบคทีเรียได้ในอนาคต

สาขาวิชา จุลชีววิทยาและเทคโนโลยีจีโนม

ปีการศึกษา 2561

ลายมือชื่อ นิสิต

ลายมือชื่อ อ.ที่ปรึกษาหลัก

5972150523 : MAJOR MICROBIOLOGY AND MICROBIAL TECHNOLOGY

KEYWORD: Lipid accumulation, Salt stress, Gene expression, Lipid profile, FAMES analysis

Thanapa Atikij : GENE EXPRESSION AND LIPID ACCUMULATION IN GREEN MICROALGA *Chlamydomonas reinhardtii* (137c) UNDER SALT STRESS CONDITION. Advisor: Assoc. Prof. Rungaroon Waditee-Sirisattha, Ph.D.

Biodiesel is an important alternative energy that can reduce CO₂ emission, the main cause of Global warming. Algal biomass has been considered to be the third generation biofuels. One of the important strategies that enhance lipid accumulation; precursor of biodiesel production, is stress cultivation. High salt concentration is one of a potential approach to enhance lipid accumulation in microalgae. Here, we investigated the impacts of salt on lipid accumulation in green microalga *Chlamydomonas reinhardtii* (137c). The results revealed that higher concentrations of NaCl, KCl, and LiCl led to increasing of saturated fatty acid contents for 1.8, 1.2, and 1.1 folds compared with control condition. Poly-unsaturated fatty acid contents were found to be statistically significant decreased. The expression level of seven genes involved in lipid biosynthesis was examined under NaCl stress. *PDH2*, *MAT*, and *KAS2* were up-regulated significantly for 1.83 ± 0.20 , 1.82 ± 0.06 , and 1.70 ± 0.05 folds, respectively. In this study, we were interested in the expression *ChMAT* and overexpression of *SynMAT* in the model freshwater cyanobacterium *Synechococcus elongatus* PCC 7942. Expression of *ChMAT* could be detected at transcriptional level but not translational level. In case of *SynMAT* overexpressor, gene and protein expression obviously detected. Under different growth phase of *SynMAT/7942*, gene and protein expressions were not different. *SynMAT* and *SynLACS* mRNA expression under salt stress; however, seemed to be down-regulated. Fatty acid composition was modulated in the overexpressor. FAMES analysis demonstrated that overexpression of *SynMAT* in *S. elongatus* PCC 7942 resulted in increasing of total saturated fatty acid while mono-unsaturated fatty acid content was decreased. Moreover, overexpression of *SynMAT* affected to the content of C16 and C18 in particular. This study would lead to the improvement of lipid accumulation in microalgae or cyanobacteria in the future.

Field of Study: Microbiology and Microbial Technology Student's Signature

Academic Year: 2018 Advisor's Signature

ACKNOWLEDGEMENTS

I would like to express my sincere gratitude and deep appreciation to my super advisor, Associate Professor Dr. Rungaroon Waditee Sirisattha for her benevolent instruction, expert guidance, encouragement, inspiration, and support throughout my research. In addition, I would like to express my special appreciation to thesis committee, Associate Professor Dr. Naraporn Somboonna, Assistant Professor Dr. Panan Remngsamran, and Dr. Sophon Sirisattha for their beneficial comments and valuable recommendation in this research. Furthermore, my heartfelt appreciation is also expressed to Associate Professor Dr. Hakuto Kageyama, Miss Pokchut Kusolkumbot and Miss Nuanjun Jaisai for their help and kind corporation on this project. I would like to gratefully acknowledge the Scholarship from the Graduate School, Chulalongkorn University to commemorate the 72nd anniversary of his Majesty King Bhumibol Adulyadej and the 90th anniversary of Chulalongkorn University fund (Ratchadaphiseksomphot Endowment Fund). Special thanks to my dear friends and colleagues in laboratory room 1904/17 for encouragement and camaraderie. Finally, I am much obliged to my family for their profound love, comfort, encouragement, attention, and patience during my difficulties.



จุฬาลงกรณ์มหาวิทยาลัย
CHULALONGKORN UNIVERSITY

Thanapa Atikij

TABLE OF CONTENTS

	Page
ABSTRACT (THAI).....	iii
ABSTRACT (ENGLISH).....	iv
ACKNOWLEDGEMENTS.....	v
TABLE OF CONTENTS.....	vi
LIST OF FIGURES.....	xii
LIST OF TABLES.....	xv
LIST OF ABBREVIATIONS.....	xvi
CHAPTER I INTRODUCTION.....	1
CHAPTER II LITERATURE REVIEWS.....	4
2.1 Global warming and alternative energy.....	4
2.2 Microalgae and cyanobacteria as sources of biofuels and high-value products.....	6
2.3 Lipid biosynthesis.....	9
2.4 Lipid enhancing strategies.....	12
2.4.1 Stress condition.....	12
2.4.1.1 Nitrogen starvation.....	12
2.4.1.2 High carbon concentration.....	13
2.4.1.3 Light intensity.....	14
2.4.1.4 Salinity stress.....	14
2.4.2 Engineering.....	15
2.4.2.1 Enhancement of FA synthesis approach.....	15
2.4.2.1.1 Improvement of CO ₂ fixation.....	15

2.4.2.1.2 Overexpression of <i>PDHC</i> gene.....	15
2.4.2.1.3 Overexpression of pyruvate dehydrogenase kinase	16
2.4.2.1.4 Overexpression of <i>ACCase</i> gene	16
2.4.2.1.5 Overexpression of thioesterase gene.....	17
2.4.2.2 Enhancement of TAG biosynthesis approach.....	17
2.4.2.2.1 Overexpression of <i>GPAT</i> gene	17
2.4.2.2.2 Overexpression of <i>DGAT</i> gene(s).....	17
2.4.2.3 The regulation of PDH-bypass pathway.....	18
2.4.2.3.1 Overexpression of acetyl-CoA synthase.....	18
2.4.2.3.2 Overexpression of malic enzyme	18
2.4.2.4 The inhibition of competitive pathway.....	20
2.4.2.4.1 Inhibition of β -oxidation	20
2.4.2.4.2 Inhibition of starch biosynthesis	20
2.4.2.5 Transcriptional engineering	20
2.5 Photosynthetic microorganism models	21
2.5.1 <i>C. reinhardtii</i>	21
2.5.2 <i>S. elongatus</i> PCC 7942.....	22
CHAPTER III MATERIALS AND METHODS	24
3.1 Instruments.....	24
3.2 Chemicals.....	25
3.3 Membrane.....	28
3.4 Kits.....	28
3.5 Enzymes	29
3.6 Bacterial, microalgal strains and plasmids	30

3.7 Bioinformatics analysis	32
3.8 Cultures and stress treatment.....	33
3.8.1 <i>C. reinhardtii</i> (137c) cultivation.....	33
3.8.2 <i>S. elongatus</i> PCC 7942 cultivation	33
3.8.3 <i>Escherichia coli</i> DH5 α cultivation.....	33
3.9 Lipid analysis.....	34
3.9.1 Observation of lipid accumulation under fluorescent microscope	34
3.9.1.1 Stress treatment.....	34
3.9.1.2 Nile red staining.....	34
3.9.2 Lipid profiling by FAMES analysis.....	35
3.9.2.1 Stress treatment.....	35
3.9.2.2 FAMES analysis.....	35
3.10 Genes expression analysis.....	36
3.10.1 Culture condition and stress treatment	36
3.10.2 Total RNA extraction and complementary DNA conversion	36
3.10.3 Semiquantitative RT-PCR.....	37
3.11 Construction of expression plasmid harboring <i>ChMAT</i>	38
3.11.1 <i>ChMAT</i> gene amplification and purification	38
3.11.2 Construction of <i>ChMAT</i> into pBSK ⁺ II vector	38
3.11.2.1 Construction of ChMAT/pBSK ⁺ II plasmid and transformation.....	38
3.11.2.2 ChMAT/pBSK ⁺ II plasmid extraction	39
3.11.3 Construction of <i>ChMAT</i> into pSyn_6 expression vector.....	40
3.11.4 Transformation of <i>ChMAT</i> /pSyn_6 into <i>S. elongatus</i> PCC 7942	40
3.12 Construction of expression plasmid harboring <i>SynMAT</i>	41

3.12.1 <i>S. elongatus</i> PCC 7942 genomic extraction	41
3.12.2 <i>SynMAT</i> gene amplification	42
3.12.3 Construction of <i>SynMAT</i> into pBSK ⁺ II vector	42
3.12.3 Construction of <i>SynMAT</i> into pSyn_6 vector.....	42
3.12.4 Transformation of <i>SynMAT</i> /pSyn_6 into <i>S. elongatus</i> PCC 7942	43
3.13 Analysis of expressing cells harboring <i>ChMAT</i> and <i>SynMAT</i>	43
3.13.1 Transformants cultivation	43
3.13.2 Phenotypic observation	43
3.13.3 Semiquantitative RT-PCR.....	44
3.13.3.1 Cultivation condition	44
3.13.3.2 Gene expression analysis.....	44
3.13.4 Protein expression analysis.....	45
3.13.4.1 Crude protein preparation.....	45
3.13.4.2 SDS-PAGE analysis	45
3.13.4.3 Western blot analysis	46
3.13.5 FAMES analysis.....	46
CHAPTER IV RESULTS AND DISCUSSION	48
4.1 Bioinformatics analysis	48
4.2 lipid analysis.....	55
4.2.1 Observation of lipid accumulation by Nile red staining	55
4.2.1.1 Effect of NaCl stress.....	55
4.2.1.1 Effect of KCl stress	59
4.2.1.3 Effect of LiCl stress.....	62
4.2.1.4 Effect of sodium acetate.....	65

4.2.2 Observation of lipid accumulation by FAMES analysis	69
4.3 Gene expression analysis.....	73
4.4 Construction of the expression plasmid harboring <i>ChMAT</i>	75
4.4.1 <i>ChMAT</i> gene amplification and purification	75
4.4.2 Plasmid extraction and restriction enzyme analysis	76
4.4.3 Transformation of <i>S. elongatus</i> PCC 7942 harboring <i>ChMAT</i> gene	78
4.5 Construction of expression plasmid harboring <i>SynMAT</i>	81
4.5.1 Construction of cloning vector harboring <i>SynMAT</i> gene	81
4.5.2 Construction of expression vector of <i>SynMAT</i> /pSyn_6	83
4.5.3 Transformation of <i>SynMAT</i> /pSyn_6 into <i>S. elongatus</i> PCC 7942.....	86
4.6 Analysis of expressing cells harboring <i>ChMAT</i> and <i>SynMAT</i>	88
4.6.1 Morphology of expressing cells	88
4.6.2 Screening and comparing transformants harboring <i>ChMAT</i> and <i>SynMAT</i> . 89	
4.6.2.1 Expression analysis.....	89
4.6.2.2 Transcriptional analysis	90
4.6.2.2.1 Growth phase.....	90
4.6.2.2.2 Salt stress.....	92
4.6.2.3 Protein expression analysis.....	93
4.6.2.3.1 Growth phase.....	93
4.6.2.3.2 Salt stress.....	95
4.6.3 FAMES analysis of <i>ChMAT</i> and <i>SynMAT</i> expressing cells.....	96
4.6.3.1 Growth phase	96
4.6.3.2 Salt stress	99
CHAPTER V CONCLUSIONS.....	102

APPENDICES..... 117



จุฬาลงกรณ์มหาวิทยาลัย
CHULALONGKORN UNIVERSITY

LIST OF FIGURES

	Page
Figure 1 Figure 1 Percentage of GHG in the atmosphere (2016).....	5
Figure 2 Lipid biosynthesis in microalgae.....	11
Figure 3 The schematic of citrate-pyruvate shuttle in eukaryote organisms.....	19
Figure 4 Topological analysis of protein associated with lipid biosynthesis in <i>C. reinhardtii</i>	49
Figure 5 Protein domain and protein interaction analyses.....	51
Figure 6 Protein domain and protein interaction analyses.....	52
Figure 7 Phylogenetic analysis of ChMAT (A) and SynMAT (B) and ortholog sequences.....	54
Figure 8 Image of <i>C. reinhardtii</i> (137c) cells observed under bright field light microscope (BF) and fluorescent microscope (NR).....	57
Figure 9 Image of <i>C. reinhardtii</i> (137c) cells observed under light microscope (A-F) and fluorescent microscope (G-L). Relative intensity of lipid accumulation in algal cells (M).....	58
Figure 10 Image of <i>C. reinhardtii</i> (137c) cells observed under bright field light microscope (BF) and fluorescent microscope (NR).....	60
Figure 11 Image of <i>C. reinhardtii</i> (137c) cells observed under light microscope (A-F) and fluorescent microscope (G-L). Relative intensity of lipid accumulation in algal cells (M).....	61
Figure 12 Image of <i>C. reinhardtii</i> (137c) cells observed under bright field light microscope (BF) and fluorescent microscope (NR).....	63
Figure 13 Image of <i>C. reinhardtii</i> (137c) cells observed under light microscope (A-F) and fluorescent microscope (G-L). Relative intensity of lipid accumulation in algal cells (M).....	64

Figure 14 Image of <i>C. reinhardtii</i> (137c) cells observed under bright field light microscope (BF) and fluorescent microscope (NR).....	67
Figure 15 Image of <i>C. reinhardtii</i> (137c) cells observed under light microscope (A-F) and fluorescent microscope (G-L). Relative intensity of lipid accumulation in algal cells (M).	68
Figure 16 FAMEs analysis for salt stressed cells; 200 mM NaCl and KCl, and 120 mM LiCl.	72
Figure 17 Semiquantitative RT-PCR analysis of stressed cells under 200 mM NaCl conditions at 0 (control), 6, and 12 hours (A). Relative expression analysis of stressed cells (B)	74
Figure 18 <i>ChMAT</i> gene amplification.....	75
Figure 19 Colony PCR of the candidate transformants <i>ChMAT</i> in <i>E. coli</i> DH5 α (A). Restriction enzyme analysis of <i>ChMAT</i> in cloning vector, pBSK ⁺ II (B).....	77
Figure 20 Plasmid of <i>ChMAT</i> /pSyn_6 (A). Colony PCR of the candidate transformants <i>ChMAT</i> /pSyn_6 in <i>E. coli</i> DH5 α (B). Plasmid extraction of <i>ChMAT</i> /pSyn_6 (C).....	79
Figure 21 Natural transformation of <i>ChMAT</i> /pSyn_6 in a fresh water cyanobacterium <i>S. elongatus</i> PCC 7942 on BG-11 agar plate (supplemented with 10 μ g/ml spectinomycin) plate (A). Colony PCR of 16 candidate transformants <i>ChMAT</i> /pSyn_6 in <i>S. elongatus</i> PCC 7942 (B).	80
Figure 22 Genomic DNA extracted from <i>S. elongatus</i> PCC 7942 (A). <i>SynMAT</i> gene amplification (B). Colony PCR of the candidate transformants <i>SynMAT</i> in <i>E. coli</i> DH5 α (C).....	82
Figure 23 Plasmid of <i>SynMAT</i> /pSyn_6 (A). Colony PCR of the candidate transformants <i>SynMAT</i> /pSyn_6 in <i>E. coli</i> DH5 α (B).	84
Figure 24 <i>SynMAT</i> /pSyn_6 extraction (A). Restriction enzyme analysis of <i>SynMAT</i> /pSyn_6 (B)..	85

Figure 25 Natural transformation of <i>SynMAT</i> /pSyn_6 in a fresh water cyanobacterium <i>S. elongatus</i> PCC 7942 on BG-11 agar plate (supplemented with 10 µg/ml spectinomycin) plate (A). Colony PCR of 16 candidate transformants <i>SynMAT</i> /pSyn_6 in <i>S. elongatus</i> PCC 7942 (B).	87
Figure 26 Morphology of <i>S. elongatus</i> PCC 7942 cells under light microscope.	88
Figure 27 Western blot analysis of <i>ChMAT</i> (A) and <i>SynMAT</i> (B) expressing cells.....	89
Figure 28 Semiquantitative RT-PCR analysis of two candidate transformants (A). Relative expression analysis of stressed cells (B)	91
Figure 29 Semiquantitative RT-PCR analysis of two candidate transformants.....	92
Figure 30 Western blot analysis of <i>SynMAT</i> expressing cells in different growth phase.	94
Figure 31 Western blot analysis of <i>SynMAT</i> expressing cells under 300 mM NaCl stress.	95

LIST OF TABLES

	Page
Table 1 A list of representative microalgae and cyanobacteria and their lipid contents.....	7
Table 2 Microorganisms and plasmids used in this study	30
Table 3 Primers used in this study.....	31
Table 4 Lipid profile of <i>C. reinhardtii</i> (137c) cells subjected to salt stress (NaCl, KCl, and LiCl) at day 3, 5, and 7, respectively.....	71
Table 5 Lipid profile of <i>ChMAT/7942</i> and <i>SynMAT/7942</i> cells at the exponential growth phase.....	98
Table 6 Lipid profile of <i>SynMAT/7942</i> cells under 300 mM NaCl stress.	101

LIST OF ABBREVIATIONS

ACAT; Acetyl-CoA:ACP transacylase

ACCase; Acetyl-CoA carboxylase

ACP; Acyl carrier protein

CFC; Chlorofluorocarbons

CH₄; Methane

CO₂; Carbon dioxide

DCW; Dry cell weight

DGAT; Diacyl-glycerol acyltransferase

ENR; Enoyl-ACP reductase

FA; Fatty acid

FAME; Fatty acid methyl ester

FAS; Fatty acid synthase

FAT; Fatty acid thioesterase

FFA; Free fatty acid

G3PDH; Glyceral-3-phosphate dehydrogenase

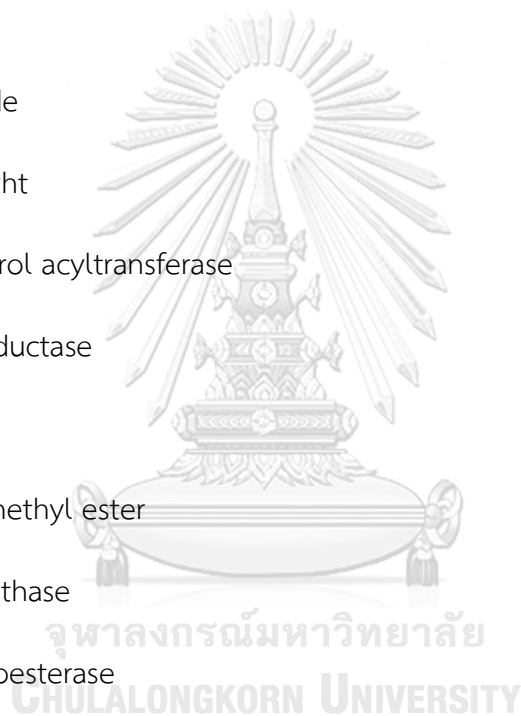
GHG; Greenhouse gas

GPAT; Glycerol-3-phosphate acyltransferase

HD; 3-hydroxyacyl-ACP dehydratase

KAR; 3-ketoacyl-ACP reductase

KAS; 3-ketoacyl-ACP synthase



LACS; Long-chain acyl-CoA synthetase

LPAAT; Lysophosphatidic acid acyl-transferase

LPAT; Lisophosphatidylcholine acyltransferase

MAT; Malonyl-CoA:ACP transacylase

ME; Malic enzyme

MCFA; Medium chain fatty acid

MUFA; Mono-unsaturated fatty acid

N₂O; Nitrous oxide

PDHC; Pyruvate dehydrogenase complex

PUFA; Poly-unsaturated fatty acid

PVDF; Polyvinylidene fluoride

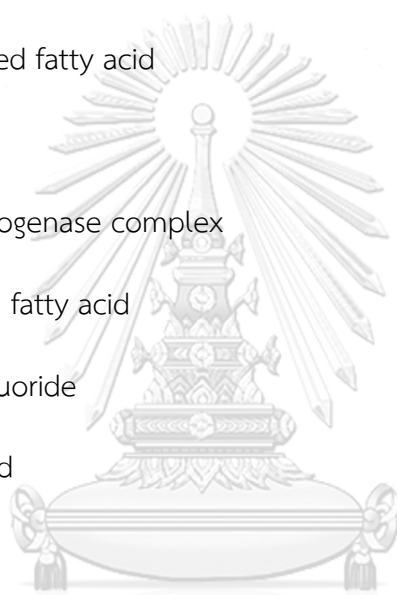
SFA; Saturated fatty acid

TAG; Triacylglycerol

TM; Transmembrane protein

UFA; Unsaturated fatty acid

WT; Wild type



จุฬาลงกรณ์มหาวิทยาลัย
CHULALONGKORN UNIVERSITY

CHAPTER I

INTRODUCTION

Biofuels gain much interesting as alternative energy. To date, the sources of biofuels production are divided into 4 generations. First and second generations represent biofuels generated food crops and wastes, respectively. Drawbacks of these two generations are the competition between food and biofuels production including the requirement of pretreatment. The third generation biofuels are generated from algal biomass. It keeps promising to be one of the most attractive alternative energies in the near future. And last, the so-called fourth generation biofuels. This generation is an advance production of biofuels by engineering photosynthetic organisms, *i.e.* plants and algae. Biodiesel is one of the most important biofuels. It is generated from transesterification which generates one molecule of glycerol and three molecules of fatty methyl esters.

Photosynthetic microorganisms including microalgae and cyanobacteria are recognized to be the feedstock of biodiesel. They are considered to be the third generation due to their several advantages. They gain energy via photosynthesis and fix CO₂ as carbon source. Moreover, they have short life cycles and do not require an arable land and water for cultivation. Microalgae accumulate high lipid content which is a precursor for biodiesel production under specific conditions. The most comprehensive study focusses on nitrogen starvation and high carbon concentration. For cyanobacteria, they do not commonly accumulate neutral lipid or triacylglycerol (TAG) as an energy supply but in the form of fatty acid (FA) or fatty alcohol (Oliver *et al.*, 2016). Moreover, both microalgae and cyanobacteria can produce high value co-products such as carotenoids, glycerol, and polyhydroxyalkanoates. These products are widely used in many industries including cosmetics, foods and beverages, pharmaceuticals, and oleochemicals.

Lipid biosynthesis in microalgae initiates in the chloroplast by fixing CO₂ and converting into pyruvate via Calvin cycle and Glycolysis pathway, respectively. FA

synthesis consequently takes place through various enzymes. Two key steps involved in enzyme complex of acetyl-coenzyme A carboxylase (ACCase) and elongation step by fatty acid synthase (FAS). Finally, free FA (FFA) is released out of the chloroplast and used as a precursor for TAG biosynthesis. In cyanobacteria; however, lipid biosynthesis only occurs in cytoplasm due to the lack of chloroplast in their cells.

Strategies to improve lipid production in photosynthetic microorganisms have been demonstrated for years. Stress condition is one of the most well-known approaches. However, some stress conditions lead to the reduction of biomass productivity. Another noticeable strategy of lipid production improvement is metabolic engineering. This approach can be divided depend upon the target site including enhancement of FA, enhancement of TAG, Improvement of PDH-bypass pathway, inhibition of competitive pathway, and transcriptional engineering.

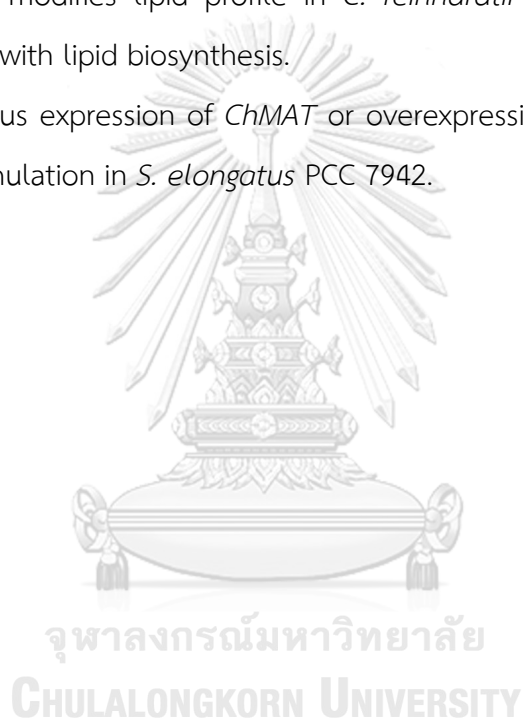
Salt stress is one of attractive approaches for lipid enhancing strategy due to its inexpensive and abundant in nature source, such as seawater (Reig *et al.*, 2014; Minhas *et al.*, 2016). To date, little is known about effect of salt stress on gene expression including regulation at transcriptional level. In this study, we aimed to examine the effects of salts (NaCl, KCl, and LiCl) on lipid accumulation and the alteration of lipid composition in the model freshwater green microalga *Chlamydomonas reinhardtii* (137c). The impacts of NaCl on expression of genes involved in FA and TAG biosynthetic pathway were also investigated. Furthermore, *MAT* from *C. reinhardtii* (137c) (*ChMAT*) was heterologously expressed in the freshwater cyanobacterium *Synechococcus elongatus* PCC 7942. We also constructed the overexpressor harboring *Synechococcus MAT* (*SynMAT*) for comparative analysis. Information gained in all aspects covering the molecular and cellular levels and productions would allow the understanding of the mechanism behind the physiological plasticity upon salt stress.

The objectives of this research:

1. To investigate lipid accumulation in *C. reinhardtii* (137c) under salt stress
2. To analyze gene expression for lipid biosynthesis in *C. reinhardtii* (137c)
3. To express *ChMAT* and *SynMAT* in *S. elongatus* PCC 7942
4. To study the effect of growth phase and NaCl stress in the transformant cells

Hypotheses of this study:

1. Salt stress modifies lipid profile in *C. reinhardtii* (137c) and triggers genes associated with lipid biosynthesis.
2. Heterologous expression of *ChMAT* or overexpression of *SynMAT* contributes lipid accumulation in *S. elongatus* PCC 7942.



CHAPTER II

LITERATURE REVIEWS

2.1 Global warming and alternative energy

Nowadays, we are facing with the changing of weather events, it is anomalous hot in summer and severe freeze in winter in some country. In 2016 and 2018, we faced to warmest summer. The temperature was increased approximately 0.8 °C compared to the 1951-1980 June (NASA, 2018: online). It was reported that the temperature of the Earth's surface rises 0.4–0.8 °C over the past 100 years. This phenomenon would continuously increase to 1.4-5.8 °C by the year 2100. Moreover, because of the rising temperature on the Earth affects the rising of sea levels due to the melting of the polar ice caps (Lifescience, 2018: online), these effects are well known as the Global warming. The main cause of Global warming crisis is greenhouse gas (GHG), e.g. carbon dioxide (CO₂), methane (CH₄), nitrous oxide (N₂O), and chlorofluorocarbons (CFC). These gases form as a barrier and trap the heat in the atmosphere. In addition, it depletes the ozone layer in the stratosphere and allows more ultraviolet (UVB) which is harmful to living organisms to pass through the Earth (Douglass *et al.*, 2011). The United States Environmental Protection Agency reported that CO₂ is the most important GHG followed by CH₄ (Figure 1). The sources of CO₂ emission are not only from natural phenomena (e.g. respiration, and volcanic eruption) but also human activities especially transportation and electricity usage (NASA, 2018: online). It has been decades that we use fossil fuel as an energy; however, this energy is not sustainable and renewable. To solve these problems, alternative energies have been invented. Since it is a green energy which means it causes much less GHG than fossil fuel and reusable.

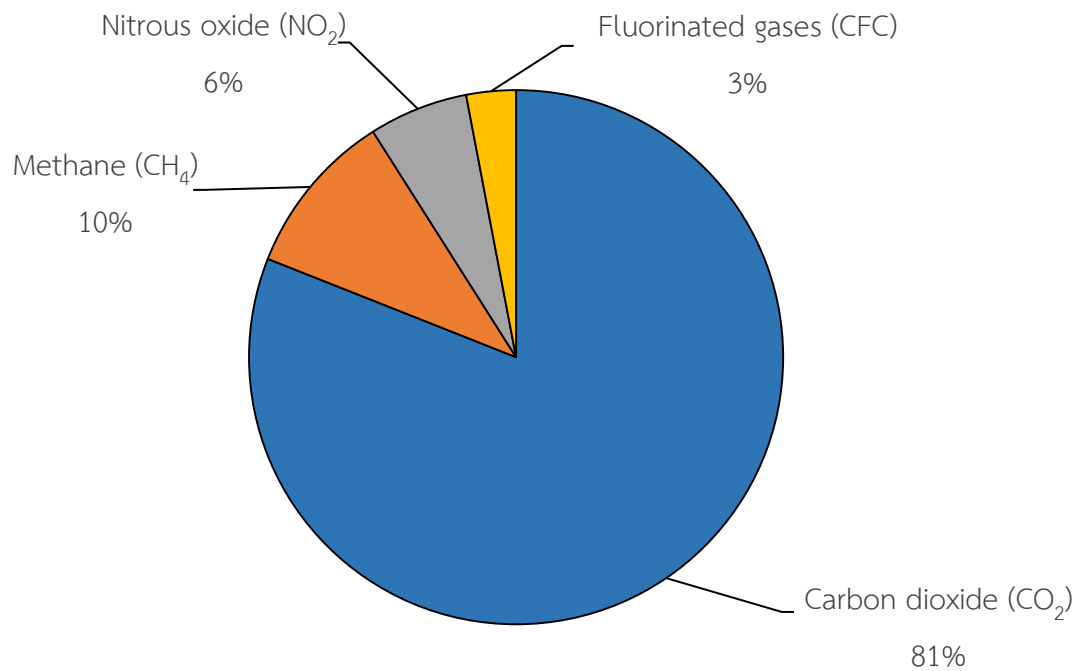
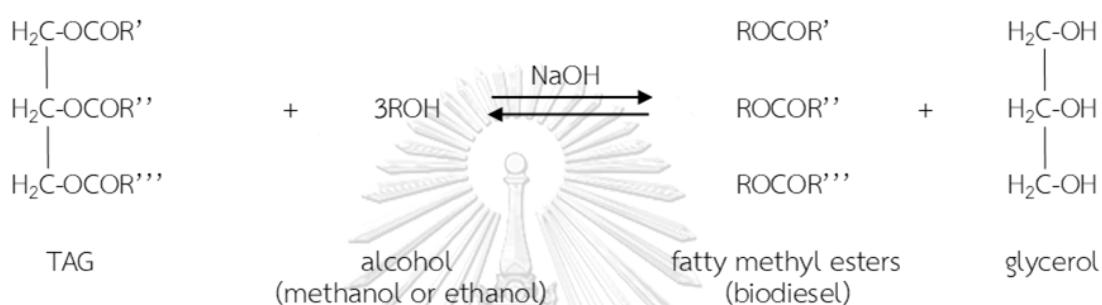


Figure 1 Figure 1 Percentage of GHG in the atmosphere (2016). The United States Environmental Protection Agency reported that CO₂ is the major component of GHG follow by CH₄ (United States Environmental Protection Agency, 2018: online).

There are many alternative energies including solar energy, wind power, hydroelectric power, geothermal energy, and biofuels. Biofuels are an energy produced from biomass. Thus far, biofuels can be divided into 4 generations (Aro, 2016; Gambelli *et al.*, 2017); (1) First generation biofuels are directly derived from food crops, *e.g.* cassava, seed and sugar cane. Nonetheless, since they produced from food crops; therefore, there is an argument between foods and biofuels, (2) Second generation biofuels have been developed to overcome the limitation of the first generation. The second generation biofuels are the fuels which generated from non-food crops and wastes, *e.g.* agricultural waste, food waste, and animal dung. The limitation of this generation is the need of pretreatment, (3) Third generation biofuels are the fuels which produced from algal biomass. This generation biofuels keeps promising to be one of the most important alternative energy in the future, (4) The last one, the so-called fourth generation biofuels. They are the fuels from photosynthetic organisms

(plants or algae) which have been engineered to improve CO₂ capturing or enhance lipid productivity (Lü *et al.*, 2011). One of the most important biofuels is biodiesel. It is generated by transesterification reaction of TAG with alcohol and generates three molecules of fatty methyl esters which is used as biodiesel and one molecule of glycerol as shown below (Brennan and Owende, 2010)



2.2 Microalgae and cyanobacteria as sources of biofuels and high-value products

Microalgae and cyanobacteria are photosynthetic organisms. Solar energy is the most important energy source for these organisms. They fix CO₂ in the atmosphere and use as a carbon source via Calvin cycle. The advantages of these organisms are not only having a short life cycles compared to higher plants, but also surviving in all habitats including harsh environments. Besides, the arable lands are not required for microalgae and cyanobacteria cultivation; hence, the area competition between food crops cultivation and biofuels production is not the major obstacle. More importantly, they can accumulate high lipid contents which are precursors for biodiesel production. Table 1 represents a list of representative lipid producing microalgae and cyanobacteria and their lipid contents.

Table 1 A list of representative microalgae and cyanobacteria and their lipid contents

Organism	Lipid content (% of dry cell weight; DCW)	Reference
Microalgae		
<i>Botryococcus braunii</i>	25-75	(Noraini <i>et al.</i> , 2014)
<i>Chlamydomonas mexicana</i>	15-37	(Salama <i>et al.</i> , 2013)
<i>Chlamydomonas reinhardtii</i>	21	(Demirbas and Demirbas, 2011)
<i>Chlorella protothecoides</i>	55	(Mata <i>et al.</i> , 2010)
<i>Chlorella vulgaris</i>	14-22/56	(Mata <i>et al.</i> , 2010)
<i>Chlorococcum</i> sp.	10-30	(Harwati <i>et al.</i> , 2012)
<i>Dunaliella tertiolecta</i>	17-71	(Mata <i>et al.</i> , 2010)
<i>Haematococcus pluvialis</i>	25	(Mata <i>et al.</i> , 2010)
<i>Nannochloropsis oculata</i>	23-30	(Mata <i>et al.</i> , 2010)
<i>Nannochloris</i> sp.	31-68	(Noraini <i>et al.</i> , 2014)
<i>Phaeodactylum tricornutum</i>	20-30	(Noraini <i>et al.</i> , 2014)
<i>Scenedesmus obliquus</i>	12-14	(Milano <i>et al.</i> , 2016)
<i>Scenedesmus obliquus</i>	18-34	(Salama <i>et al.</i> , 2013)
<i>Thalassiosira pseudonana</i>	20.6	(Mata <i>et al.</i> , 2010)
Cyanobacteria		
<i>Anabaena cylindrica</i>	4-7	(Milano <i>et al.</i> , 2016)
<i>Arthrospira maxima</i>	6-7	(Milano <i>et al.</i> , 2016)
<i>Cyanobacterium aponinum</i>	20-50	(Karatay and Dönmez, 2011)
<i>Nostoc commune</i>	8	(Vargas <i>et al.</i> , 1998)
<i>Oscillatoria</i> sp.	13	(Griffiths and Harrison, 2009)
<i>Spirulina platensis</i>	18.02	(Ambrozova <i>et al.</i> , 2014)
<i>Synechococcus</i> sp.	22-42	(Karatay and Dönmez, 2011)
<i>Synechocystis</i> sp.	50	(Rittmann, 2008)

Lipid is not only used in a biodiesel factory but in food additives (Bharathiraja *et al.*, 2017). Microalgae and cyanobacteria also can be used as microbial cell factories for high-value biocompound productions in various industries, such as cosmetics, foods and beverages, and pharmaceuticals (Spolaore *et al.*, 2006; Michalak and Chojnacka, 2015). Glycerol is a major byproduct from biodiesel production and widely used in a cosmetic industry as a solvent and humectant (Tan *et al.*, 2013). Furthermore, it also can be used as a precursor for biofuels production including hydrogen and ethanol via streaming processes and fermentation, respectively (Fan *et al.*, 2010). One of the most valuable co-products from lipid production is poly-unsaturated fatty acids (PUFAs), *e.g.* α -linolenic acid, eicosapentaenoic acid, docosahexaenoic acid, γ -linolenic acid, and dihomo- γ -linolenic acid (Brennan and Owende, 2010). These PUFAs are well-known as ω -3 (α -linolenic acid, eicosapentaenoic acid, and docosahexaenoic acid) and ω -6 (γ -linolenic acid and dihomo- γ -linolenic acid). On account of the fact that docosahexaenoic acid is a key component in brain tissue, retina of the eyes and heart tissue, it is widely used as a nutritional supplement for infants and adults (Spolaore *et al.*, 2006). Carotenoids are another one of the most important high-value co-products from microalgae and cyanobacteria. Carotenoids are a group of accessory pigments that enhance the photosynthetic system efficiency in these organisms. Because of their strong anti-oxidant and anti-inflammatory activities (Gammone *et al.*, 2015), these pigments were used as an anti-aging substance in pharmaceutical and cosmetic industries (Wang *et al.*, 2015). Besides, microalgal cells (such as *Spirulina* and *Chlorella*) also can be directly used as an animal feed and dietary supplement for human due to its high nutritional value (Vigani *et al.*, 2015).

Although these microorganisms accumulate large contents of lipids as serving for biodiesel production, limitation of using these organisms as biodiesel producer is their low biomass productivity under stress condition. Pancha *et al.* (2015) reported that when freshwater microalga *Scenedesmus* sp. CCNM 1077 was cultured in saline condition, the biomass productivity was reduced from 22.74 mg/L/day (0 mM NaCl) to 10 mg/L/day (400 mM NaCl). Under this condition; however, the lipid productivity was increased 1.7 folds compared to the control condition. The engineering of the microalgal strain might be one of alternative solutions; nonetheless, the improvement of microalgal strain to endure the stress condition resulted in the decreasing of lipid productivity in *Chlamydomonas* sp. JSC4 (Kato *et al.*, 2017). Therefore, enhancing the lipid production approaches might be a better solution.

2.3 Lipid biosynthesis

Lipid biosynthesis in microalgae can be divided into two main steps (Figure 2). The initiation step is fatty acid biosynthesis follows by TAG biosynthesis. FA biosynthesis mainly occurs in the chloroplast. The process initiates with the CO₂ fixation. Then, CO₂ is converted into pyruvate through Calvin cycle and Glycolysis pathway, respectively. Pyruvate is further converted into acetyl-CoA by the activity of pyruvate dehydrogenase complex (PDHC). After that, acetyl-CoA is added the carbonyl group to form malonyl-CoA by ACCase. This step is regarded as a rate limiting step for FA biosynthesis (Zalutskaya *et al.*, 2015). The coenzyme A that attached to the acetyl and malonyl is replaced by acyl carrier protein (ACP) to form acetyl-ACP and malonyl-ACP by acetyl-CoA:ACP transacylase (ACAT) and malonyl-CoA:ACP transacylase (MAT), respectively. Either ACAT or MAT plays an important role in FA elongation. To synthesize FAs, several enzymes involved in FA synthesis as a sequential reaction of reduction-dehydration-reduction (Bellou *et al.*, 2014) FA synthesis starts with the condensation of acetyl-CoA and malonyl-CoA by 3-ketoacyl-ACP synthase (KAS) to form 3-ketoacyl-ACP. Next, 3-ketoacyl-ACP is converted into 3-hydroxyacyl-ACP and trans-enoyl-ACP through 3-ketoacyl-ACP reductase (KAR) and 3-hydroxyacyl-ACP dehydratase (HD), respectively. The cycle is repeated until the formation of palmitoyl-

ACP. The FAs are released from ACP and transferred into cytosol via fatty acid thioesterase (FAT) and long-chain acyl-CoA synthetase (LACS). For unsaturated FA formation, it is synthesized after FA synthesis cycle is completed. Desaturase is the key enzyme for unsaturated fatty acids (UFAs) formation (Bellou *et al.*, 2016). The position of the double bond depends on the present of desaturase encoding gene in the individual strain. The sequence of desaturation of the FA is normally initiated with $\Delta 9$ position by $\Delta 9$ desaturase, following by $\Delta 12$ and $\Delta 15$ (or $\Delta 6$) positions, respectively (Mühlroth *et al.*, 2013).

In microalgae, TAG biosynthesis can be generated via three biosynthetic pathways; (1) TAG that is catalyzed by phospholipid:diacylglycerol acyltransferase (PDAT), (2) monoacylglycerol (MAG) pathway which forms TAG via the conversion of monoacylglycerol into diacylglycerol (DAG) by monoacylglycerol acyltransferase activity. The last pathway which is the main contribution to synthesize TAG, the so-called (3) Kennedy pathway (or glycerol phosphate pathway). This pathway is recognized to be the main pathway for TAG biosynthesis in microalgae. It initially converts dihydroxyacetone phosphate (DHAP) into glycerol-3-phosphate by glycerol-3-phosphate dehydrogenase (G3PDH). Glycerol-3-phosphate is then acylated with acyl-CoA which is transformed from free FA (FFA) by addition of CoA and continuously converted into TAG by various enzymes including glycerol-3-phosphate acyltransferase (GPAT), lysophosphatidic acid acyl-transferase (LPAAT), and lysophosphatidylcholine acyltransferase (LPAT), respectively. Then diacylglycerol acyltransferase (DGAT) converts DAG into TAG. Finally, TAG assembles together to form lipid body in algal cells (Zienkiewicz *et al.*, 2016).

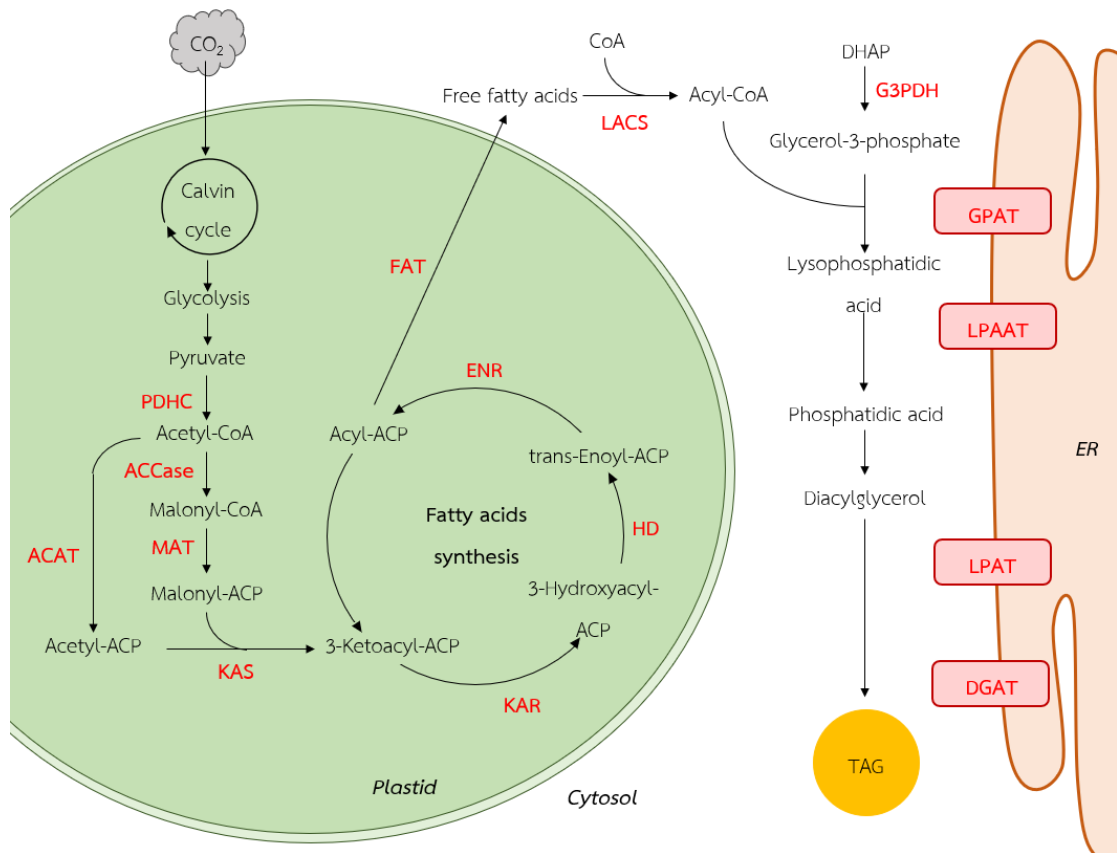


Figure 2 Lipid biosynthesis in microalgae. Fatty acid synthesis (FAS) occurs in the chloroplast and Kennedy pathway occurs in cytosol (Modified from Radakovits *et al.*, 2010). PDHC; pyruvate dehydrogenase complex, ACCase; acetyl-CoA carboxylase, ACAT; acetyl-CoA:ACP transacylase, MAT; malonyl-CoA:ACP transacylase, KAS; 3-ketoacyl-ACP synthase, KAR; 3-ketoacyl-ACP reductase, HD; 3-hydroxyacyl-ACP dehydratase, ENR; enoyl-ACP reductase, FAT; fatty acid thioesterase, LACS; long-chain acyl-CoA synthetase, G3PDH; glycerol-3-phosphate dehydrogenase, GPAT; glycerol-3-phosphate acyltransferase, LPAAT; lysophosphatidic acid acyl-transferase, LPAT; lysophosphatidylcholine acyltransferase, and DGAT; diacyl-glycerol acyltransferase.

In cyanobacteria, lipid biosynthesis is only occurred in the cytosol due to the lack of chloroplast. Thylakoid membrane where the photosynthesis takes place is the most important compartment for cyanobacteria (van Eerden *et al.*, 2015). The biosynthesis is similar as in microalgae. It starts with the conversion of CO₂ into pyruvate. Then, pyruvate is transformed into acetyl-CoA following by malonyl-CoA via the activities of PDH and ACCase, respectively. FAs are synthesized by type II FAS as the same sequential as mentioned above (Ryall *et al.*, 2003; Quintana *et al.*, 2011; Janßen and Steinbüchel, 2014). Most bacteria, including cyanobacteria, prefer to store FAs in the form of fatty alcohol or converts them into alkane (or alkene). TAG is an unusual energy storage for cyanobacteria (Alvarez and Steinbüchel, 2002). However, there was the first publish discovered TAG accumulation in the form of lipid body in filamentous cyanobacterium, *Nostoc punctiforme* (Peramuna and Summers, 2014). Different from the microalgae, owing to the lack of TAG accumulation property, FFA and glycolipid are used for biodiesel production with the same method as TAG conversion (Machado and Atsumi, 2012; Yu *et al.*, 2014).

2.4 Lipid enhancing strategies

To enhance lipid production in microalgae and/or cyanobacteria, both optimization condition and engineering approaches are the good strategies. Stress treatment, for example nitrogen starvation, high carbon concentration, temperature, and salinity stress, are effective approaches to induce lipid accumulation. However, each condition has a different affect to the cells. Moreover, individual strain of microalgae and cyanobacteria has a distinct affect by each condition.

2.4.1 Stress condition

2.4.1.1 Nitrogen starvation

Nitrogen is one of the most important components for either amino acids which are the precursor for protein synthesis or ribonucleic acids which are precursor(s) for genetic materials. Culturing of microalgae or cyanobacteria under nitrogen starvation mainly effected to the protein synthesis. This makes the cells to

adapt themselves to cope with the unfavorable environment. Ho *et al.* (2014) reported that when the green microalga *Chlamydomonas* sp. JSC4 was cultured in nitrogen depleted media, the lipid content was found to be increased 2.7 folds compared to the normal condition. In contrast, the content of protein was dramatically declined from 45.4% of DCW in nitrogen repletion condition to 17.9% of DCW in the depletion condition. This indicated that this microalga reduced the protein production and stored the influx carbon in the form of lipid instead. As similar as the previous study, Avidan *et al.* (2015) found that *Chlorella desiccata* accumulated higher lipid content when the cells were cultured in nitrogen deficient condition. Genes expression analysis revealed that the PDH-E1 α encoding gene was highly up-regulated for 3-folds within 24 hours of cultivation. The up-regulation of this gene consequently resulting in enhancing of the conversion of pyruvate into acetyl-CoA rate. Nitrogen starvation is not only effect to the protein content but also the abundance of the protein (Hockin *et al.*, 2012).

2.4.1.2 High carbon concentration

Carbon is a major component for almost all molecules in living organisms. Hence, the high concentration of both CO₂ and organic carbon would enhance carbon flux into the central carbon metabolism. Nakanishi *et al.* (2014) reported that *Chlamydomonas* sp. JSC4 accumulated higher lipid content when it was cultured in higher concentration of CO₂. However, when the concentration reached too high (4-8%), this led more an acidic environment. So that, the microalgal growth was slow down (biomass production was low) thus, consequently affected to lipid production.

Heterotrophic cultivation can also be performed with the microalgae (Najafabadi *et al.*, 2015). Thus, the use of microalgae in waste water treatment process along with lipid production have become an interesting approach (Mohan *et al.*, 2015; Higgins *et al.*, 2016). Similar to the CO₂, the increasing of glucose concentration also induced lipid accumulation in microalgae (Gim *et al.*, 2016).

2.4.1.3 Light intensity

High light intensity condition was found to be one of effective conditions to induce lipid accumulation in some microalgae and cyanobacteria (Xiao *et al.*, 2015; Shukla *et al.*, 2016). When *Chlorella* sp. and *Monoraphidium* sp. were cultured under high light intensity ($400 \mu\text{mol m}^{-2} \text{s}^{-1}$), the lipid content was reached to 33.03 % and 43.47% of DCW, respectively (Ho *et al.*, 2015). While in the low light condition ($40 \mu\text{mol m}^{-2} \text{s}^{-1}$), the lipid content of *Chlorella* sp. was 22.90% of DCW and *Monoraphidium* sp. was 30.70% of DCW. Furthermore, carbohydrate and protein content were found to be decreased when the microalgae were treated with the high light intensity. In addition, Ho *et al.* (2017) reported the increasing of pyruvate, acetyl-CoA, and glycerol-3-phosphate in *Chlamydomonas* sp. JSC4 which was cultured under high light intensity ($300 \mu\text{mol m}^{-2} \text{s}^{-1}$). This specific condition resulted in an overproduction of TAG in the cells. However, the mechanism by which light intensity impacts on lipid production remains elusive.

2.4.1.4 Salinity stress

High salinity stress is another attractive method to improve lipid production in microalgae. In a previous study, the unicellular green microalga *Chlorella protothecoides* which were cultured under 20 g/L NaCl can accumulated lipid content at 43.4% of DCW (Campenni *et al.*, 2013). In addition, the carotenoids content was found to be increased with increasing of NaCl concentration. This result suggested that free radicals produced from osmotic stress might affect to lipid and carotenoids production (Pancha *et al.*, 2015). In green microalga *C. protothecoides* accumulated higher lipid content under higher NaCl concentration (Wang *et al.*, 2016). This is likely due to the decreased activity of phosphoenolpyruvate carboxykinase and isocitrate dehydrogenase. These enzymes play important roles in gluconeogenesis and Krebs' cycle. Thus, this condition causes an inhibition of glucose synthesis. Whereas, the activity of key enzyme in FA biosynthesis, ACCase, was significantly increased. This indicated that carbon flux was altered to the lipid production instead of carbohydrate production. It was demonstrated that the activity of the enzymes involved in starch

synthesis pathway were down-regulated under salt stress condition (Ho *et al.*, 2017). On the other hand, genes involved in lipid biosynthesis and starch degradation were found to be up-regulated. These studies proved the hypothesis that salinity stress induces lipid production via switching the metabolism from protein and carbohydrate into lipid synthesis.

2.4.2 Engineering

Genetic and metabolic engineering keep promising to be a good strategy to improve lipid production in microalgae and cyanobacteria. Unfortunately, a big obstacle to engineer the microorganisms is an insufficient genetic database. It seems more difficult to engineer microalgae which is eukaryotic microorganism. Like other eukaryotes, microalgae have complicate transcription and translation processes. However, the attempt to enhance lipid accumulation in these microorganisms by genetic or metabolic engineering still gain attention these days. Approaches for engineering can be divided into 5 categories according to the target of interest (Liang and Jiang, 2013; Bajhaiya *et al.*, 2017).

2.4.2.1 Enhancement of FA synthesis approach

2.4.2.1.1 Improvement of CO₂ fixation

Both cyanobacteria and microalgae are CO₂ fixing microorganisms and use as carbon source. Since carbon is a major component of all metabolites in living organism, the improvement of CO₂ fixation efficiency might induce FFA and total lipid accumulation (Ducat *et al.*, 2011; Nozzi *et al.*, 2013). Ruffing (2014) reported that overexpression of RuBisCO encoding gene (*rbclS*) under *psbAI* promoter resulted in increasing of FFA production for 3 folds compared in the parental strain. Moreover, enhancement of CO₂ fixation consequently resulted in the higher stress tolerance capability in cyanobacteria (Kitchener and Grunden, 2018).

2.4.2.1.2 Overexpression of PDHC gene

PDHC is a complex enzyme that plays an important role in converting pyruvate into acetyl-CoA; a precursor for FA synthesis. The PDHC comprises

of three catalytic enzymes including (1) pyruvate dehydrogenase (E1 subunit), (2) dihydrolipoyl transacetylase (E2 subunit), and (3) dihydrolipoyl dehydrogenase (E3 subunit) (Patel *et al.*, 2014; Sutendra *et al.*, 2014). The enhancement of acetyl-CoA production could increase FA productivity. Downregulation of PDHC-E1 α subunit drastically decreased the *de novo* FA synthesis in *C. reinhardtii* (Shtaida *et al.*, 2014). TAG accumulation was steeply declined when the microalgae was cultured photoautotrophically. In addition, PDHC-E1 α knockout led to damage of photosynthetic activity. Hence, it can conclude that *PDH* is an important gene.

2.4.2.1.3 Overexpression of pyruvate dehydrogenase kinase

Pyruvate dehydrogenase kinase (PDK) enzyme is an inhibitor of PDHC by phosphorylation. This process leads to the alteration of PDHC structure and inactivation of the enzyme (Sutendra and Michelakis, 2013). The knockdown of *PDK* gene promoted TAG accumulation in *Phaeodactylum tricornutum* (Ma *et al.*, 2014). The interference of *PDK* gene expression by using RNA-interference (RNAi) technology caused the overexpression of *PDHC* (Ma *et al.*, 2017). Both TAG accumulation and FA production were determined to be increased without disturbing the growth of the cells. Besides, supplementation of sodium dichloroacetate which is a PDK inhibitor induced the acetyl-CoA production and TAG overproduction. Thus, the inhibition of PDK activity can enhance the activity of PDHC and induced acetyl-CoA production (Yao *et al.*, 2017).

2.4.2.1.4 Overexpression of ACCase gene

As mentioned in section 2.3, ACCase is a rate limiting step in FA synthesis. ACCase is as well as a metabolic direction regulator. Owing to the fact that acetyl-CoA participates in many metabolisms, including protein, carbohydrate, and lipid. However, it must accept that the overexpression of *ACCase* gene has a limitation due to the complication of metabolism in the microalgal cells (Klok *et al.*, 2014). Nevertheless, the overexpression of *ACCase* gene in non-oleaginous yeast, *Mucor*

rouxii, was achieved (Ruenwai *et al.*, 2009). The result showed 40% increasing of lipid in *M. rouxii*.

2.4.2.1.5 Overexpression of thioesterase gene

In cyanobacteria, thioesterase plays a key role in FA synthesis. The overexpression of thioesterase encoding gene caused over FFA production (Savakis and Hellingwerf, 2015). It was shown that the freshwater cyanobacterium *Synechocystis* sp. PCC6803 excreted higher concentration of FFA when thioesterase gene was overexpressed (Liu *et al.*, 2011). The FA production reached to 194 ± 14 mg/L of culture. This proved that not only the improvement of up-stream FA synthesis, but down-stream FA synthesis engineering could induce lipid accumulation in cyanobacteria.

2.4.2.2 Enhancement of TAG biosynthesis approach

2.4.2.2.1 Overexpression of *GPAT* gene

GPAT plays an important role in TAG biosynthesis via converting FFA into lysophosphatidic acid (Figure 2). Niu *et al.* (2016) reported that the overexpression of *GPAT* gene in *P. tricornutum* affected the enhancing of TAG accumulation for 2 folds compared to the wild type. The knockdown of this gene reversibly affected in lipid accumulation (Amiar *et al.*, 2016).

2.4.2.2.2 Overexpression of *DGAT* gene(s)

Because of the importance of DGAT to be a key enzyme in TAG biosynthesis, this enzyme gets a lot of attention among lipid enhancing studies. DGAT can be divided into several families. Type 1 and type 2 DGATs are the main family. They have the same activity but different in structure and catalytic domain. Moreover, they have distinct protein sequences which suggested that they evolved separately (Zienkiewicz *et al.*, 2016). The third type of DGAT (type 3 DGAT) is a soluble cytosolic enzyme first discovered in *Arachis hypogaea*. The last type of DGAT is type 4 DGAT. It acts as both wax ester synthase and DGAT (Miller, 2015; Wagner *et al.*, 2010). Among these DGATs, type 2 DGAT (DGTT) plays the most important role in lipid production in

microalgae (Chen and Smith, 2012) . The heterologous *DGTT1* expression from *C. reinhardtii* in *S. obliquus* led to the increasing of TAG accumulation for approximately 2 folds compared to the wild type. In addition, the biomass production was found to be improved for 29% (Chen *et al.*, 2016). Úbeda-Mínguez *et al.* (2017) reported in the green microalga *Tetraselmis chui*, lipid accumulation was induced by overexpression of *Saccharomyces cerevisiae* *DGAT1* and *Echium pitardii* *DGAT2*.

2.4.2.3 The regulation of PDH-bypass pathway

2.4.2.3.1 Overexpression of acetyl-CoA synthase

Acetyl-CoA is not only directly generated from PDHC but also the activity of Acetyl-CoA synthase (ACS). This enzyme localizes in mitochondria and plays important role in converting pyruvate into acetyl-CoA, so-called PDH-bypass pathway (Shtaida *et al.*, 2015). The oleaginous green microalga *C. desiccata* accumulated higher lipid content when the ACS gene was overexpressed (Avidan and Pick, 2015). They also found that the content of acetyl-CoA was increased when the microalga was treated with nitrogen depletion condition.

2.4.2.3.2 Overexpression of malic enzyme

Malic enzyme acts in converting of malate into pyruvate in cytoplasm. It was hypothesized that the overexpression of malic enzyme might lead to the enhancement malate to pyruvate conversion rate (Figure 3). However, there is a few studies of this enzyme in microalgae and cyanobacteria. Nonetheless, there was a report that *P. tricornutum* can accumulate lipid content for 57.8% of DCW when it was overexpressed the ME encoding gene. Additionally, the transgenic strain of *P. tricornutum* was accumulated TAG 66% higher than that of the wild type (Xue *et al.*, 2015).

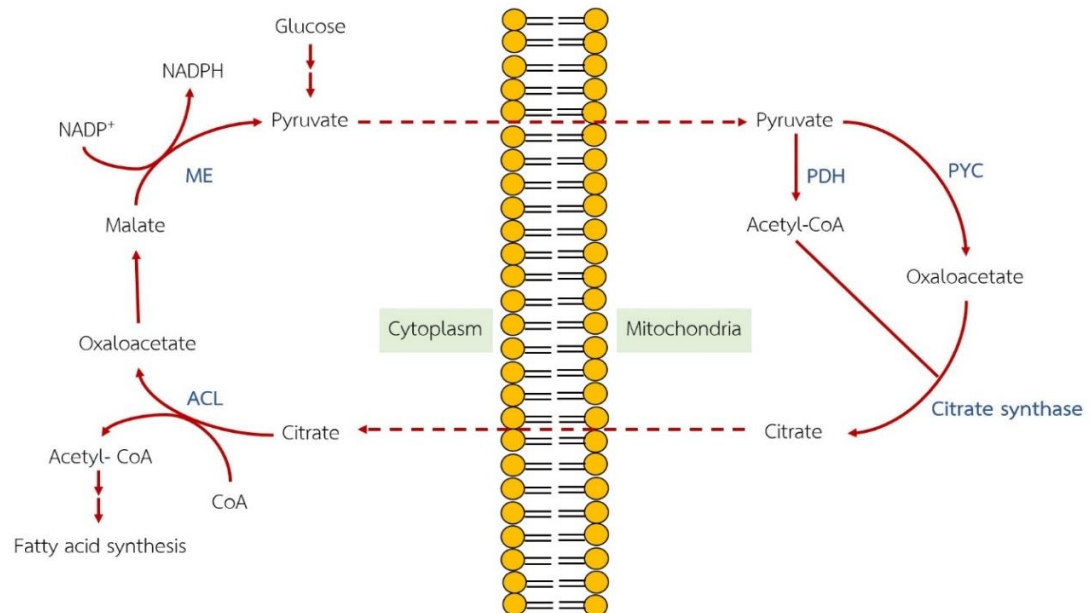


Figure 3 The schematic of citrate-pyruvate shuttle in eukaryote organisms (modified from Liang and Jiang (2016). PDH; pyruvate dehydrogenase, PYC; pyruvate carboxylase, ACL; ATP citrate lyase, and ME; malic enzyme.

2.4.2.4 The inhibition of competitive pathway

2.4.2.4.1 Inhibition of β -oxidation

β -oxidation is a lipid degradation pathway. In photosynthetic organisms, lipid biosynthesis is naturally occurred during the daytime and will be degraded at night. Unfortunately, the inhibition of this pathway is not a good strategy for lipid enhancement due to highly impact to growth rate. The only solution for this problem is continuous light cultivation so that the cells reduce the rate of β -oxidation. However, Ruffing and Jones (2012) had succeeded in inhibition of β -oxidation in *S. elongatus* PCC 7942. The knockout of acyl-ACP synthetase combined with expression of thioesterase resulted in higher FFA in this cyanobacterium. Nonetheless, the photosynthetic efficiency in the engineered strain was weakened due to the reduction of chlorophyll-a content and the alteration of photosynthetic accessory allocation.

2.4.2.4.2 Inhibition of starch biosynthesis

Starch is a primary energy feedstock in all living organisms. Starch biosynthesis starts with the conversion of glucose-1-phosphate into adenosine diphosphate-glucose (ADP-glucose) via the activity of ADP-glucose phosphorylase. The inhibition of this pathway caused the dramatic increase in lipid accumulation in microalgae (Sirikhachornkit *et al.*, 2016). Li *et al.* (2010) reported that making of starchless mutant of *C. reinhardtii* induced TAG accumulation over than 8 folds compared to the wild type. Similar to the inhibition of β -oxidation, starch synthesis inhibition also affects to the cell growth rate as well as the efficiency to cope with the extreme environment.

2.4.2.5 Transcriptional engineering

Transcriptional engineering is an engineering of transcription factor (TF). Transcriptional engineering is recently interested in enhancement of lipid biosynthesis (Chen *et al.*, 2018). Attempts were made by knockout TFs in *Nannochloropsis gaditana* by CRIPR-CAS9 technique. Among 20 TFs, only the knockout of *Zn(II)₂Cys₆* (*ZnCys*) resulted in lipid overproduction (Ajjawi *et al.*, 2017). On the other hand, the inhibition

of *ZnCys* expression affected to lower total organic carbon (TOC) productivity. Thus, the down regulated of *ZnCys* was performed instead. The result showed that the lipid accumulation of *ZnCys*-RNAi-7 strain; the *N. gaditana* that was interfered the *ZnCys* expression by using RNAi technique, was found to be sharply increased without interfere the growth rate. Transcriptional engineering becomes a new interesting strategy to improve lipid accumulation in microalgae and/or cyanobacteria.

2.5 Photosynthetic microorganism models

2.5.1 *C. reinhardtii*

Chlamydomonas sp. is a unicellular green microalga that live in a diverse environment. This microalga has oval shape and 2 flagella. Their cell wall mainly consists of glycoprotein with no cellulose. The outstanding compartment of *Chlamydomonas* is an eyespot in the chloroplast which is used as photoreceptor (Kreimer *et al.*, 1992). *Chlamydomonas* is classified in the class of Chlorophyceae, order Chlamydomonadales, family Chlamydomonadaceae. They contain several species, but the most well-known is *C. reinhardtii*. This freshwater green microalga is suitable to be a model organism due to its ease cultivation in simple medium and more importantly, its entire genome sequence has been completed and available in the databases (Siaut *et al.*, 2011). In fact, *C. reinhardtii* is less recognized as the best model for lipid accumulation due to their low lipid production compared to another model such as *C. vulgaris*, *D. tertiolecta*, and *N. gaditana* (Rismani-Yazdi *et al.*, 2011; Radakovits *et al.*, 2012; Çakmak *et al.*, 2014; Avidan and Pick, 2015). However, because of *C. reinhardtii* is more simply to understand and there are a lot of genetic tools and databases, hence *C. reinhardtii* is wildly used as a model in lipid production studies. The understanding of high salinity effect on lipid accumulation is limited. Recent study revealed that salinity stress induced starch-to-lipid conversion in *Chlamydomonas* sp. JSC4 (Ho *et al.*, 2017). The lipid content was reached to the highest at 56.9% of DCW in 2% of sea salt condition. While, the starch content was reduced to 20% of DCW. Genes involved in lipid biosynthesis including biotin carboxyl carrier protein (BCCP), biotin carboxylase (BC), carboxyl transferase α subunit (α CT) and carboxyl transferase

β subunit (β_{CT}) which are the subunit of ACCase enzyme were found to be significantly increased when the cells were treated with 2% of sea salt. Nevertheless, the expression of *PDH* remained stable.

2.5.2 *S. elongatus* PCC 7942

Cyanobacteria are one of the good candidates for biodiesel feedstock due to several potentials as mentioned above (section 2.2) (Sarsekeyeva *et al.*, 2015). Various cyanobacteria can be used as model studies. For instance, the freshwater unicellular cyanobacterium *S. elongatus* PCC 7942 is one of the most widely used microorganisms. Cultivation of *S. elongatus* PCC 7942 under high light intensity in the medium enriched with Na_2CO_3 resulted in enhancement of linoleic content and lipid productivity was accounted for 35.9 ± 0.5 mg/L/day (Silva *et al.*, 2014). Furthermore, very recently it was reported the improvement *S. elongatus* PCC 7942 strain to produce omega-3 by overexpressing and deleted various genes (Santos-Merino *et al.*, 2018). They found that the overexpression of putative *fabD* gene (annotated as *SynMAT*) led to alteration of FA composition. The content of C14:0 and C16:1 were found to be slightly increased while C16:0, C18:0, and C18:1 were declined. On the other hand, overexpression of *fabH* gene (*KASII*) led to the extremely overproduction of long chain fatty acids (LCFAs) which are C18:0 and C18:1. As similar as the overexpression of *fabH* gene, deletion of *fadD* which encoded long-chain fatty acyl-CoA ligase (annotated as *LACS*) caused the significantly increasing of LCFAs.

In this study, *C. reinhardtii* (137c) was chosen to be the model organism. This strain is the combination of wild type strain CC-125 (mt^+) and CC-124 (mt^-) (Chlamydomonas Resource Center). The microalga was treated with salts at appropriate concentration. The accumulation of lipid body was observed by Nile red staining and lipid content was determined by fatty acid methyl esters (FAMES) analysis. Moreover, genes associated with lipid biosynthesis were investigated after treating the cells with appropriate concentration of NaCl. The gene that was highly expressed was further studied in the heterologous photosynthetic organism, *S. elongatus* PCC 7942,

together with the overexpression of native gene as comparative analysis. Information gained on all aspects covering the molecular and cellular levels and productions could allow the understanding of the mechanism behind the physiological plasticity upon salt stress.



CHAPTER III

MATERIALS AND METHODS

3.1 Instruments

Autoclave: Model ES-215, TOMY Digital Biology, Japan

Balance: Model PG2002-S, Mettler Toledo, USA

Cell culture plate (12-well plate): SPL Life Science, Korea

Centrifuge bottle: Nalgene™, USA

Cuvette: Spectronic 401, Milton Roy, USA

Fluorescence microscope: Model BX51, Olympus, Japan

Freeze dryer: FlexiDry MP, Kinetics, USA

Gas chromatography: Model Agilent 6890N, Agilent, USA

Gel electrophoresis: Model MJ-105, Major Science, USA

Gel imaging: Model Gel Doc EZ™, Bio-Rad Laboratories, USA

High speed refrigerated centrifuge: Model 6500, Kubota, Japan

Horizontal laminar flow: Model H1, Microtech, Thailand

Hot air oven: Model UE600, Memmert, Germany

HP-INNOWax GC column: Agilent, USA

Incubator shaker: Model Innova 4330, New Brunswick Scientific, USA

Incubator: Model ULE800, Memmert, Germany

Laboratory glassware: Pyrex, USA

Magnetic stirrer: Model MMS-3000, Biosan, Latvia

Micropipette: Eppendorf Research Plus, Eppendorf, Germany

Nanodrop 200 UV-Vis Spectrophotometer: Thermo Scientific, USA

Orbital shaker: Model TT-20, Hercuvan Lab Systems, Malaysia

Power supply: PowerPac™ HC, Bio-Rad Laboratories, USA

Precision balance: Model ME3002, Mettler Toledo, USA

Refrigerated centrifuge: Model 5922, Kubota, Japan

Refrigerated microcentrifuge: Model 5418 R, Eppendorf, Germany

Rocking platform: Mini Rocker, Bio-Rad Laboratories, USA

Semi-dry transfer cell: Model Trans-Blot® SD Cell, Bio-Rad Laboratories, USA

Sodium dodecyl sulfate polyacrylamide gel electrophoresis: Model MiniPROTEIN II®
Tetra Cell, Bio-Rad Laboratories, USA

Sonicator: Vibra-Cell™ Ultrasonic Liquid Processors VCX 130, Sonics, USA

Spectrophotometer: GENESYS 20, Thermo Fisher Scientific, USA

Thermal cycler: Model C1000 Touch™, Bio-Rad Laboratories, USA

Thermal cycler: Model T100™, Bio-Rad Laboratories, USA

UV-Vis Spectrophotometer: UV-240, Shimadzu, Japan

Vortex mixer: Model K-550-GE, Scientific Industries, USA

3.2 Chemicals

2-Mercaptoethanol: Sigma-Aldrich, USA

30% Acrylamide/Bis Solution: Bio-Rad Laboratories, USA

Acetic acid: Merck, Germany

Acrylamide/Bis solution (40%): Bio-Rad Laboratories, USA

Agar powder: Himedia, India

Agarose gel: Bio-Rad Laboratories, USA

Ammonium chloride: Emsure, Germany

Ammonium molybdate: Emsure, Germany

Ammonium persulfate: Merck, USA

Antibody raised against 6-histidine: R&D system, USA

Antibody raised against mouse-IgG HRP conjugated: New England Biolabs, USA

Bacto[®] tryptone: Merck, Germany

Bio-Rad protein assay (dye reagent concentrate), Bio-Rad Laboratories, USA

Boric acid: Merck, Germany

BSA (Bovine serum albumin): New England Biolabs, USA

Butylated hydrotoluene, USA

Calcium chloride: Merck, Germany

Chloroform: RCI Labscan Limited, Thailand

Citric acid: Merck, Germany

Cobalt (II) chloride: Ajax Finechem Pty Limited, Australia

Cobalt (II) nitrate: Ajax Finechem Pty Limited, Australia

Coomassie brilliant blue G-250: Sigma-Aldrich: USA

Copper (II) sulfate: Ajax Finechem Pty Limited, Australia

DEPC (Diethylpyrocarbonate): Amresco, USA

Dipotassium phosphate: Ajax Finechem Pty Limited, Australia

Disodium phosphate: Ajax Finechem Pty Limited, Australia

EDTA (Ethylenediaminetetraacetic acid): Amresco, USA

Ethanol: Merck, Germany

Ferric ammonium nitrate: Merck, Germany

Glycerol: Merck, Germany

Glycine: Ajax Finechem Pty Limited, Australia

Hexane: USA

Hydrochloric acid: Merck, USA

IPTG (Isopropyl β -D-1-thiogalactopyranoside): Sigma-Aldrich, USA

Iron (II) sulfate: Ajax Finechem Pty Limited, Australia

Isopropanol: Merck, Germany

Lithium chloride: Merck, Germany

Magnesium sulfate: Merck, Germany

Manganese (II) chloride: Ajax Finechem Pty Limited, Australia

Methanol: Merck, Germany

Penicillin: Amresco, USA

Potassium chloride: Merck, Germany

Potassium dihydrogen phosphate: Merck, Germany

Skim milk: Himedia, India

Sodium carbonate: Merck, Germany



Sodium chloride: Ajax Finechem Pty Limited, Australia

Sodium lauryl sulfate: Ajax Finechem Pty Limited, Australia

Sodium nitrate: Merck, Germany

Sodium sulfate: Japan

Spectinomycin: Sigma-Aldrich, USA

Sulfuric acid: Merck, Germany

SYBR[®] safe DNA gel stain: Invitrogen, USA

TEMED (Tetramethylethylenediamine): Bio-Rad Laboratories, USA

Trizma (2-amino-2-(hydroxymethyl)-1,3-propanedial): Sigma, USA

TRIzol[®] reagent: Invitrogen, USA

Tween 20: Merck, Germany

X-gal: Amresco, USA

Yeast extract powder: Himedia, India

Zinc sulfate: Ajax Finechem Pty Limited, Australia

3.3 Membrane

PVDF (Polyvinylidene difluoride): Millipore Cooperation, USA

3.4 Kits

DNeasy[®] Plant Mini Kit: Qiagen, Germany

GenepHlow[™] Gel/PCR Kit, Geneaid, Taiwan

HiYield[™] Plasmid Mini Kit, RBC Bioscience, Taiwan

Horseshoe Peroxidase Conjugate Substrate kit (Bio-Rad Laboratories, USA)

SuperScript® III First Strand Synthesis system, Invitrogen, USA

3.5 Enzymes

*Bam*HI: New England Biolabs, USA

KOD polymerase: KOD-Plus-Neo, Toyobo, Japan

*Nde*I: New England Biolabs, USA

T4 DNA ligase: Takara, Japan

Taq DNA polymerase: Vivantis, Malaysia



3.6 Bacterial, microalgal strains and plasmids

Table 2 Microorganisms and plasmids used in this study

Strain and plasmid	Description	Source/reference
<i>C. reinhardtii</i> (137c)	Fresh water green alga	Invitrogen, USA
<i>S. elongatus</i> PCC 7942	Fresh water cyanobacterium	Invitrogen, USA
<i>E. coli</i> DH5 α	ϕ 80 <i>lacZ</i> Δ M15 Δ (<i>lacZYA-argF</i>)U169 <i>recA1 endA1 hsdR17</i> (rK ⁻ , mK ⁺) <i>phoA</i> <i>supE44</i> λ^- <i>thi-1 gyrA96 relA1</i>	Invitrogen, USA
pBSK ⁺ II	Cloning vector	Toyobo, Japan
pSyn_6	Expressing vector	Invitrogen, USA
<i>ChMAT</i> /pBSK ⁺ II	0.99 kb <i>ChMAT</i> fragment cloned into pBSK ⁺ II	This study
<i>ChMAT</i> /pSyn_6	0.99 kb <i>ChMAT</i> fragment cloned into pSyn_6	This study
<i>SynMAT</i> /pBSK ⁺ II	0.92 kb <i>SynMAT</i> fragment cloned into pBSK ⁺ II	This study
<i>SynMAT</i> /pSyn_6	0.92 kb <i>SynMAT</i> fragment cloned into pSyn_6	This study

Table 3 Primers used in this study

Primers	Sequences (5' → 3')	Base pairs
ChlmyPDH2_Foward	CCCATTGTGGAGGGC	15
ChlmyPDH2_Reverse	ACAGCAGAACGTGCT	15
ChlmyACCCase_Foward	TCTGCAAGTCGCTCG	15
ChlmyACCCase_Reverse	CGTGTCCACGAAGGT	15
ChlmyMAT_Foward	CCGTGAGTCAGCCCCG	15
ChlmyMAT_Reverse	TGGACCGGCTTGTCC	15
ChlmyKAS2_Foward	CGCGGACTACACGAC	15
ChlmyKAS2_Reverse	GGCGAAGGGAATGCA	15
ChlmyGPD1_Foward	CAAAGGCCTTGAGGT	15
ChlmyGPD1_Reverse	CAAGTCCATGCCCTC	15
ChlmyFAT 1_Foward	TCAGGAGTCGCGGTG	15
ChlmyFAT 1_Reverse	GCACTTGCAGGCGTG	15
ChlmyDGTT1_Foward	GATTAAGACCGCCGA	15
ChlmyDGTT1_Reverse	AGCGCCTCAGACGCG	15
ChlmyDGTT2_Foward	TCCTGTCCTTCTGGT	15
ChlmyDGTT2_Reverse	TGAACACCACATTCG	15
ChlmyDGTT3_Foward	TACCTCGCACTTGAC	15
ChlmyDGTT3_Reverse	AAGTAGTGACGCCAG	15
ChlmyDGTT4_Foward	GGCTACTTGTTTCGGA	15
ChlmyDGTT4_Reverse	GCTGGAGAGGTAGGC	15
Chlmy18s rRNA_Foward	CGGAACCCGCTGGTC	15
Chlmy18s rRNA_Reverse	TGAAGGTGAGCGGCG	15
ChMAT_NdeI_Foward	ATCATATGGTCGCTGTCC	18
ChMAT_BamHI_Reverse	GGATCCAGCGGTGAT	16
SynMAT_NdeI_Foward	CATATGGCTAAAACGGTGTGGGTGT	25
SynMAT_BamHI_Reverse	GGATCCGACCGTGAGGTCTGC	21

Primers	Sequences (5'→3')	Base pairs
pSyn_psbA	TCTTGCCCTTTACAACCT	18
pSyn_rrnB	CGCTACTGCCGCCAG	15
7942rnpB_Forward	GAGGAAAGTCCGGGCTCCC	19
7942rnpB_Reverse	TAAGCCGGGTTCTGTTCTC	19
7942MAT_Forward	CAGCCCTCTACACCG	15
7942MAT_Reverse	GCCATAAACGGCGAG	15
7942LACS_Forward	TGCTTTCTCACGGCA	15
7942LACS_Reverse	TCGATCAAGCGACGT	15

3.7 Bioinformatics analysis

Gene and protein sequences including predicted lipid biosynthesis involved in FA and TAG biosynthetic pathways in the green microalga *C. reinhardtii* were searched and retrieved from Kyoto Encyclopedia of Genes and Genomes (KEGG) (<http://www.genome.jp/kegg/>), KEGG PATHWAY Database (<https://www.genome.jp/kegg/pathway.html>), National Center for Biotechnology Information (NCBI) (<https://www.ncbi.nlm.nih.gov/>) and Joint Genome Institute (JGI) (<https://jgi.doe.gov/>) databases. Each sequence was analyzed for topological modelling by using PROTTER software (<http://wlab.ethz.ch/protter/start/>). Amino acid sequences of *C. reinhardtii* malonyl-CoA:ACP transacylase (*ChMAT*) and *S. elongatus* PCC 7942 malonyl-CoA:ACP transacylase (*SynMAT*) were retrieved from KEGG and NCBI databases (Appendix 1). The ChMAT and SynMAT proteins were analyzed for protein domain and interaction between other proteins via SMART software (http://smart.embl-heidelberg.de/smart/change_mode.pl) and STRING software (<https://string-db.org/>), respectively. To analyze the phylogeny of ChMAT and SynMAT, the protein sequences were blasted by using NCBI (<https://blast.ncbi.nlm.nih.gov/Blast.cgi>) and compared with malonyl-CoA:ACP transacylase orthologs. The phylogenetic tree was analyzed by using Molecular

Evolutionary Genetics Analysis Version 6.0 (MEGA6) software (<https://www.mega-software.net/>).

3.8 Cultures and stress treatment

3.8.1 *C. reinhardtii* (137c) cultivation

The unicellular green microalga *C. reinhardtii* (137c) was cultured in Tris-Acetate-Phosphate medium (TAP) (Appendix 2) at 26 ± 1 °C under continuous light ($50 \mu\text{mol m}^{-2}\text{s}^{-1}$) in 250 ml Erlenmeyer flask and shaking at 110 rpm. The culture was used as stock culture for all experiments. The growth of cells was determined by spectrophotometer (Shimadzu, Japan) at absorbance 730 nm.

3.8.2 *S. elongatus* PCC 7942 cultivation

Fresh water cyanobacterium *S. elongatus* PCC 7942 was cultured in Blue-Green 11 medium (BG11) (Appendix 3) at 26 ± 1 °C under continuous light ($50 \mu\text{mol m}^{-2}\text{s}^{-1}$) in 250 ml Erlenmeyer flask and shaking at 110 rpm. The growth of cells was determined by spectrophotometer at absorbance 730 nm.

3.8.3 *Escherichia coli* DH5 α cultivation

E. coli DH5 α was incubated on 1.5% Luria-Bertani agar (LB) (Appendix 4) at 37 °C for overnight (approximately 16 hours) to get a single colony. Bacterial inoculum was done by picking the single colony into 3 ml LB broth and incubated overnight at 37 °C in the incubator shaker (200 rpm). After that, one percent of *E. coli* DH5 α was inoculated into new LB broth for 50 ml. The culture was incubated at 37 °C with shaking at 80 rpm all along the incubation. The growth of bacterial culture was determined by spectrophotometer at absorbance 620 nm. To maintain as stock culture, equal volume of 80% glycerol was added into *E. coli* DH5 α culture and stored at -80 °C.

3.9 Lipid analysis

3.9.1 Observation of lipid accumulation under fluorescent microscope

3.9.1.1 Stress treatment

For lipid accumulation observation under fluorescence microscope, the stock culture of *C. reinhardtii* (137c) (obtained from step 3.8.1) was cultured until the growth reached to the exponential phase ($OD_{730} = 0.5$). Three milliliters of cell culture were harvested by centrifugation at 12,000 rpm at 4 °C for 10 minutes. The cell pellet was washed twice with fresh TAP medium before transferring into the new media which contained salt at appropriate concentrations of NaCl and KCl at 0, 50, 100, 150, 200 and 250 mM and LiCl at 0, 30, 60, 90, 120, and 150 mM in 12-well plate. Sodium acetate at concentration of 0, 50, 100, 150, 200 and 250 mM was served as a positive control to induce lipid accumulation. The stressed cultures were incubated for 0, 3, 5 and 7 days at 26 ± 1 °C under continuous light ($50 \mu\text{mol m}^{-2}\text{s}^{-1}$).

3.9.1.2 Nile red staining

The stressed cells in each condition from step 3.9.1.1 was harvested for 200 μl by centrifugation at 12,000 rpm for 10 minutes. The supernatant was discarded completely. Total cell pellet was stained with Nile red solution (Appendix 5) and 15% DMSO at the ratio of 1:5 (v/v). The mixture was dropped on glass slide and covered with coverslip. The lipid accumulation was observed under fluorescent microscope (model BX51, Olympus, Japan). Images were captured by using the DP Controller microscope software. Relative intensity of accumulated lipid was measured by using ImageJ software (<https://imagej.nih.gov/ij/>) and statistical significance was analyzed by GraphPad Prism® program version 5 (<https://www.graphpad.com/>).

3.9.2 Lipid profiling by FAMES analysis

3.9.2.1 Stress treatment

One percent of stock culture obtained from step 3.8.1 was incubated in 1 L flask and measured the growth by spectrophotometer at absorbance 730 nm until reach to the exponential phase ($OD_{730} = 0.5$). Cells were harvested by centrifugation at 8,000 rpm at 4°C for 20 minutes. Cell pellet was transferred into new media that contained salt at concentration: NaCl and KCl at 200 mM and LiCl at 120 mM in 250 ml flask. The stressed cultures were incubated under continuous light ($50 \mu\text{mol m}^{-2}\text{s}^{-1}$) at 26 ± 1 °C for 0, 3, 5 and 7 days, respectively.

3.9.2.2 FAMES analysis

To perform FAMES analysis, the stressed cells were harvested to get approximately 1000 mg fresh weight by centrifugation at 8,000 rpm at 4 °C for 20 minutes. Cells were dehydrated by using freeze dryer (FlexiDry MP, Kinetics, USA). The intracellular fatty acids were extracted from cells powder by methanol-hydrochloric acid (95:5 V/V). Then, mixed well and incubated at 85 °C for 90 min. One milliliter of distilled water was added into the mixture. For FAMES extraction, hexane containing 0.01% butylated hydrotoluene was used and conducted at room temperature. The extracts were centrifuged and separated the organic and aqueous phase. For remaining water absorption, sodium sulfate was added to aqueous phase and mixed well. Next, FAMES were evaporated and dry residues were redissolved in hexane. The extracts were injected to HP-INNOWax column (ID 0.25 μM) and analyzed by gas chromatography (Model Agilent 6890N, Agilent, USA) equipped with flame ionization detector (FID). The temperature of injection and detection were maintained at 250 °C. Helium gas was used as mobile phase. Fatty acid contents in extract were calculated by comparing with authentic compounds.

3.10 Genes expression analysis

3.10.1 Culture condition and stress treatment

C. reinhardtii (137c) was inoculated into TAP medium for 1% and incubated at the same condition as step 3.8.1. The cultures were incubated until the OD₇₃₀ reach to 0.5. Cells were harvested by centrifugation at 8,000 rpm at 4 °C for 20 minutes. Cell pellets were transferred to new TAP media contained 200 mM NaCl. The stressed cultures were incubated for 0, 6 and 12 hours at 26 ± 1 °C under continuous light (50 μmol m⁻²s⁻¹). The cultures were then harvested by centrifugation at 8,000 rpm at 4 °C for 20 minutes. The pellets were washed twice by fresh TAP medium and aliquoted into 1.5 ml microcentrifuge tube. Cell wet weights were measured by precision balance (Model ME3002, Mettler Toledo, USA) to gain 30 - 50 mg wet weight. The cell pellets were kept in -80 °C prior RNA extraction.

3.10.2 Total RNA extraction and complementary DNA conversion

Total RNA was extracted by using TRIzol[®] reagent (Invitrogen, USA) according to the manufacturer's protocol. Briefly, one milliliter of TRIzol[®] reagent was added to the cell pellet. The mixture was mixed by pipetting and incubated on ice for 5 minutes. Secondly, chloroform was added 200 μl into the mixture and inverted the tube for 20 seconds. The mixture was incubated on ice for 2 minutes and was then centrifuged at 12,000 rpm for 15 minutes at 4 °C. Next, the aqueous phase was carefully transferred (approximately 50% of the total volume) into a new tube. To isolate RNA, five hundred microliters of 100% isopropanol was added to the aqueous phase and mixed by inverting the tube for 20 seconds. The mixture was incubated on ice for 10 minutes. Then, precipitation of the RNA was performed by centrifugation at 12,000 rpm for 10 minutes at 4 °C. After that, discarded all supernatant and washed the RNA pellet with 1 ml of 70% ethanol by gently pipetting and then centrifuged at 7,500 rpm for 5 minutes at 4 °C. Ethanol was removed and dried the RNA pellet for 10 minutes. The pellet was dissolved by adding 35 μl of DEPC-treated water and incubate at 60 °C for

10 minutes. The quantity and quality of the extracted RNA were measured by using Nanodrop 200 UV-Vis Spectrophotometer and agarose gel electrophoresis, respectively.

Total RNA was converted to cDNA by using SuperScript® III First-Strand Synthesis system (Invitrogen, USA). Following to the manufacturer's instruction. Three micrograms of total RNA were added to the cDNA conversion reaction which containing 5 μ M oligo[dT]₂₀ and 1 mM dNTP mix. The reaction was incubated at 65 °C for 5 minutes to stretching the RNA strand. The reaction was cooled down by placing on ice at least 1 minute. To convert RNA to cDNA, ten millimolar of MgCl₂, 20 mM DTT, 40 U of RNase OUT™ and 200 U of SuperScript® III RT were added to the reaction. Then, incubated the reaction at 50 °C for 50 minutes following at 85 °C for 5 minutes. The reaction was chilled on ice before adding 2 U of *E. coli* RNase H and incubated at 37 °C for 20 minutes to eliminate the leftover RNA in the reaction. The cDNA was stored at -20 °C for using as a template in reverse transcription-polymerase chain reaction (RT-PCR) step.

3.10.3 Semiquantitative RT-PCR

The cDNA products obtained from the previous step were used as templates in RT-PCR with specific primer pairs (Table 3 and Appendix 6). *18s rRNA* gene was used as an internal control. The PCR products were analyzed by 1.2% (w/v) agarose gel electrophoresis (Appendix 7) and were imaged by using Gel Doc EZ™ (Bio-Rad Laboratories, USA). The relative intensity was quantitated by Image Lab™ software (<http://www.bio-rad.com/en-th/product/image-lab-software?ID=KRE6P5E8Z>) and the statistic differential (two-way ANOVA) was analyzed by using GraphPad Prism® program version 5.

3.11 Construction of expression plasmid harboring *ChMAT*

3.11.1 *ChMAT* gene amplification and purification

The cDNA obtained from step 3.10.2 was used as a template for gene amplification. All primers were designed by using OligoAnalyzer program (<https://sg.idtdna.com/calc/analyzer>). Briefly, whole *ChMAT* gene sequence was acquired from KEGG (Appendix 6). The restriction site, *Nde*I (5'-CATATG-3'), was introduced to the gene at the up-stream (forward primer). Another restriction site, *Bam*HI (5'-GGATCC-3'), was introduced to the down-stream of the gene and used as reverse primer. To amplify the gene, KOD-Plus-Neo (Toyobo, Japan) was used as DNA polymerase and touch down PCR technique was used in this study. The melting temperature was started at 60 °C and then decreased for 0.3 °C per cycle. The PCR was performed for 50 cycles.

The PCR product was analyzed by gel electrophoresis. The bands of the product were imaged by using Gel Doc EZ™. The agarose gel was digested and purified by using GenepHlow™ Gel/PCR Kit (Geneaid, Taiwan). After purification, the PCR product was measured for the concentration and analyzed by gel electrophoresis.

3.11.2 Construction of *ChMAT* into pBSK⁺II vector

3.11.2.1 Construction of *ChMAT*/pBSK⁺II plasmid and transformation

Cloning vector, pBSK⁺II (Toyobo, Japan) (Appendix 8), was digested with *Eco*RV to make blunt end site. Then, the plasmid was purified by using GenepHlow™ Gel/PCR Kit and was measured for the concentration by using Nanodrop 200 UV-Vis Spectrophotometer. To construct the *ChMAT*/pBSK⁺II vector, the pBSK⁺II was melted at 37 °C for 15 minutes before ligation step. One hundred nanograms of purified PCR product (from step 3.11.1) were put into the reaction that contained 50 ng of the plasmid. The reaction was incubated at 65 °C for 3 minutes before adding T4 DNA

ligase (Takara, Japan). The reaction was then incubated overnight at 16 °C. After that, the ligation product was transformed into the competent *E. coli* DH5 α prepared by CaCl₂ method.

Five microliters of the ligation product were put into 100 microliters of competent cells. The mixture was put on ice for 30 minutes before incubation at 42 °C for 90 seconds. The mixture was immediately transferred into the ice bath and keep on ice for 5 minutes. The cells were recovered by adding 900 milliliters of fresh LB broth and incubated at 37 °C with shaking for 1 hour. After incubation, the cells were spread on 1.5% (w/v) LB (supplemented with 50 μ g/ml ampicillin, 0.1 mM IPTG, and 2 mg/ml X-gal). The empty vector pBSK⁺II was also transformed into the *E. coli* DH5 α for serving as control empty vector. The plates of the transformants were incubated at 37 °C for approximately 16 hours. The white single colonies were picked and streaked on new LB agar plate. The existing of the gene was confirmed by colony PCR. The clones which gave positive result on colony PCR were selected for the next experiment.

3.11.2.2 *ChMAT*/pBSK⁺II plasmid extraction

The transformants from step 3.11.2.1 were cultured in LB broth (supplemented with 50 μ g/ml ampicillin) for 3 ml. The cultures were incubated at 37 °C overnight (approximately 16 hours) with shaking at 200 rpm. The plasmid was extracted by using HiYieldTM Plasmid Mini Kit (RBC Bioscience, Taiwan). The procedure was modified from the manufacturer's instruction. The transformant cultures were harvested by centrifugation at 12,000 rpm for 5 minutes at 4 °C. The supernatant was discarded from the cultures and then PD1 was added for 100 μ l and mixed by vortex. Lysis buffer (PD2) was added for 100 μ l into the mixture and the tube was inverted for 10 times. PD3 which is the neutralizing solution was then added for 150 μ l and immediately mixed by inverting the tube. The mixture was centrifuged at 12,000 rpm for 10 minutes and then the supernatant was transferred into the new microcentrifuge tube. To precipitate plasmid, absolute ethanol was added for 3 volumes of the solution and centrifuged at 12,000 rpm for 10 minutes. The pellet was washed with

70% ethanol for 2 times thereafter. After washing, the pellet was dried for 10 minutes and then resuspended with Tris-EDTA buffer (TE).

The purified plasmid was analyzed for quality and quantity by gel electrophoresis and using Nanodrop 200 UV-Vis Spectrophotometer, respectively. The restriction enzyme analysis was also determined by using *NdeI* and *BamHI*. Furthermore, the accuracy of *ChMAT* sequence was confirmed by sequencing analysis (Macrogen, Korea).

3.11.3 Construction of *ChMAT* into pSyn_6 expression vector

To generate the *ChMAT*/pSyn_6 vector, the plasmid of *ChMAT*/pBSK⁺II (from step 3.11.2.2) and pSyn_6 vector (Appendix 9) were first digested with restriction enzymes; *NdeI* and *BamHI*. The initial plasmid in the reaction was 4,000 ng. The reaction was incubated overnight at 37 °C. Gel purification was performed to purify both *ChMAT* gene and pSyn_6 vector. The purified gene and plasmid were then ligated using T4 DNA ligase as similar as step 3.11.2.1. The ligation product was propagated by transforming into *E. coli* DH5 α . The transformant was spread on 1.5% (w/v) LB agar (supplemented with 100 μ g/ml spectinomycin). After incubation at 37 °C, individual colony was analyzed for the presence of target gene by colony PCR. The positive colonies were picked up and cultured in LB broth that contained 100 μ g/ml spectinomycin, and then the plasmid was extracted as same as step 3.11.2.2.

3.11.4 Transformation of *ChMAT*/pSyn_6 into *S. elongatus* PCC 7942

S. elongatus PCC 7942 was phototrophically cultured in BG11 medium at 26 \pm 1 °C under continuous light (50 μ mol m⁻²s⁻¹) until the absorbance at 730 nm reached to 1.0. The cells were harvested for 10 ml by centrifugation at 12,000 rpm for 5 minutes at 4 °C. The cell pellet was washed with fresh medium for 3 times and resuspended in BG11 for 1 ml. The cells were aliquoted for 100 μ l per tube before adding 100 ng of *ChMAT*/pSyn_6. Sterile distilled water was put into the prepared cells to serve as negative control (mock). Empty vector, pSyn_6, was used as positive control. The

mixtures were incubated at 34 °C in the dark for 4 hours. After incubation, the tubes must be cleaned with 70% ethanol. Fresh BG11 was added into the transformants to gain 500 µl of cultures, the transformants were then over-layered on 1.5% (w/v) BG11 agar plate (supplemented with 10 µg/ml spectinomycin). The plates were incubated at 26 ± 1 °C under continuous light (50 µmol m⁻²s⁻¹) until the colonies appeared on the plates (approximately 2 weeks). The colonies were randomly selected for colony PCR analysis. Three positive colonies were inoculated into 20 ml of BG11 medium containing spectinomycin at the same concentration as aforementioned, and the cultures were incubated under continuous light at 26 ± 1 °C with shaking at 110 rpm. The transformant cultures were used as stock for the next experiments.

3.12 Construction of expression plasmid harboring *SynMAT*

3.12.1 *S. elongatus* PCC 7942 genomic extraction

The stock culture of *S. elongatus* PCC 7942 from section 3.8.2 was inoculated for 5% (v/v) into BG11 medium. The cultures were incubated at the same condition as 3.8.2 until the growth reached to the exponential growth phase (OD₇₃₀ = 1.0). Cells were harvested for 10 ml by centrifugation at 12,000 rpm for 5 minutes at 4 °C. To extract genomic DNA of cyanobacterium, DNeasy[®] Plant Mini Kit (Qiagen, Germany) was used in this study. According to the manufacturer's protocol, four hundred microliters of AP1 was added into the cell pellet and mixed by vortex. The mixture was incubated at 65 °C for 10 minutes to lysis the cells. After that, AP2 solution was added into the mixture and incubated on ice for 5 minutes. The cells were precipitated by centrifugation at 12,000 rpm for 7 minutes. The supernatant was transferred to QIAshredder spin column and centrifuged at 12,000 rpm for 5 minutes to clear the cells completely. The flow-through which was left at the collection tube was transferred to the new microcentrifuge tube. Then, AP3/E was added for 1.5 volume of the solution and mixed by pipetting. The solution was transferred to the new DNeasy[®] mini spin column and centrifuged at 7,000 rpm for 1 minute. The flow-through was discarded and the column was transferred to the new microcentrifuge tube. The column was washed twice with AW. After discarded all the AW by centrifugation at

7,000 rpm for 1 minute, AE buffer was added for 35 μ l and centrifuged to elute the DNA from the column. The extracted gDNA was analyzed by gel electrophoresis and the concentration of gDNA was measured by using Nanodrop 200 UV-Vis Spectrophotometer.

3.12.2 *SynMAT* gene amplification

Similar as *ChMAT* amplification, *SynMAT* was amplified by using KOD-Plus-Neo. However, to amplify *SynMAT* gene, the gDNA from step 3.12.1 was used as template. Followed by the instruction from the manufacturer, the temperature of denature and elongation were set at 94 °C for 15 seconds and 68 °C for 1 minute, respectively. The melting temperature for annealing step was set at 68 °C due to the GC richness of the primers. The PCR product was analyzed by gel electrophoresis and purified by using GenepHlow™ Gel/PCR Kit. The purified product was electrophorized on 1.2% (w/v) agarose gel and measured for the concentration by using spectrophotometer. The product was next ligated into cloning vector pBSK⁺II.

3.12.3 Construction of *SynMAT* into pBSK⁺II vector

The blunt ended PCR products were ligated into cloning vector, pBSK⁺II, by using T4 DNA ligase as same procedures as mentioned in section 3.11.2. The *SynMAT*/pBSK⁺II was transformed into the competent *E. coli* DH5 α cells. To select the transformant cells, *E. coli* DH5 α was cultured on 1.5% (w/v) LB agar plates (supplemented with 50 μ g/ml ampicillin, 2 mg/ml X-gal, and 0.1 mM IPTG). The agar plates were incubated at 37 °C for approximately 16 hours. The white colonies were then picked and streaked on new agar plate and incubated overnight. Colony PCR was performed to confirm the existence of the gene.

3.12.3 Construction of *SynMAT* into pSyn_6 vector

The transformants that gave positive result on colony PCR were cultured in LB broth (supplemented with 100 μ g/ml spectinomycin) for 3 ml in incubator shaker (200 rpm) at 37 °C for 16 hours. The vector of *SynMAT*/pSyn_6 was extracted by using

HiYield™ Plasmid Mini Kit following the manufacturer's protocol (as described in section 3.11.2.2). The plasmid was double digested with *Nde*I and *Bam*HI. The gene was purified by using GenepHlow™ Gel/PCR Kit. After that, *SynMAT* was ligated into the expressing vector and propagated with the same protocol as step 3.11.3.

3.12.4 Transformation of *SynMAT/pSyn_6* into *S. elongatus* PCC 7942

SynMAT/pSyn_6 was first extracted and purified before transformation. The fresh cyanobacterium, *S. elongatus* PCC 7942, was cultured until the optical density of 730 nm over than 1.0. The plasmid was transformed into the cyanobacterium with the same method as described in section 3.11.4. The transformants was also confirmed by colony PCR and nucleotide sequencing analysis (Eurofins Genomics, Japan). Three independent clones of *SynMAT/7942* were inoculated into 20 ml of BG11 medium (supplemented with 10 µg/ml spectinomycin) and the cultures were incubated under continuous light at 26 ± 1 °C with shaking at 110 rpm. The transformant cultures were used as stock for the next experiments.

3.13 Analysis of expressing cells harboring *ChMAT* and *SynMAT*

3.13.1 Transformants cultivation

Three independent clones of the transformants for *ChMAT/7942* and *SynMAT/7942* were cultured in BG11 (supplemented with 10 µg/ml spectinomycin) in 250 ml flask. The wild type (WT) and empty vector *pSyn_6/7942* were cultured as control. The cultures were incubated at 26 ± 1 °C with shaking at 110 rpm under continuous light ($50 \mu\text{mol m}^{-2}\text{s}^{-1}$). The growth of the cells was determined by spectrophotometer at the absorbance of 730 nm.

3.13.2 Phenotypic observation

The transformant cells were analyzed for morphology under light microscope. Ten microliters of cells (WT, empty vector, *ChMAT/7942*, and *SynMAT/7942*) were

dropped on glass slide and covered with coverslip. Images were captured by using the DP Controller microscope software.

3.13.3 Semiquantitative RT-PCR

3.13.3.1 Cultivation condition

Cell cultures obtained from step 3.13.1 was incubated in 250 ml flasks. The cells were harvested at 2 phases, first was at exponential phase ($OD_{730} \sim 0.8-1.0$) and second was early stationary phase ($OD_{730} \sim 1.8-2.0$). In addition, to study the effect of salt (NaCl) on the expression of the genes, the WT, empty vector and transformants cells (*SynMAT/7942*) were cultured until the OD_{730} reached to 0.8. The cells were harvested by centrifugation at 8,000 rpm for 20 minutes at 4 °C. The cell pellet was subjected into the new media that contained 300 mM NaCl. The cultures were incubated for 0, 6, and 12 hours and harvested by centrifugation. The cells were stored in -80 °C until RNA extraction.

3.13.3.2 Gene expression analysis

To analyze the expression level of the *ChMAT* or *SynMAT* gene in the expressing cells, semiquantitative RT-PCR was performed in this study. Moreover, the expression level of the gene encoding long-chain acyl-CoA synthetase (*LACS*) (Appendix 6) which involved in lipid degradation in *S. elongatus* PCC 7942 was investigated. To analyze the gene expression, total RNA of the transformants was firstly extracted from 30-50 mg fresh cells weight by TRIzol[®] reagent and was converted into cDNA as the same procedures as described in section 3.10.2. The cDNA was used as template for PCR with specific primer pairs (Table 3). The *mpB* gene was used as an internal control. The PCR products were analyzed by 1.2% (w/v) agarose gel electrophoresis and were imaged by using Gel Doc EZ[™]. The relative intensity was quantitated by Image Lab[™] software and the statistic differential (two-way ANOVA) was analyzed by using GraphPad Prism[®] program version 5.

3.13.4 Protein expression analysis

3.13.4.1 Crude protein preparation

S. elongatus PCC 7942 (WT) and transformants of empty vector/7942, *ChMAT*/7942 and *SynMAT*/7942 were cultured for 2 weeks ($OD_{730} \sim 0.8-1.0$) and 4 weeks ($OD_{730} \sim 1.8-2.0$). For stress experiment, the cells were treated with 300 mM NaCl for 0, 24, and 48 hours. After incubation, cells of each transformant were harvested for 10 ml by centrifugation at 12,000 rpm for 5 minutes at 4 °C. The cell pellet was washed twice with Tris-Cl pH 8.2 and resuspended with the same solution for 300 μ l. Cells were lysed by using sonicator (Vibra-Cell™ Ultrasonic Liquid Processors VCX 130, Sonics, USA). The amplitude was set at 70% and the pulse interval was 30 /10 (seconds) for 2 minutes per sample. Since the sonication would generate heat, thus; the tube must be put on ice all the time. The lysed cells were separated from the supernatant by centrifugation at 12,000 rpm at 4 °C for 10 minutes. The supernatant was transferred into the new microcentrifuge tube. The extracted crude protein was analyzed for total protein quantity following the standard Bradford protein assay protocol (Bio-Rad Laboratories, USA). Bovine serum albumin (BSA) was used as standard protein (Appendix 10). The total protein concentration was calculated by comparing to the standard protein curve. Next, the protein was analyzed by SDS-PAGE and western blot analyses.

3.13.4.2 SDS-PAGE analysis

The extracted crude protein from step 3.13.4.1 was performed for SDS-PAGE by standard protocol (Laemmli, 1970). Briefly, twenty micrograms total protein of the transformants was loaded to 10% (v/v) acrylamide gel (1.5 mm thickness). The SDS-PAGE was electrophorized for 1.30 hours at 75 volts. To stain the gel, Coomassie brilliant blue (CBB) staining (Appendix 11) was used. The gel was shaken for 20 minutes before detained overnight with destain solution (methanol and acetic acid). The destain solution was removed and the gel was rinsed with distilled water for several

times. For western blot analysis, the acrylamide gel was not stained with CBB, but was washed with distilled water for several times to discard the SDS-running buffer.

3.13.4.3 Western blot analysis

The ChMAT or SynMAT protein expression was observed by western blot analysis according to the standard protocol (Timmons and Dunbar, 1990). Polyvinylidene difluoride (PVDF) membrane was pretreated with 90% (v/v) methanol for 10 seconds followed by soaking in western blotting buffer (Glycine, Tris base, and methanol) before used. The protein was blotted by using semi-dry transfer cell (Model Trans-Blot[®] SD Cell, Bio-Rad Laboratories, USA). The ampere was fixed at 0.12 A and the blotting was run for 50 minutes. After finishing, the PVDF membrane was blocked with 5% (w/v) skim milk (Appendix 12) for 1 hour. The blocking solution was discarded before the primary antibody which is an antibody raised against 6x His-tag (R&D system, USA) was added into the blotting chamber. The membrane was incubated with primary antibody overnight. After that, the membrane was washed thrice with 5% (w/v) skim milk for 20, 10, and 10 minutes, respectively. To wash the membrane completely, 1x PBS buffer was added into the chamber and was discarded for three rounds as same as the first wash. The anti-mouse IgG-HRP conjugated (New England Biolab, USA) which was used as secondary antibody was added afterward. The membrane was incubated with secondary antibody for 2 hours and then was washed with 5% (w/v) skim milk and 1x PBS buffer as the same procedure as aforementioned. Color development was performed by using Horseradish Peroxidase Conjugate Substrate kit (Bio-Rad Laboratories, USA) according to the manufacturer's protocol. The specific protein bands were quantitated with ImageJ software.

3.13.5 FAMEs analysis

Cells obtained from step 3.13.1 were inoculated into new media and were cultured for 4 weeks. Moreover, cells at exponential growth phase ($OD_{730} = 0.8$) were subjected into new media containing 300 mM NaCl and incubated for 0, 48, and 72 hours. After that, cells of each condition were harvested by centrifugation at 8,000 rpm

at 4°C for 20 min to get approximately 300 mg of fresh weight. The cell pellet was extracted for lipid and analyzed as the same protocol as mentioned in section 3.9.2.2.



CHAPTER IV

RESULTS AND DISCUSSION

4.1 Bioinformatics analysis

As one of the most important macromolecules in all living organisms, lipid biosynthesis has been extensively studied. In photosynthetic organisms (e.g. microalgae), the *de novo* pathway comprises of two main steps; (1) FA biosynthesis takes place in chloroplast and (2) TAG biosynthesis takes place in cytosol (Mühlroth *et al.*, 2013; Bellou *et al.*, 2014; De Bhowmick *et al.*, 2015). As mentioned in section 2.3, TAG can be generated via three biosynthetic pathways. Kennedy pathway is recognized to be the common pathway observing in algae and plants (Moellering *et al.*, 2009). In this study, genes involved in both biosynthetic pathway of green microalga *C. reinhardtii* were searched via KEGG database. There are five genes responsible for FA synthesis i.e. *PDH2*, *ACCase*, *MAT*, *KAS2*, and *FAT1* and two key genes in Kennedy pathway i.e. *GPD1* and *DGAT2* (or *DGTTs*).

Seven genes focusing in this study were predicted for the localization in different compartments; therefore, topological modelling was also performed. As shown in Figure 4, most of the proteins are predicted to be non-membrane proteins except for DGTTs including DGTT1 to DGTT4. For DGTT1, DGTT2, and DGTT4, they have only two segments of transmembranes (TMs) while DGTT3 compresses of three segments of TMs.

Protein	Topology	Protein	Topology
PDH		GPD1	
ACCCase		DGTT1	
MAT		DGTT2	
KAS2		DGTT3	
FAT1		DGTT4	

Figure 4 Topological analysis of protein associated with lipid biosynthesis in *C. reinhardtii*. Amino acid sequence of each protein was retrieved from KEGG database. Topology was analyzed by PROTTOR software. PDH; pyruvate dehydrogenase, ACCCase; acetyl-CoA carboxylase, MAT; malonyl-CoA:ACP tranacylase, KAS2; 3-ketoacyl-ACP-synthase, FAT1; fatty acyl-ACP thioesterase A, GPD1; glycerol-3-phosphate dehydrogenase, DGTT1 to DGTT4; type 2 diacylglycerol acyltransferase. The orange bar represents plasma membrane (PM).

From our previous study, we found that *MAT* gene was highly up-regulated under NaCl stress (Atikij, 2015). In addition, due to *MAT* is not a complex enzyme, thus allowing the expression and functional characterization of *MAT* is of interest for us to investigate in detail. In this study, *MAT* gene from *C. reinhardtii* (137c) was therefore selected to overexpress in a freshwater cyanobacterium *S. elongatus* PCC 7942. Furthermore, *MAT* gene also present in this cyanobacterium; so that, the overexpression of putative *MAT* of *S. elongatus* PCC 7942 was parallelly studied. Protein sequences of ChMAT and SynMAT were retrieved from KEGG database. The sequences were analyzed for protein domain by SMART software and interaction between other proteins by STRING software. The results showed that both ChMAT and SynMAT were classified as acyltransferase family (Figure 5, 6). The position of amino acid residue from 29 to 111 of ChMAT was predicted to be the domain position (Figure 5A). The protein-protein interaction analysis revealed that there were 10 candidate proteins that highly associated with ChMAT (EDP09600). The most related proteins were the proteins in FAS complex including KAS2, KAS1, the predicted protein of ACP-synthase (EDO96631), and 3-ketoacyl-CoA-synthase (EDP05644) which were scored in all cases 0.992 (Figure 5B). For SynMAT, the domain of this protein was located at position 5 to 289 of amino acid residues (Figure 6A). Protein-protein interaction revealed that 10 candidate proteins were predicted to be associated with SynMAT (Figure 6B). Based on the analytic score, KAS2 (Synpcc7942_0537) (scored of 0.999) was the most interacted protein to SynMAT followed by KAS3 (or fabH) (scored of 0.998).

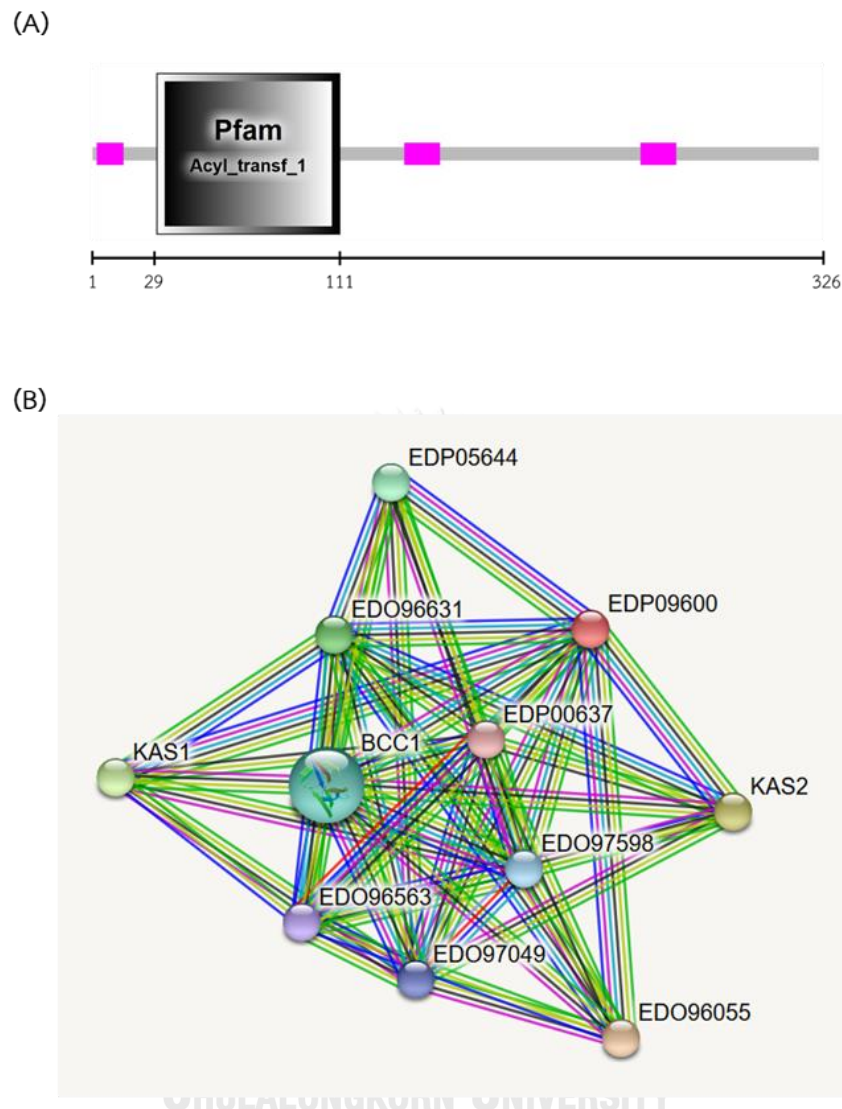


Figure 5 Protein domain and protein interaction analyses. The amino acid sequences of ChMAT (XP_001689862) was analyzed for protein domain by using SMART program. The numbers indicate amino acid residues (A). The gradient box indicated the family of the protein domain and the pink boxes implied for the low complexity sequences. The protein-protein interaction was performed by using STRING program (B). The red node (EDP09600) was ChMAT protein. The green nodes were indicated of related proteins including KAS2, KAS1, the predicted protein of ACP-synthase (EDO96631), and 3-ketoacyl-CoA-synthase (EDP05644) were scored of 0.992 by STRING.

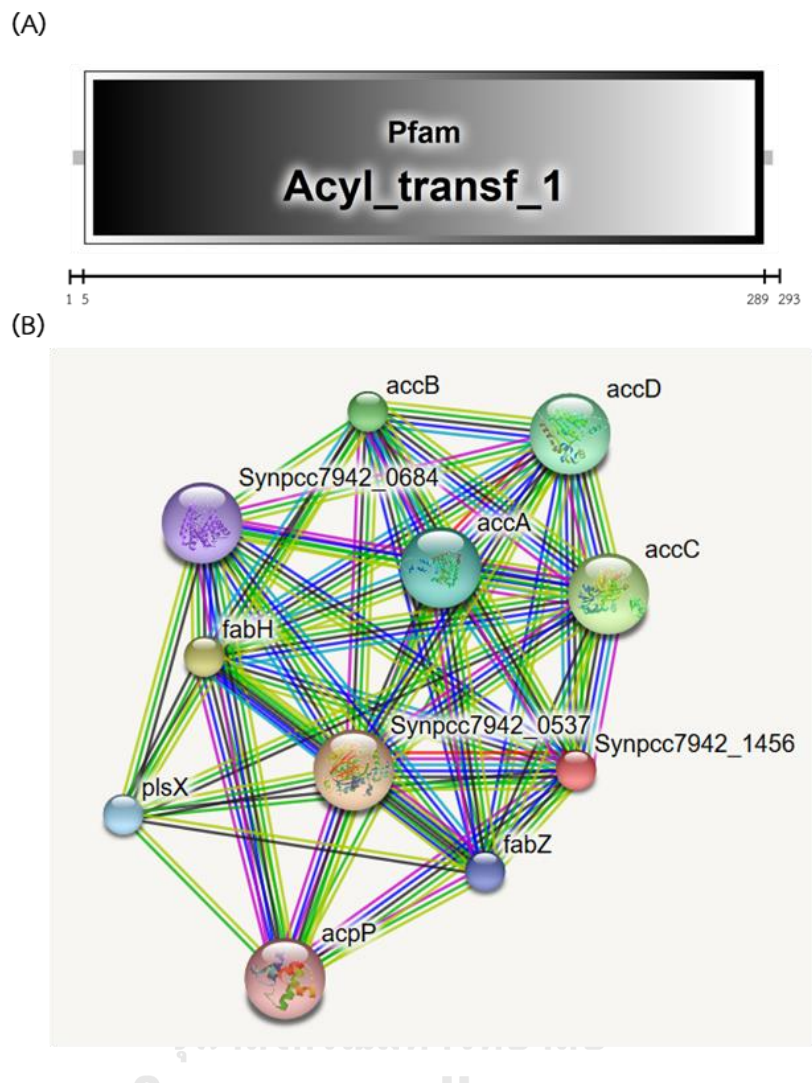
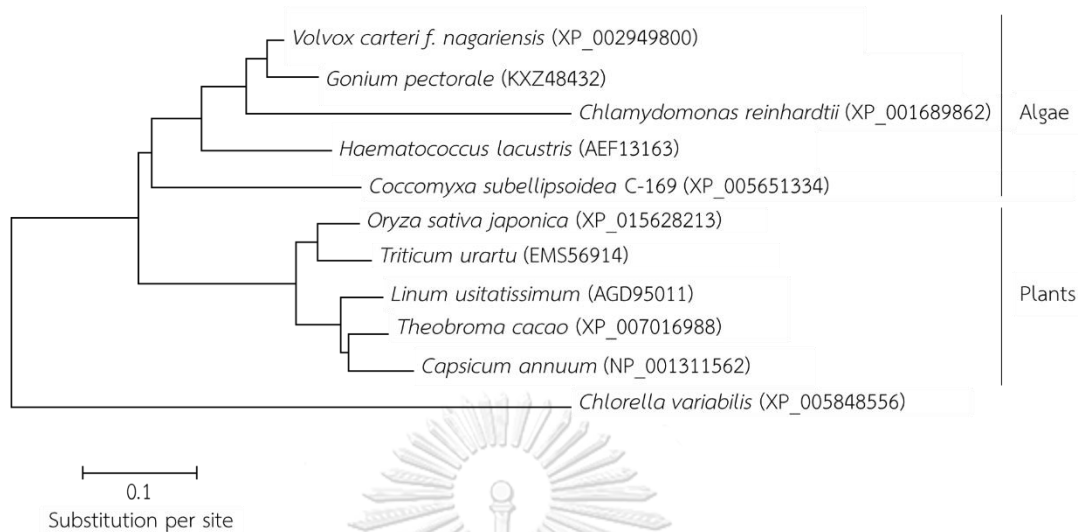


Figure 6 Protein domain and protein interaction analyses. The amino acid sequences of SynMAT (ABB57486) was analyzed for protein domain by using SMART program. The numbers indicate amino acid residues (A). The gradient box indicated the family of the protein domain. The protein-protein interaction was performed by using STRING program (B). The red node (Synpcc7942_1456) was MAT protein. The large yellow node (Synpcc7942_0537) was indicate the most related protein at scored of 0.999 and the olive-green node (*fabH*) was scored at 0.998 by STIRNG.

Phylogenetic tree was analyzed (Figure 7A). Ten candidate orthologs for MAT were selected for alignment compared with ChMAT. Algorithm clearly divided into two groups between microalgae and plants. ChMAT was closely related to *Volvox carteri f. nagarensis* and *Gonium pectorale* which are the colonial microalgae. Both of them were classified in the same order of *Chlamydomonas*, Chlamydomonadales. It should be noted that the unicellular green microalga *C. variabilis* was far separated branch. This alga was classified in the order Chlorellales. Because of the closed relation of microalgae and plants, ChMAT was found to be closely related to the higher plants, i.e. *Oryza sativa japonica*, *Linum usitatissimum*, *Theobroma cacao*, *Triticum urartu*, and *Capsicum annum*.

For the analysis of SynMAT, 10 orthologs including cyanobacteria and bacteria were used. The phylogenetic tree can be grouped distinctly into 2 groups; the unicellular and filamentous cyanobacteria (Figure 7B). The unicellular cyanobacteria including *S. elongatus* PCC 7942, *S. elongatus* PCC 6301 (100% amino acid identity), *Synechocystis* sp. PCC 6803 (62% amino acid identity), and *Halothece* sp. 7418 (58% amino acid identity) were grouped together as a closely related of the sequences. The filamentous cyanobacteria including *Arthrospira platensis*, *Oscillatoria acuminata*, *Nostoc punctiforme*, and *Geitlerinema* sp. PCC 7407 were clustered together. *E. coli* which is a Gram-negative bacterium was chosen to align as outgroup with *S. elongatus* PCC 7942. The tree revealed that even though the amino acid sequences of cyanobacteria have considerably homology to *E. coli* (40% amino acid identity), the branch of *E. coli* was far separated.

(A)



(B)

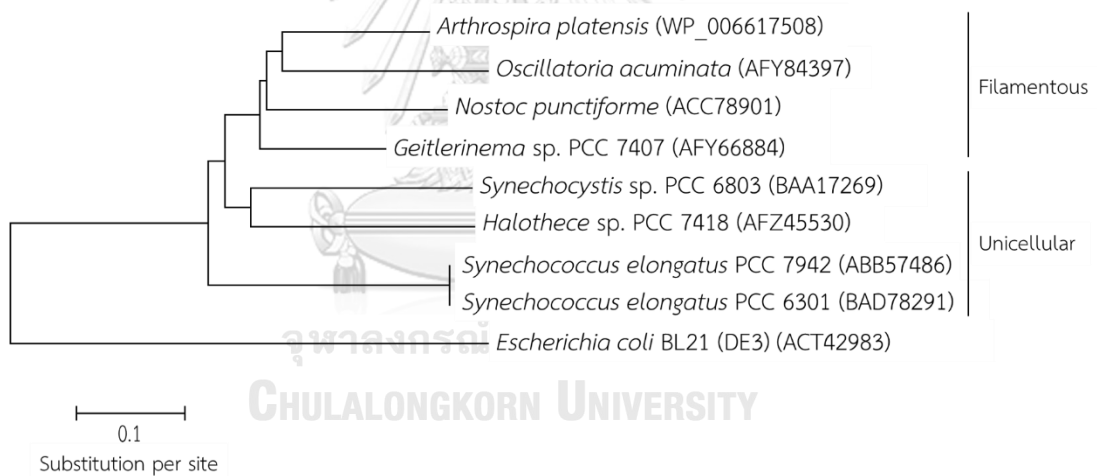


Figure 7 Phylogenetic analysis of ChMAT (A) and SynMAT (B) and ortholog sequences. The MAT amino acid sequences were obtained from KEGG database as described in Materials and Methods. Accession number of each sequence was indicated in blanket. These sequences were compared and aligned by using Molecular Evolutionary Genetics Analysis Version 6.0 (MEGA6) software with Neighbor joining system (bootstrap values from 500 replicates).

4.2 lipid analysis

4.2.1 Observation of lipid accumulation by Nile red staining

4.2.1.1 Effect of NaCl stress

In preliminary study, *C. reinhardtii* (137c) was found to be died during 7 days under salt stress. To study lipid accumulation under salt stress, we therefore investigated the accumulation in appropriate of time. *C. reinhardtii* (137c) cells were treated with various NaCl concentrations (0, 50, 100, 150, 200, and 250 mM) for 0, 3, 5, and 7 days, respectively. The lipid droplets in the cells were observed by Nile red staining and using fluorescent microscope for imaging. Figure 8 demonstrated the changes of cells morphology under light microscope and lipid accumulation. Lipid droplet accumulation was not observed under control condition (day 0). After subjecting the cells to salt stress, the yellow spots which suggested to be lipid bodies were found to be increased with the longer cultivation time. Lipid droplets were firstly observed at a concentration of 250 mM at 3 days of cultivation. At day 5 and 7, the signal of lipid droplets was much higher than control ones. The higher salt concentration induced lipid accumulation. As shown in Figure 8, lipid bodies were found to be increased along with its concentrations. The bright yellow spots were clearly observed under 150 – 250 mM NaCl. The highest lipid accumulation observed by Nile red staining was observed at 250 mM at 7 days. These results suggested that the concentration of 250 mM NaCl was the most effective condition to induce lipid droplet accumulation at day 7.

Cell sizes upon stress condition were found to be slightly larger compared to the control set. Moreover, cells cultured under 250 mM NaCl for 7 days were appeared to be aggregated as palmelloid to deal with the stress environment. This observation appeared to be similar morphological changes as observing in Khona *et al.* (2016).

After measuring the intensity of the images by using ImageJ program, the results revealed that when the microalga was cultured under higher NaCl concentration, the intensities of lipid droplets were increased (Figure 9). At the first 3 days of cultivation using 100 and 200 mM NaCl; however, the relative intensities were reduced compare to the control cells. Yet when the cells were stressed for 5 days, the relative intensities tend to increase significantly at concentration of 150 mM to 250 mM. The highest relative intensity was observed in the cells that were cultured for 7 days under 250 mM NaCl (2.01 ± 0.2 folds).



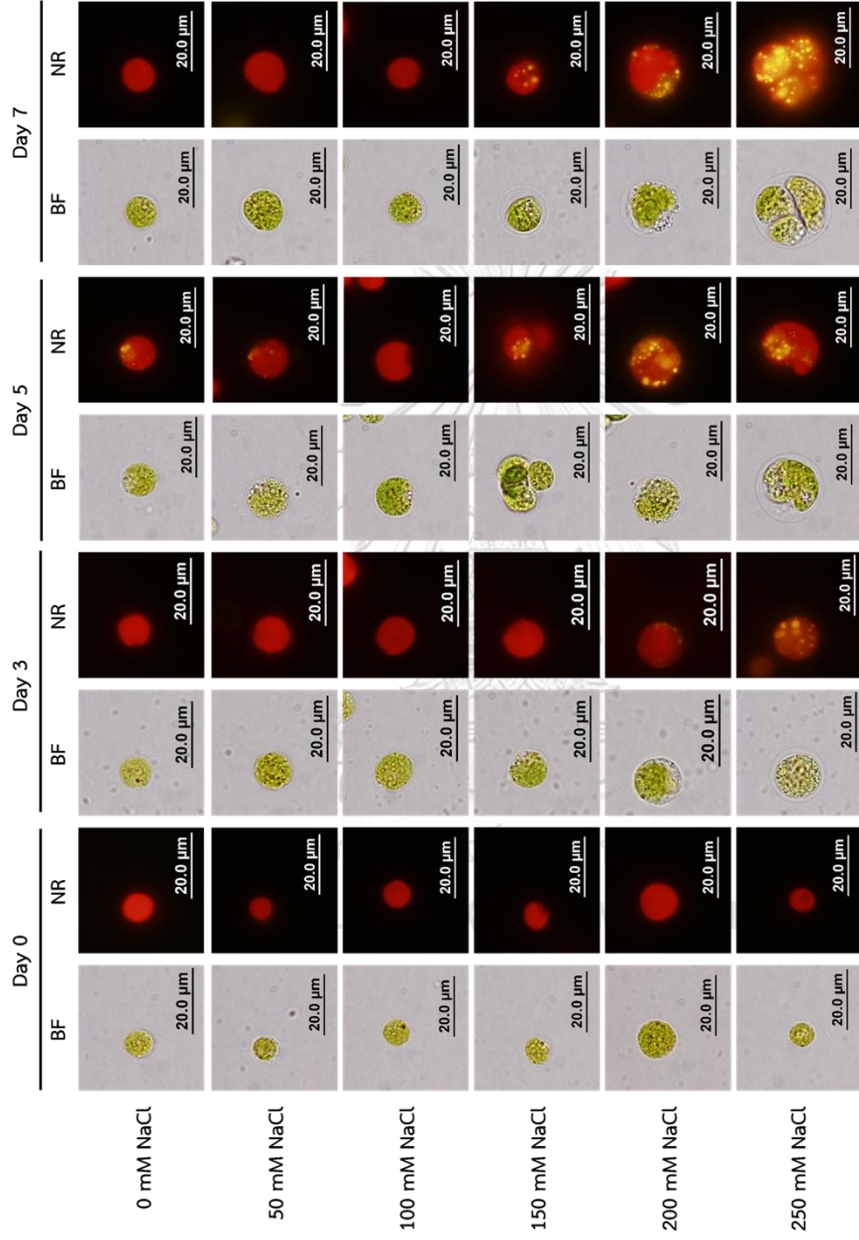


Figure 8 Image of *C. reinhardtii* (137c) cells observed under bright field light microscope (BF) and fluorescent microscope (NR). Cells at exponential growth phase were subjected to salt stress (NaCl) at various concentrations; 0 mM, 50 mM, 100 mM, 150 mM, 200 mM, and 250 mM for 0, 3, 5, and 7 days. Morphology and lipid body were observed by Nile red staining as described in section 3.9.1.2.

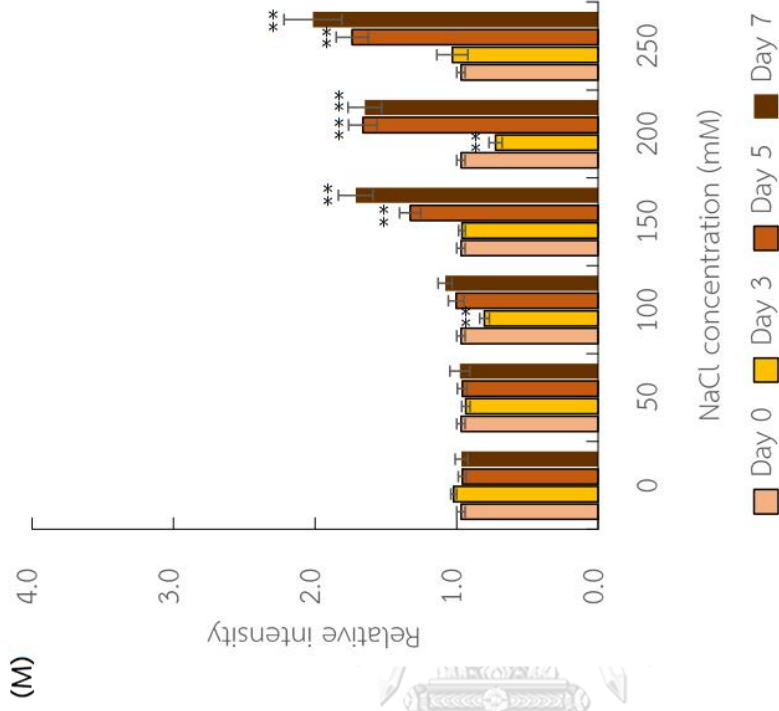
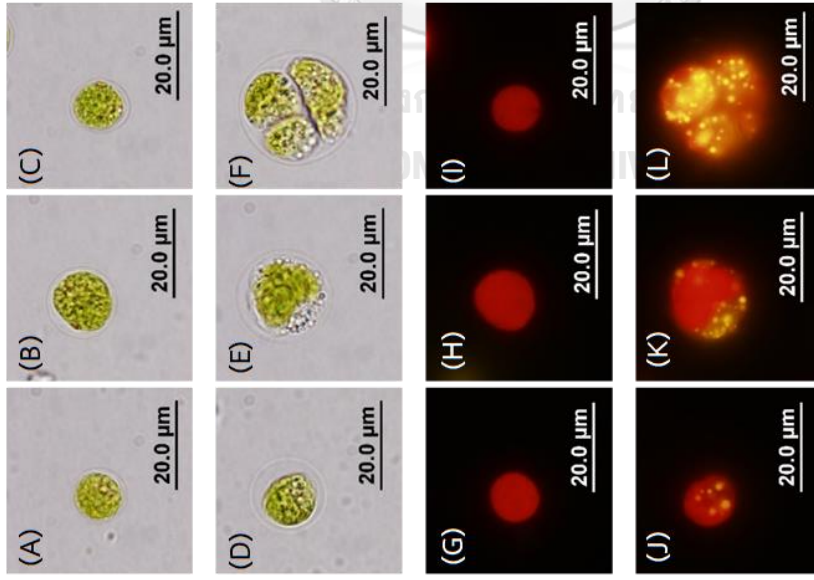


Figure 9 Image of *C. reinhardtii* (137c) cells observed under light microscope (A-F) and fluorescent microscope (G-L). Cells at exponential growth phase were subjected to salt stress (NaCl) at various concentrations; 0 mM (A, G), 50 mM (B, H), 100 mM (C, I), 150 mM (D, J), 200 mM (E, K), and 250 mM (F, L) for 7 days. Morphology and lipid body were observed by Nile red staining as described in section 3.9.1.2. Relative intensity of lipid accumulation in algal cells was analyzed by using ImageJ software (M). Data are mean \pm SE from at least 10 independent cells ($*p < 0.01$, $**p < 0.001$ by unpaired T-test).

4.2.1.1 Effect of KCl stress

The green microalga *C. reinhardtii* (137c) was cultured in TAP medium that contained 0, 50, 100, 150, 200 and 250 mM KCl for 0, 3, 5 and 7 day, respectively. Figure 10 represented the morphology changes and lipid body accumulation. Morphology (in terms of cell size) observed under light microscope remaining unchanged in all tested conditions. However, the cells were not homogenous, observing that the continuous light cultivation affected to the cell division and cell cycle (Jüppner *et al.*, 2017). The palmelloid formation was obviously observed at the first 5 days of cultivation under 200 and 250 mM. This morphological change implicates that the cells adapted themselves to cope with KCl stress. The cells were quantitated for lipid accumulation using the same protocol as described in section 3.9.1.2. The result revealed that KCl induced lipid accumulation in *C. reinhardtii* (137c) as similar trend as observing in NaCl. Quantification of lipid droplets intensity revealed that the lipid accumulations under 50 and 100 mM KCl fluctuated during the cultivation time. Nonetheless, when KCl concentration was over than 150 mM, intensity was statistically increased with the longer cultivation periods. The highest signal was observed at the concentration of 200 mM at 5 days of cultivation which accounted for 2.22 ± 0.11 folds.

Lipid accumulation observed in the cells that were cultured under NaCl and KCl showed non-significant differences statistically. It should be noted that NaCl stress causes a severe effect on cell viability compared to KCl. At day 5 at the concentration of 250 mM, NaCl stress led cell death. On the other hand, under KCl stress, cells were observed to be more aggregation. The palmelloid formation observing here likely reflects to cells adaptation under the harsh environment (Lurling and Beekman, 2006).

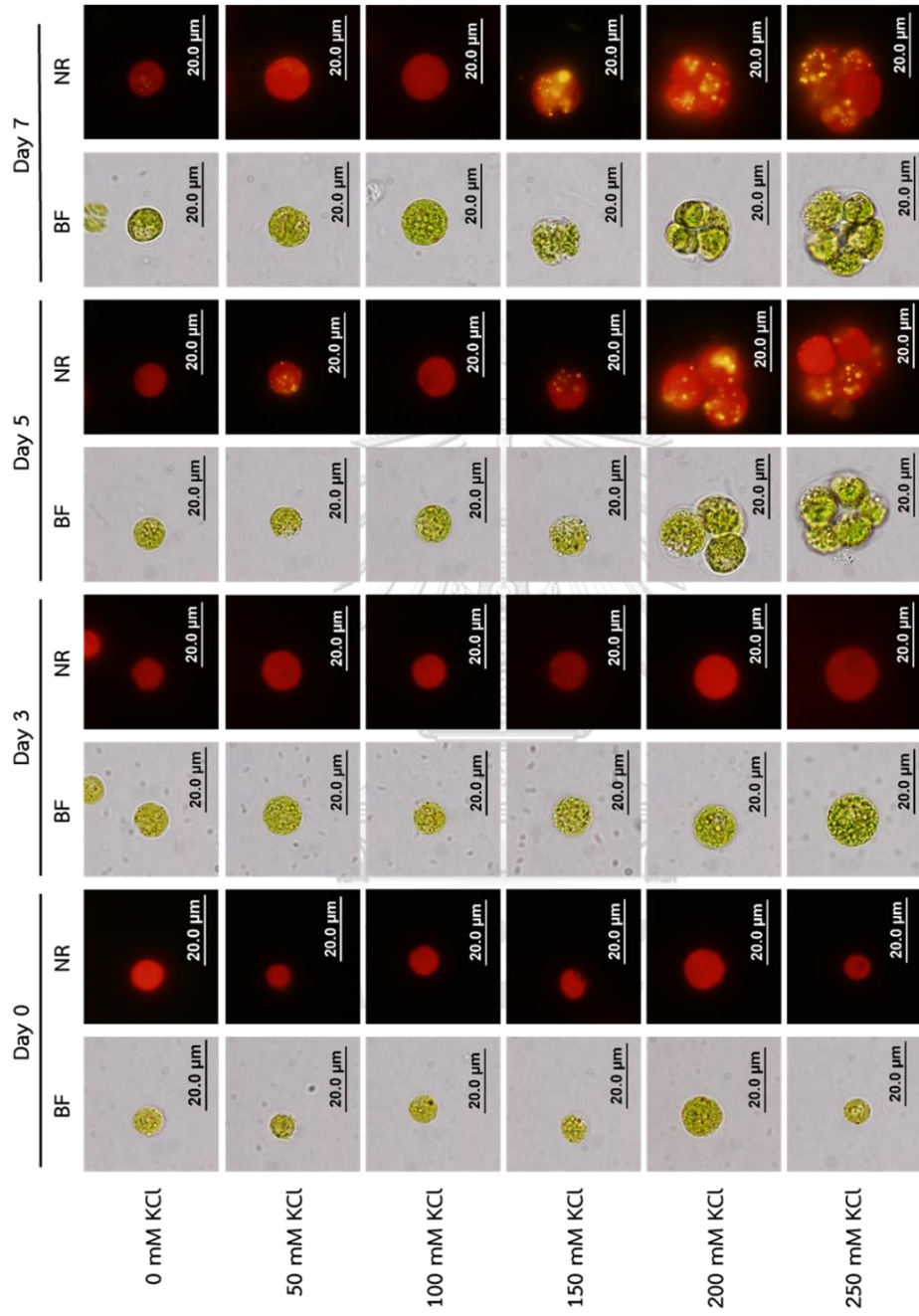


Figure 10 Image of *C. reinhardtii* (137c) cells observed under bright field light microscope (BF) and fluorescent microscope (NR). Cells at exponential growth phase were subjected to salt stress (KCl) at various concentrations; 0 mM, 50 mM, 100 mM, 150 mM, 200 mM, and 250 mM for 0, 3, 5, and 7 days. Morphology and lipid body were observed by Nile red staining as described in section 3.9.1.2.

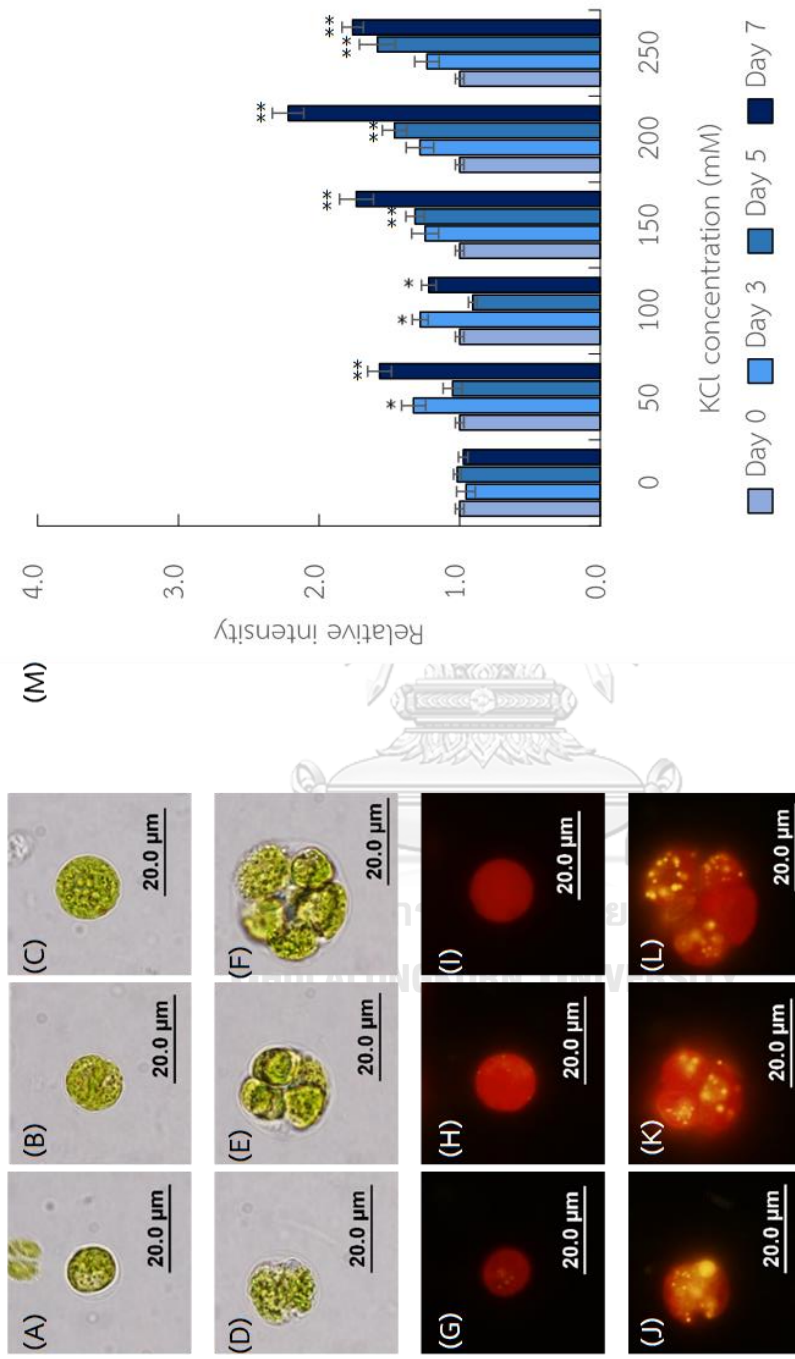


Figure 11 Image of *C. reinhardtii* (137c) cells observed under light microscope (A-F) and fluorescent microscope (G-L). Cells at exponential growth phase were subjected to salt stress (KCl) at various concentrations; 0 mM (A, G), 50 mM (B, H), 100 mM (C, I), 150 mM (D, J), 200 mM (E, K), and 250 mM (F, L) for 7 days. Morphology and lipid body were observed by Nile red staining as described in section 3.9.1.2. Relative intensity of lipid accumulation in algal cells was analyzed by using ImageJ software (M). Data are mean \pm SE from at least 10 independent cells (* $p < 0.01$, ** $p < 0.001$ by unpaired T-test).

4.2.1.3 Effect of LiCl stress

For LiCl stress condition, the concentration was reduced to 0, 30, 60, 90, 120, and 150 mM because of its toxicity. After shocking the cells for 0, 3, 5, and 7 days, respectively, cells morphology (in terms of cell size) remained unchanged. They were found to lose their survival at the first 3 days of cultivation at 120 mM LiCl. Cells were observed to be pale green in which suggested to be the result of the decreasing of chlorophyll under higher LiCl concentration (*i.e.* 60 mM LiCl at day 5). When the stressed cultures were extended to 7 days, the cells which were subjected into 90, 120, and 150 mM were all bleached and became colorless (Figure 12). Small-scattered lipid droplets in the cells were firstly observed at 3 days under 60 mM LiCl stress. The quantity of the oil droplets was increased when the cells were treated in the higher concentration and longer incubation time. For example, at 120 mM and 150 mM of day 7, the cells showed all bright yellow under fluorescent microscope. Figure 13 demonstrated that lipid droplet accumulation was highly induced under this condition. Signal intensity was reached to 2.06 ± 0.11 folds at first 3 days of cultivation at 60 mM LiCl. The lipid accumulation was significantly increased with the higher concentration of LiCl and cultivation time. The highest signal intensity was 3.27 ± 0.16 folds at 7 days of cultivation under 120 mM LiCl.

Among salt stress tested in this study, LiCl was regarded to be the strongest inducer for lipid accumulation in *C. reinhardtii* (137c). However, LiCl is extremely toxic to the cells as it caused cell death within 3 day of cultivation even under low concentration. To our knowledge, this study is the first report of LiCl induce lipid accumulation in *C. reinhardtii* (137c).

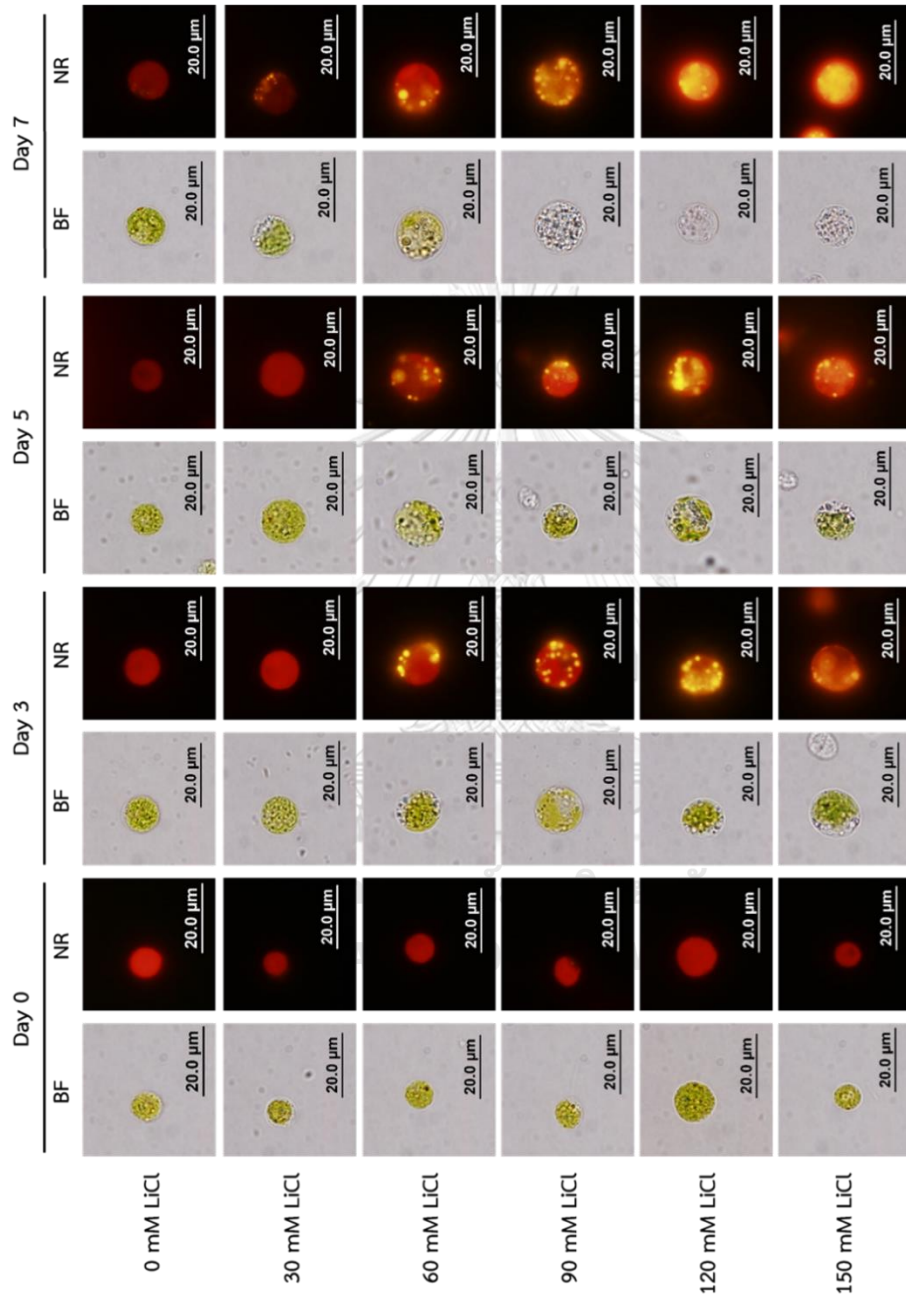


Figure 12 Image of *C. reinhardtii* (137c) cells observed under bright field light microscope (BF) and fluorescent microscope (NR). Cells at exponential growth phase were subjected to salt stress (LiCl) at various concentrations; 0 mM, 30 mM, 60 mM, 90 mM, 120 mM, and 150 mM for 0, 3, 5, and 7 days. Morphology and lipid body were observed by Nile red staining as described in section 3.9.1.2.

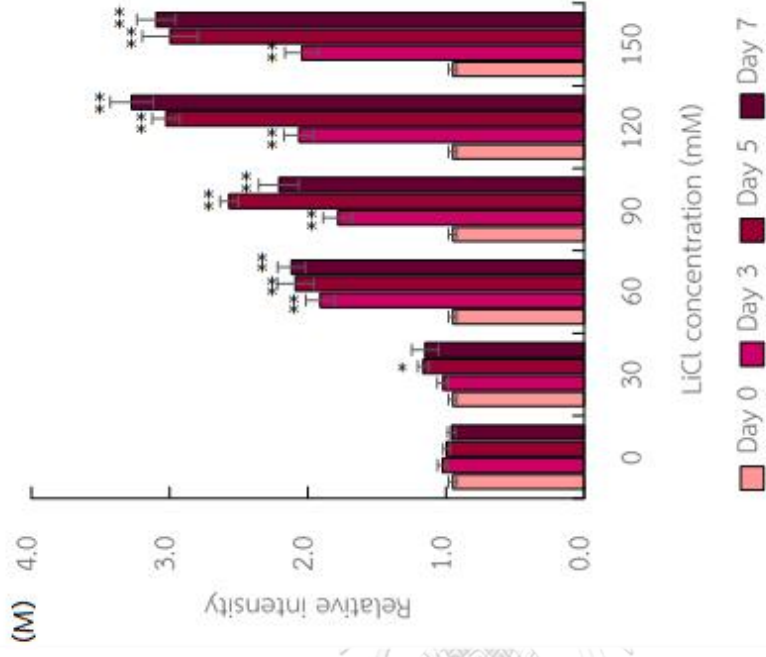
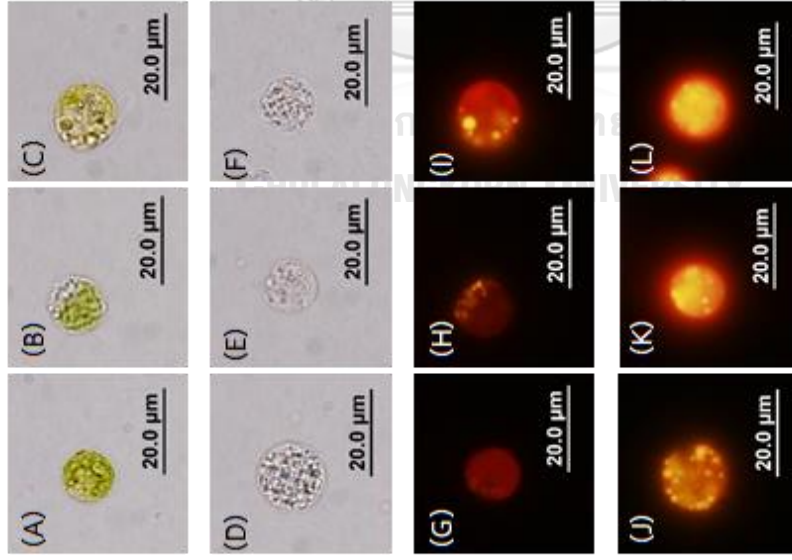


Figure 13 Image of *C. reinhardtii* (137c) cells observed under light microscope (A-F) and fluorescent microscope (G-L). Cells at exponential growth phase were subjected to salt stress (LiCl) at various concentrations; 0 mM (A, G), 30 mM (B, H), 60 mM (C, I), 90 mM (D, J), 120 mM (E, K), and 150 mM (F, L) for 7 days. Morphology and lipid body were observed by Nile red staining as described in section 3.9.1.2. Relative intensity of lipid accumulation in algal cells was analyzed by using ImageJ software (M). Data are mean \pm SE from at least 10 independent cells (* $p < 0.01$, ** $p < 0.001$ by unpaired T-test).

4.2.1.4 Effect of sodium acetate

Acetate was shown to be a substrate for acetyl-CoA production via PDH-bypass pathway (Avidan and Pick, 2015). Acetyl-CoA synthetase is the key enzyme in this pathway (Kato *et al.*, 2017). In this study, sodium acetate (CH_3COONa) was used as positive control for lipid induction, in accordance with the hypothesis that the higher concentration of sodium acetate would enhance acetyl-CoA production and lipid accumulation. Figure 14 revealed that lipid accumulation in *C. reinhardtii* (137c) was increased with the increasing of sodium acetate. However, lipid bodies observed in day 5 and 7 were reduced compared to day 3. Cell morphology remained unchanged in all tested conditions. These results suggested that *C. reinhardtii* (137c) cells utilize acetate as carbon source. The signal intensity was significantly increased with the increasing of sodium acetate concentrations at 3 days of cultivation at 100 to 250 mM (Figure 15M). Though the lipid was increased in day 5 and day 7 when the cultures were cultivated with higher acetate concentration, the relative intensities were lower than in day 3. The highest signal intensity was observed at 3 days of cultivation at 250 mM sodium acetate (2.04 ± 0.09 folds). Whereas the relative intensities of day 5 and day 7 at 250 mM sodium acetate were 1.38 ± 0.07 and 1.60 ± 0.06 folds, respectively. Moon *et al.* (2013) reported that the mixotrophic cultivation of *C. reinhardtii* could yield lipid for 16.41% of DCW and the biomass production was reached to 2.15 g/L. Moreover, the starchless mutant of *C. reinhardtii* BafJ5 showed the increasing of lipid accumulation under higher acetate concentration combined with nitrogen deprivation (Ramanan *et al.*, 2013). Not only the increasing of lipid droplets but cell growth was also observed in our study (data not shown). After cultivation for 7 days, the color of the acetate supplemented cultures was green while the control culture (without acetate) was much pale. Similar trend to the previous report observing by Taghavi *et al.* (2016), the presence of acetate in the culture medium resulted in higher biomass productivity in *C. reinhardtii* CC-125. This result suggested

that the mixotrophic cultivation might improve lipid productivity along with the biomass production.



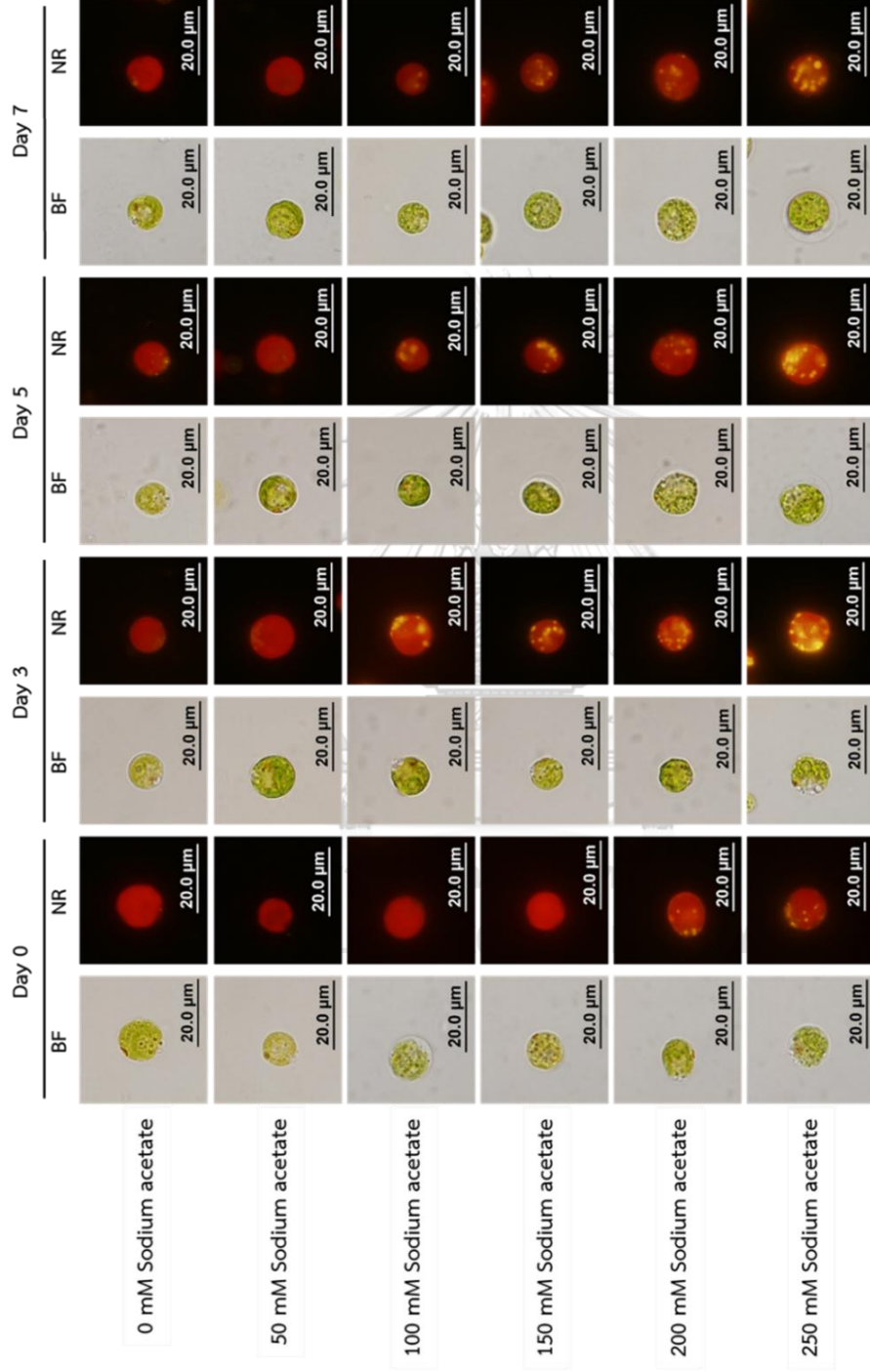


Figure 14 Image of *C. reinhardtii* (137c) cells observed under bright field light microscope (BF) and fluorescent microscope (NR). Cells at exponential growth phase were subjected to sodium acetate at various concentrations; 0 mM, 50 mM, 100 mM, 150 mM, 200 mM, and 250 mM for 0, 3, 5, and 7 days. Morphology and lipid body were observed by Nile red staining as described in section 3.9.1.2.

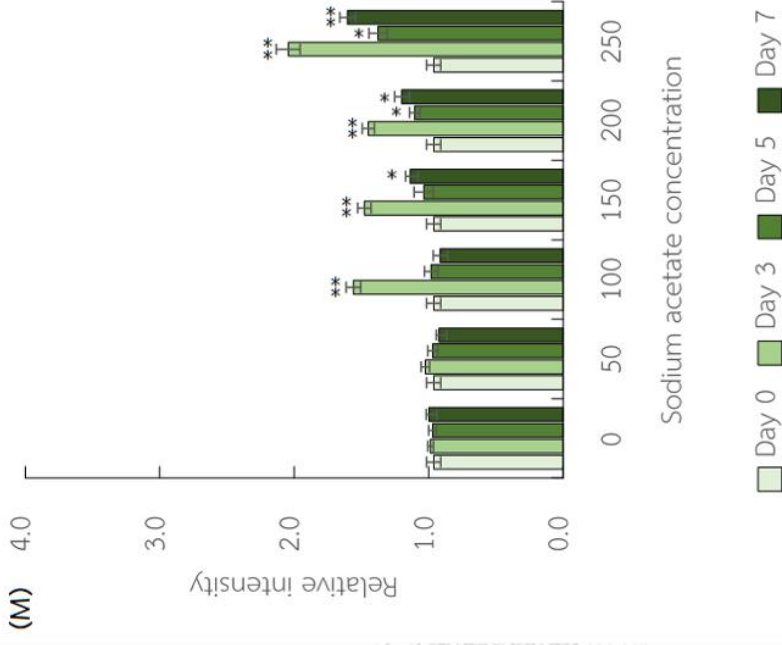
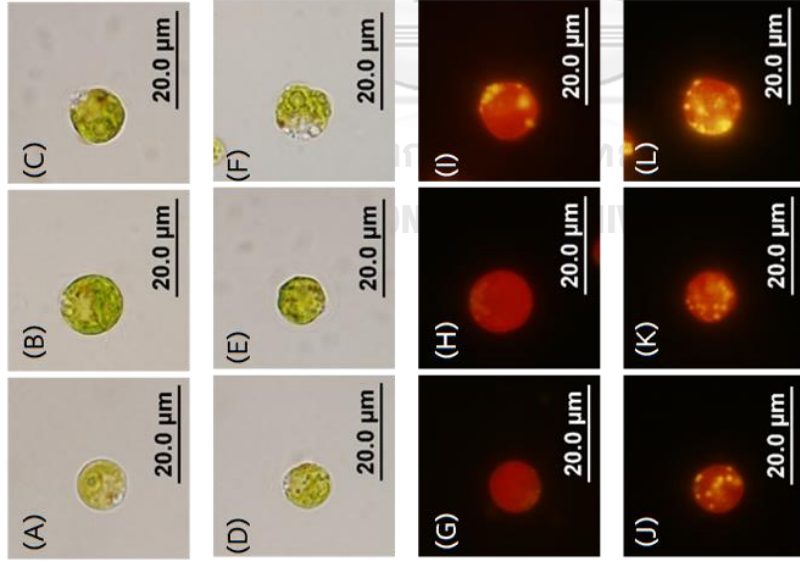


Figure 15 Image of *C. reinhardtii* (137c) cells observed under light microscope (A-F) and fluorescent microscope (G-L). Cells at exponential growth phase were subjected to sodium acetate at various concentrations; 0 mM (A, G), 50 mM (B, H), 100 mM (C, I), 150 mM (D, J), 200 mM (E, K), and 250 mM (F, L) for 7 days. Morphology and lipid body were observed by Nile red staining as described in section 3.9.1.2. Relative intensity of lipid accumulation in algal cells was analyzed by using ImageJ software (M). Data are mean \pm SE from ≥ 10 independent cells (* $p < 0.01$, ** $p < 0.001$ by unpaired T-test).

4.2.2 Observation of lipid accumulation by FAMES analysis

Next, we directly analyzed lipid accumulation by FAMES analysis based on the results obtained from section 4.2.1. It should be noted that 250 mM of NaCl was the concentration that resulted to highest lipid accumulation observed by Nile red staining. Nonetheless, this condition caused cell death within 3-5 days of cultivation. Thus, the concentration of NaCl was reduced to 200 mM for FAMES analysis. Table 4 summarized lipid profile in *C. reinhardtii* (137c) that was cultured in TAP medium (control) and was up-shocked with 200 mM NaCl, 200 mM KCl, and 120 mM LiCl, respectively. In control condition, total saturated fatty acid (SFA) was found to be $38.79 \pm 0.33\%$ of total FA while the total mono-unsaturated fatty acid (MUFA) was very low ($5.73 \pm 0.66\%$ of total FA). Total PUFA was analyzed to be $56.58 \pm 1.03\%$ of total FA. The last, total FA accounted for $7.08 \pm 0.09\%$ of DCW. Linoleic acid (C18:2), PUFA, was obviously determined to be the major component of FA in this microalga due to the highest content among other FAs ($33.64 \pm 0.04\%$ of total FA), followed by palmitic acid (C16:0). In *Chlamydomonas* sp., it was showed that palmitic acid (C16:0) is a major FA component (Sato *et al.*, 1995; Nascimento *et al.*, 2013). In our study, we found that lipid profile was changed upon salt stress. Total SFA was found to be statistic significantly increased to $50.48 \pm 6.67\%$ of total FA within 3 days of cultivation. Total SFA was reached to the highest at day 7 and accounted for $70.19 \pm 0.00\%$ of total FA (Figure 16). For MUFAs, the total content remained unchanged. On the other hand, total PUFAs was dramatically declined along with the cultivation time. PUFAs reduced to the lowest level at $16.15 \pm 0.00\%$ of total FA in day 7.

In biodiesel production, the medium chain fatty acid (MCFA) is preferable. In this study, we analyzed in terms of MCFAs as well. As shown in Table 4, myristic acid (C14:0), palmitic acid and palmitoleic acid (C16:1) were increased compared to control condition. Only palmitic acid was increased significantly. The long chain fatty acids (LCFAs) which are stearic acid (C18:0) and arachidonic acid (C20:0) were found slightly

increased, while the content of oleic acid (C18:1) was not changed. This implied that NaCl mainly affected on increasing of MCFA content, especially the palmitic acid.

In case of KCl or LiCl, the total SFA also significantly increased compared with the control condition. Total SFA reached to maximum level at 7 days of cultivation. It was accounted for 47.05 ± 0.00 and $43.09 \pm 0.00\%$ of total FA under KCl and LiCl, respectively. As well as, the stresses resulted to the decreasing of PUFAs as occurring in NaCl stress. We noticed that the results from FAMES analysis were mostly in consistency with Nile red staining.

In *Dunaliella* sp., NaCl was shown to be the strong inducer for lipid accumulation upon 2 M NaCl stress. Total SFA was found to be increased from 33.62% to 46.27% of total FA. For total MUFA, it was found to be significantly enhanced from 5.1% to 26.93% of total FA while total PUFA was decreased (BenMoussa-Dahmen *et al.*, 2016). Previously, protein biosynthesis was observed to be decreased when the freshwater green microalga *Chlorella sorokiniana* SDEC-18 (low-starch producing alga) was cultured under salt stress (Zhang *et al.*, 2018). Nevertheless, the effect of salt on FA composition alteration still unclear. Besides, the transcriptional level of genes involved in lipid biosynthesis has not been studied exclusively. In the study, we are interested in effects of NaCl on lipid biosynthesis involving genes including *PDH2*, *ACCase*, *MAT*, *KAS2*, *FAT1*, *GPD1*, *DGTT1*, *DGTT2*, *DGTT3*, and *DGTT4*.

Table 4 Lipid profile of *C. reinhardtii* (137c) cells subjected to salt stress (NaCl, KCl, and LiCl) at day 3, 5, and 7, respectively. A hundred milligram DCW of each stressed cell were collected and extracted lipid as described in section 3.9.2.2. The data were shown as mean \pm SD. (ND; not detected)

Fatty acid	Control			200 mM NaCl			200 mM KCl			120 mM LiCl		
	3 days	5 days	7 days	3 days	5 days	7 days	3 days	5 days	7 days	3 days	5 days	7 days
SATURATED FATTY ACIDS (SFAs)												
Caprylic acid (C8:0)	ND	ND	ND	ND	ND	ND	ND	ND	ND	ND	ND	ND
Capric acid (C10:0)	ND	ND	ND	ND	ND	ND	ND	ND	ND	ND	ND	ND
Lauric acid (C12:0)	ND	0.02 \pm 0.03	0.01 \pm 0.03	0.03 \pm 0.04	ND	ND	ND	0.01 \pm 0.00	ND	0.05 \pm 0.00	0.05 \pm 0.00	0.03 \pm 0.00
Myristic acid (C14:0)	1.93 \pm 0.03	0.57 \pm 0.08	1.78 \pm 1.49	2.24 \pm 1.97	2.80 \pm 0.10	2.98 \pm 0.06	3.28 \pm 0.13	0.66 \pm 0.01	0.67 \pm 0.01	0.66 \pm 0.01	0.67 \pm 0.01	0.07 \pm 0.01
Palmitic acid (C16:0)	31.94 \pm 0.16	43.14 \pm 10.56	51.20 \pm 14.96	59.80 \pm 14.46	36.20 \pm 0.00	36.28 \pm 0.01	39.32 \pm 0.03	35.98 \pm 0.04	36.57 \pm 0.03	35.98 \pm 0.04	36.57 \pm 0.03	37.51 \pm 0.03
Stearic acid (C18:0)	4.70 \pm 0.04	6.47 \pm 2.68	6.78 \pm 3.85	7.75 \pm 4.69	3.70 \pm 0.03	3.80 \pm 0.03	4.16 \pm 0.02	4.30 \pm 0.04	4.89 \pm 0.00	4.30 \pm 0.04	4.89 \pm 0.00	4.64 \pm 0.00
Arachidic acid (C20:0)	0.22 \pm 0.00	0.28 \pm 0.06	0.27 \pm 0.13	0.37 \pm 0.13	0.22 \pm 0.00	0.26 \pm 0.01	0.29 \pm 0.00	0.21 \pm 0.01	0.22 \pm 0.00	0.21 \pm 0.01	0.22 \pm 0.00	0.21 \pm 0.00
Behenic acid (C22:0)	ND	ND	ND	ND	ND	ND	ND	ND	ND	ND	ND	ND
Lignoceric acid (C24:0)	ND	ND	ND	ND	ND	ND	ND	ND	ND	ND	ND	ND
Total SFA	38.79 \pm 0.33	50.48 \pm 6.67	60.04 \pm 5.66	70.19 \pm 0.00	42.92 \pm 0.01	43.33 \pm 2.85	47.05 \pm 0.00	41.20 \pm 0.38	41.90 \pm 0.22	41.20 \pm 0.38	41.90 \pm 0.22	43.09 \pm 0.00
MONO-UNSATURATED FATTY ACIDS (MUFAs)												
Palmitoleic acid (C16:1)	0.34 \pm 0.25	0.66 \pm 0.38	0.71 \pm 0.41	0.55 \pm 0.39	0.68 \pm 0.37	0.74 \pm 0.36	0.92 \pm 0.54	0.82 \pm 0.31	0.78 \pm 0.31	0.82 \pm 0.31	0.78 \pm 0.31	0.46 \pm 0.06
Oleic acid (C18:1)	5.40 \pm 1.70	6.16 \pm 3.48	5.73 \pm 2.84	3.84 \pm 2.80	5.05 \pm 0.99	5.91 \pm 0.18	4.06 \pm 0.52	3.09 \pm 2.65	3.38 \pm 2.97	3.09 \pm 2.65	3.38 \pm 2.97	1.10 \pm 0.68
Erucic acid (C22:1)	ND	ND	ND	ND	ND	ND	ND	ND	ND	ND	ND	ND
Total MUFA	5.73 \pm 0.66	6.82 \pm 0.00	6.45 \pm 0.00	4.40 \pm 0.00	5.73 \pm 1.29	6.65 \pm 0.16	4.98 \pm 0.00	3.91 \pm 0.00	4.16 \pm 0.00	3.91 \pm 0.00	4.16 \pm 0.00	1.56 \pm 0.00
POLY-UNSATURATED FATTY ACIDS (PUFAs)												
Linoleic acid (C18:2)	33.64 \pm 0.04	26.64 \pm 7.37	21.86 \pm 8.52	11.18 \pm 12.23	29.57 \pm 2.35	26.25 \pm 5.54	15.09 \pm 18.94	34.19 \pm 2.73	34.42 \pm 3.59	34.19 \pm 2.73	34.42 \pm 3.59	18.99 \pm 25.43
Linolenic acid (C18:3)	22.94 \pm 2.36	15.93 \pm 6.60	11.73 \pm 7.37	4.96 \pm 6.42	22.26 \pm 1.61	18.22 \pm 2.19	8.94 \pm 11.81	16.65 \pm 6.10	15.32 \pm 5.54	16.65 \pm 6.10	15.32 \pm 5.54	11.56 \pm 8.74
Total PUFA	56.58 \pm 1.03	42.58 \pm 0.03	33.59 \pm 2.11	16.15 \pm 0.00	51.83 \pm 0.74	44.47 \pm 2.19	24.03 \pm 0.00	50.84 \pm 2.73	49.74 \pm 3.59	50.84 \pm 2.73	49.74 \pm 3.59	30.56 \pm 0.00
Total FA (% DCW)	7.08 \pm 0.99	7.53 \pm 0.52	6.21 \pm 0.12	6.28 \pm 0.13	6.55 \pm 1.07	6.29 \pm 0.88	5.71 \pm 0.05	7.78 \pm 2.05	7.95 \pm 3.06	7.78 \pm 2.05	7.95 \pm 3.06	6.06 \pm 0.02

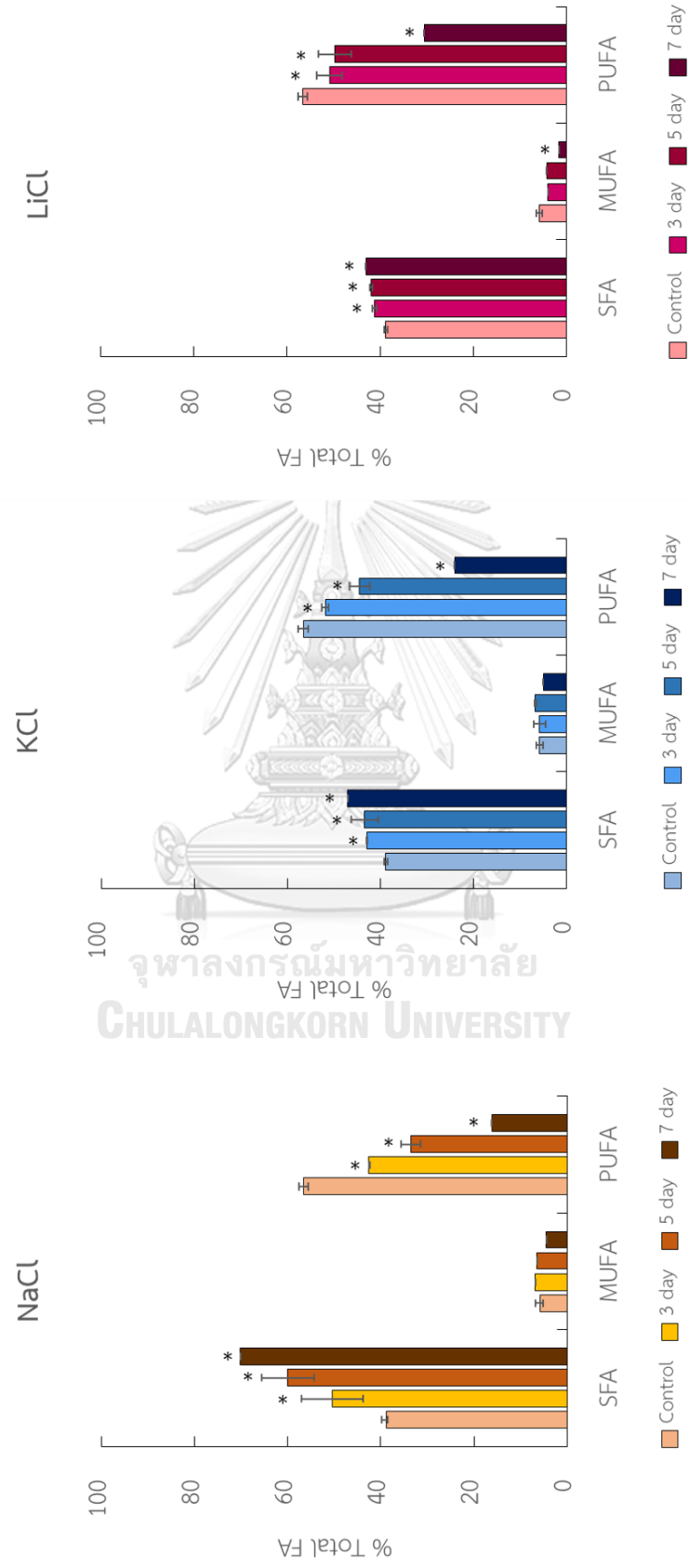


Figure 16 FAMES analysis for salt stressed cells; 200 mM NaCl and KCl, and 120 mM LiCl. A thousand milligrams of cells fresh weight were analyzed for FAMES as described in Materials and Methods. SFA; saturated fatty acid, MUFA; mono-unsaturated fatty acid, PUFA; poly-unsaturated fatty acid (* $p < 0.001$, by two-way ANOVA).

4.3 Gene expression analysis

Mechanisms behind salt stress was further investigated by employing transcriptional analysis. To this end, *C. reinhardtii* (137c) was treated with 200 mM NaCl for 0 (control), 6, and 12 hours, respectively. Genes involved in FA and TAG biosynthesis were examined their transcriptional expressions by using RT-PCR. The relative expression was analyzed by using Image Lab program. Figure 17A showed the gene expression analysis. Equality of total RNA concentrations was confirmed by using *18s rRNA* as an internal control (intensity was quantitated as ~ 1.0 in all conditions, data not shown). The result revealed that after up-shocking the microalga with salt stress for 6 and 12 hours, the expression of the genes were modulated either up- or down-regulation. The expression of *PDH2*, *MAT* and *KAS2* genes were found to be significantly up-regulated at 12 hours of cultivation compared to the control ones (0 hours of NaCl). Expression of *PDH2* and *MAT* were observed to the highest at 1.83 ± 0.20 and 1.82 ± 0.06 folds, respectively. In case of *KAS2*, the expression was significantly increased to 1.70 ± 0.05 folds. All three genes which involved in Kennedy pathway were observed to be down-regulated. *DGTT1* and *DGTT2* expressions were sharply decreased. For *ACCase*, it was significantly up-regulated (1.87 ± 0.05 folds) after 6 hours of stress and then slightly declined. In this study, three genes (*FAT1*, *DGTT3* and *DGTT4*) could not be analyzed by RT-PCR. For *FAT1*, its expression seemed to be extremely low. We could not detect even 50 cycles of amplification. The expression of *DGTT3* and *DGTT4* could not be analyzed because of non-specific PCR products (data not shown).

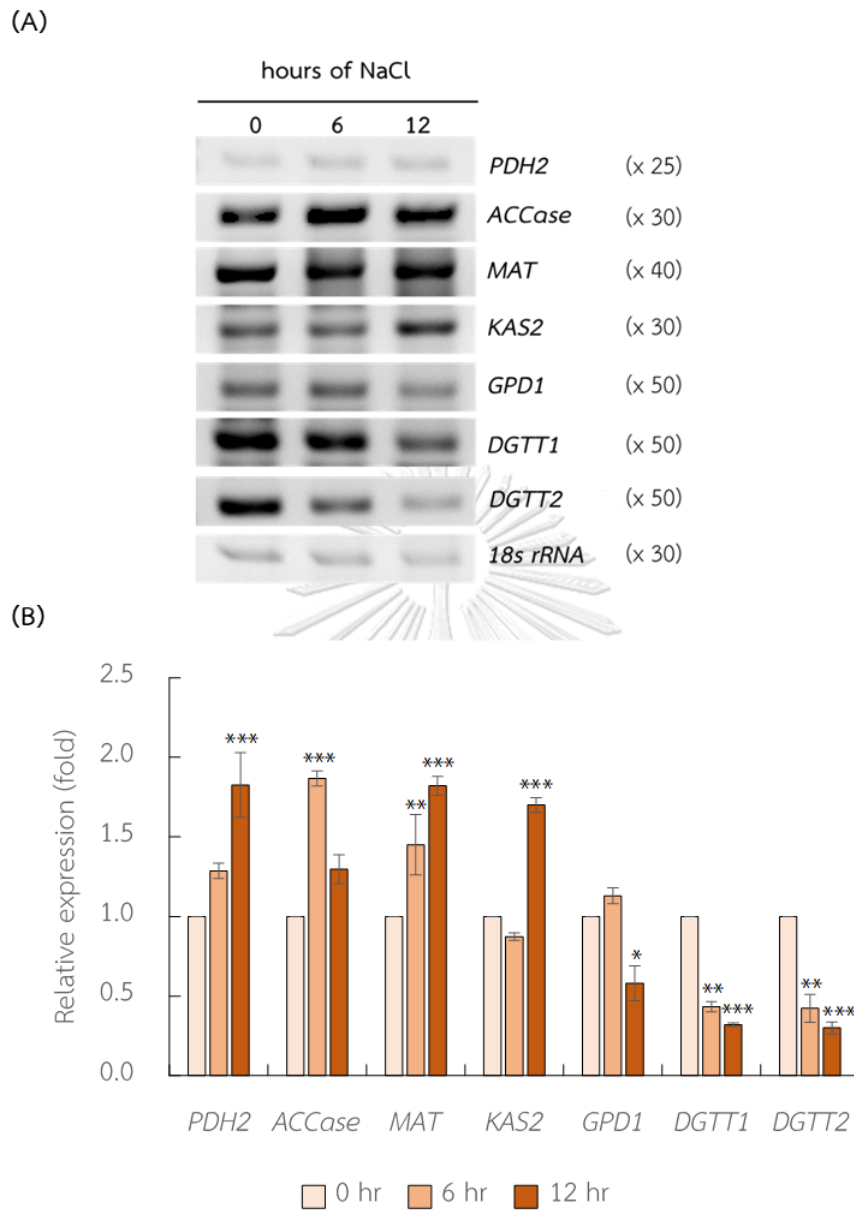


Figure 17 Semiquantitative RT-PCR analysis of stressed cells under 200 mM NaCl conditions at 0 (control), 6, and 12 hours (A). Equality of total RNA concentrations were confirmed by an internal control *18s rRNA* expression. PCR products were analyzed on 1.2% (w/v) gel electrophoresis precasted with SYBR[®] safe. Relative expression analysis of stressed cells quantitated by Image Lab program (B) (* $p < 0.05$, ** $p < 0.01$, and *** $p < 0.001$ by two-way ANOVA).

4.4 Construction of the expression plasmid harboring *ChMAT*

4.4.1 *ChMAT* gene amplification and purification

ChMAT gene was amplified by using PCR. KOD-Plus-Neo was used as DNA polymerase and cDNA obtained from step 3.10.2 was use as template. The PCR products were analyzed on 1.2% (w/v) agarose gel. Figure 18 showed gel electrophoresis of PCR products. According to NCBI database, the size of putative *ChMAT* gene is 981 base pairs. Two sizes of PCR products were obtained in this study (0.9 and 1.1 kb). Both sizes were purified and ligated into cloning vector pBSK⁺II to confirm their nucleotide by sequencing analysis.

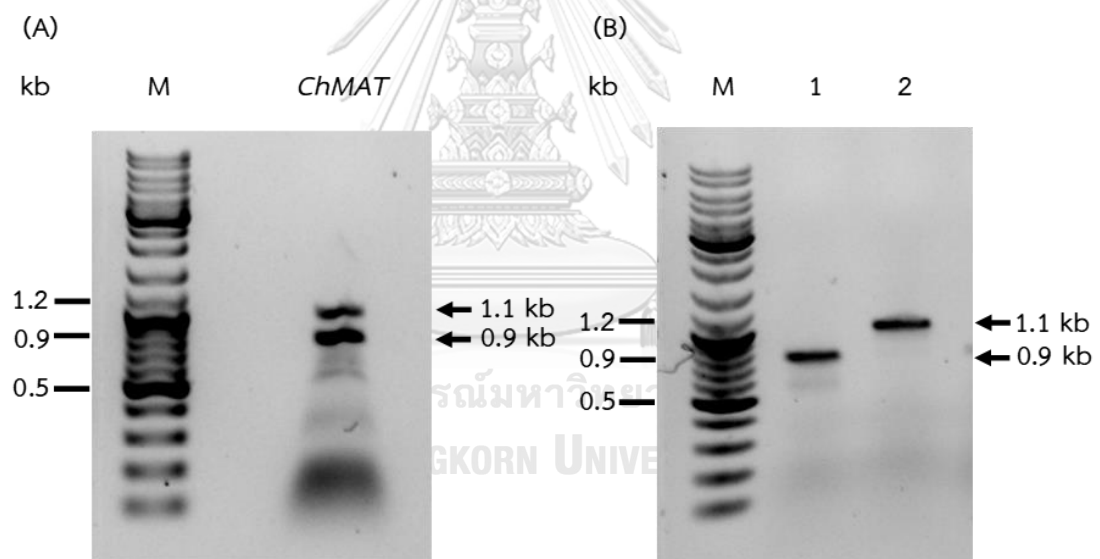


Figure 18 *ChMAT* gene amplification. PCR was performed using touch-down PCR technique (as described in section 3.11.1) with KOD-Plus-Neo and cDNA was used as template. The PCR product was electrophorized on 1.2% (w/v) agarose gel precasted with SYBR[®] safe (A). Two *ChMAT* splicing variants after purification (B). Lane M: DNA ladder, Lane 1: the lower band of PCR product (low_ *ChMAT*), and Lane 2: the upper band of PCR product (up_ *ChMAT*).

4.4.2 Plasmid extraction and restriction enzyme analysis

After transforming the *ChMAT*/pBSK⁺II (0.9 and 1.1 kb) into *E. coli* DH5 α , the transformants were incubated for 16 hours at 37 °C. The positive colony supposed to appear as white colony. To confirm the presenting of the *ChMAT* gene in cloning vector, colony PCR was performed. Figure 19A showed the target bands of the *ChMAT* corresponding 1.1 kb and 0.9 kb.

Each size of *ChMAT* was confirmed its nucleotide by DNA sequencing. The results revealed that the sequence of the 1.1 kb was similar to the deposited *ChMAT* sequence in NCBI database (100% identity, 73% query cover) (Appendix 13). While the sequence of the 0.9 kb was shown as the highest homology to the *C. reinhardtii* lecithin:cholesterol acyltransferase (*LCA1*) (38% query cover) (data not shown). Nevertheless, based on the sequencing result that the 0.9 kb band (*low_ChMAT*) was closely related to *LCA1* gene in *C. reinhardtii*. Hence, the 1.1 kb band (*up_ChMAT*) was selected for further study. To transform *ChMAT* into the expression vector, the plasmid of *ChMAT*/pBSK⁺II was double digested with *Nde*I and *Bam*HI. Figure 19B revealed that after digestion, two bands were appeared on the agarose gel. The bigger band (4.0 kb) was expected to be the uncomplete digested pBSK⁺II and the lower band (1.1 kb) was the target band of *ChMAT*. Then, the lower band was cut and purified from agarose gel. The purified product was then ligated into the expression vector, pSyn_6, as described in section 3.11.3.

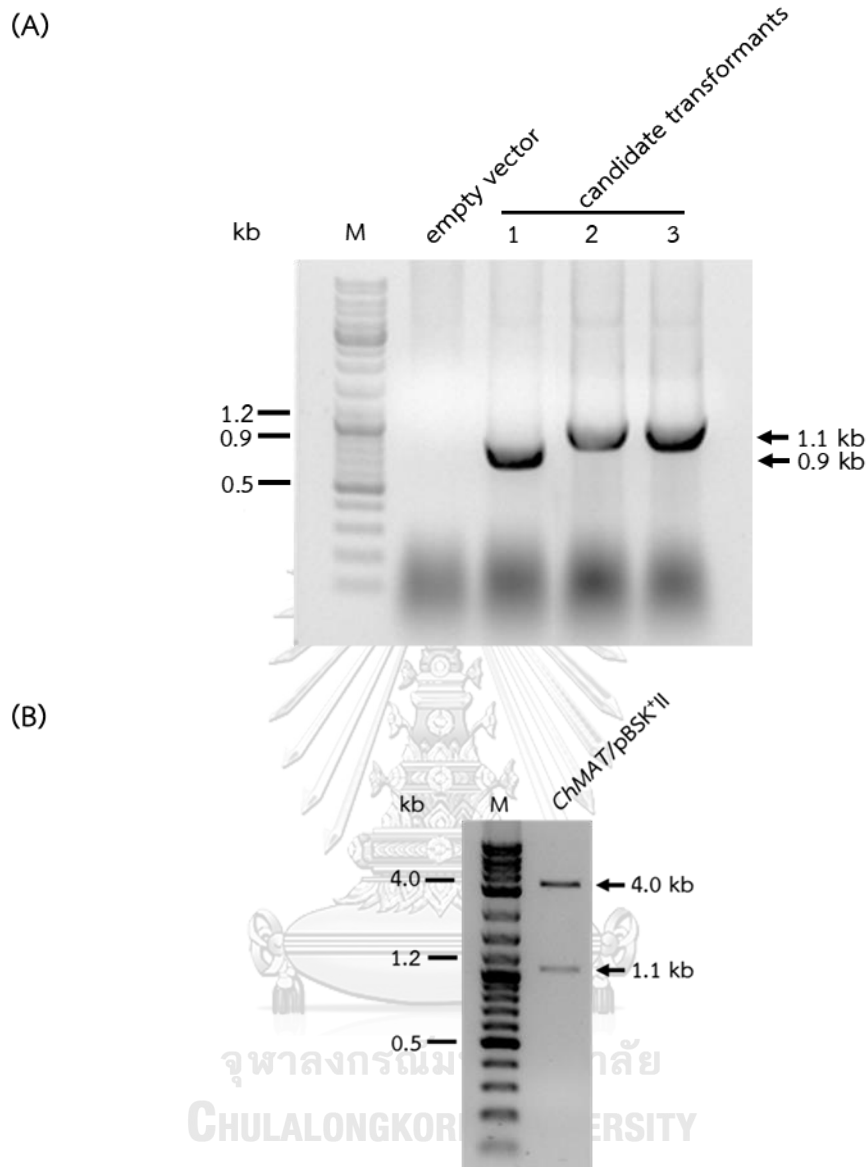


Figure 19 Colony PCR of the candidate transformants *ChMAT* in *E. coli* DH5 α (A). A single colony of the candidate transformants was picked and used as template in PCR reaction. The PCR products were analyzed by gel electrophoresis on 1.2% (w/v) agarose gel precasted with SYBR[®] safe and imaged by GelDoc[™]. Lane M: DNA ladder, and Lane 1-3: candidate transformants of *ChMAT*. Restriction enzyme analysis of *ChMAT* in cloning vector, pBSK⁺II (B). The vector harboring *ChMAT* was prepared and double digested with *Nde*I and *Bam*HI. The reaction was run by using 1.2% (w/v) agarose gel precasted with SYBR[®] safe. Lane M: DNA ladder.

4.4.3 Transformation of *S. elongatus* PCC 7942 harboring *ChMAT* gene

After purification of *ChMAT* and ligated into pSyn_6 vector. The constructed plasmids were then transformed into *E. coli* DH5 α . The transformants were spread onto LB agar plate (supplemented with 100 μ g/ml spectinomycin) and was incubated in 37 °C for 16 hours. The colonies were restreaked onto new LB agar plate supplemented with spectinomycin (100 μ g/ml) and were incubated as the same aforementioned condition. Each transformant was picked up and directly used as a template for colony PCR. Figure 20B showed colony PCR products of nine candidate transformants of *ChMAT*/pSyn_6/DH5 α . The expected band was observed at 1.1 kb. Then, the plasmids were extracted from *E. coli* DH5 α as the same protocol as mentioned in Materials and Methods. After extraction, the plasmids were electrophorized on 1.2% (w/v) agarose gel. The size of empty pSyn_6 vector was 4,461 bp and the size of *ChMAT* gene was 993 bp. Thus, the expected size of *ChMAT*/pSyn_6 vector was approximately 5.5 kb (Figure 20C).

ChMAT/pSyn_6 expressing vector was naturally transformed into the freshwater cyanobacterium *S. elongatus* PCC 7942. The transformants were over layered onto the BG11 agar plates (supplemented with 10 μ g/ml spectinomycin). They were incubated under continuous light (50 μ mol m⁻²s⁻¹) at 26 \pm 1 °C until the single colony was appeared. Figure 21A showed the growth of WT (mock), pSyn_6/7942 (empty vector), and *ChMAT*/7942 that were incubated for two weeks. There was visually no colony on the mock plate (wild type (WT) of *S. elongatus* PCC 7942) since the WT is susceptible to spectinomycin. While the empty vector and the transformants plates showed several independent colonies. To confirm the existing of *ChMAT* in the transformants, independent colony of WT (grown on BG11 agar plate), empty vector and *ChMAT*/7942 were randomly picked up. They were used as templates for colony PCR. The PCR product showed the correct size of *ChMAT* gene (Figure 21B).

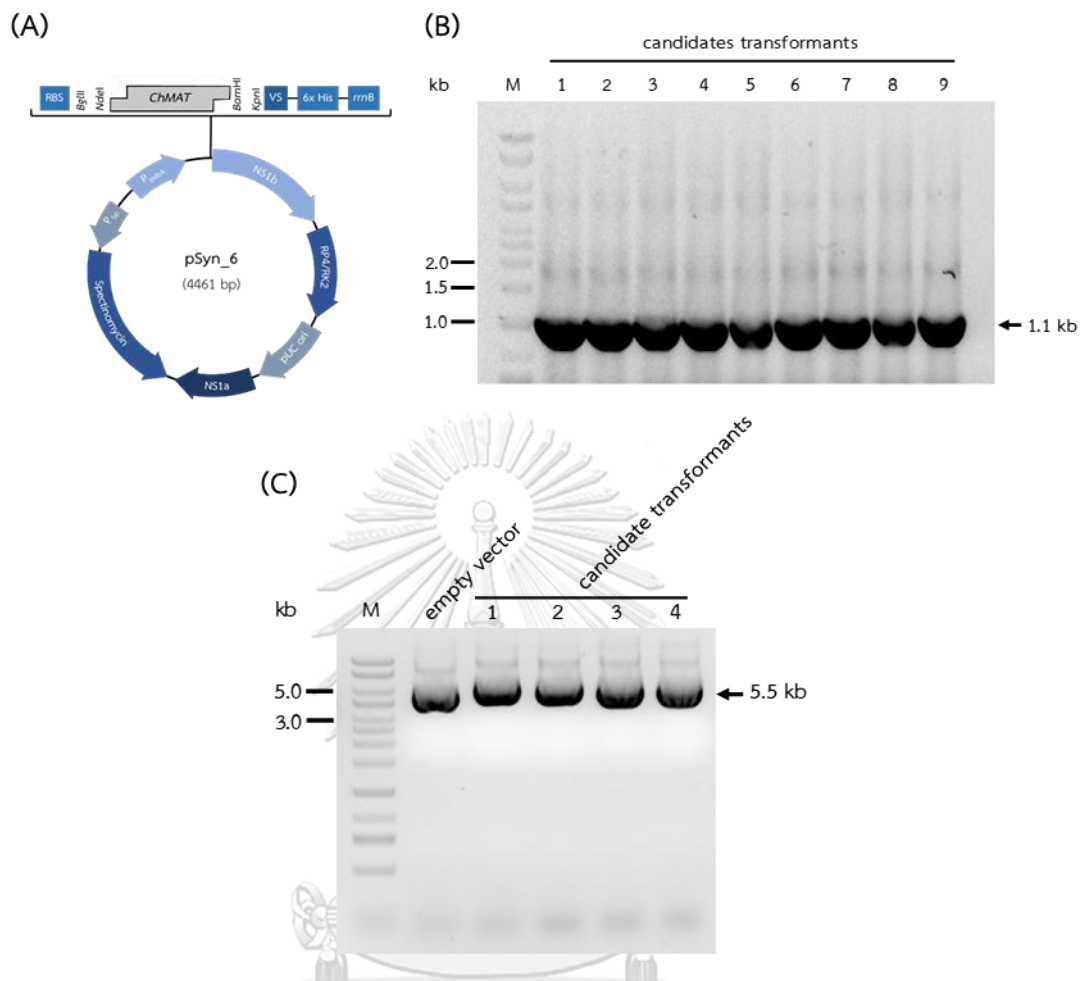


Figure 20 Plasmid of *ChMAT/pSyn_6* (A). The grey box represents as *ChMAT* gene inserted between *NdeI* and *BamHI* site. Colony PCR of the candidate transformants *ChMAT/pSyn_6* in *E. coli* DH5 α (B). A single colony of the candidate transformants was picked and used as template in PCR reaction. The PCR products were analyzed by gel electrophoresis on 1.2% (w/v) agarose gel precasted with SYBR[®] safe and imaged by GelDoc[™]. Lane M: DNA ladder, and Lane 1-9: candidate transformants of *ChMAT/pSyn_6*. Plasmid extraction of *ChMAT/pSyn_6* (C). The pSyn_6 harboring *ChMAT* gene was prepared as described in section 3.11.2.2. Lane M: DNA ladder, and Lane 1-4: *ChMAT/pSyn_6* vector extracted from candidates transformants.

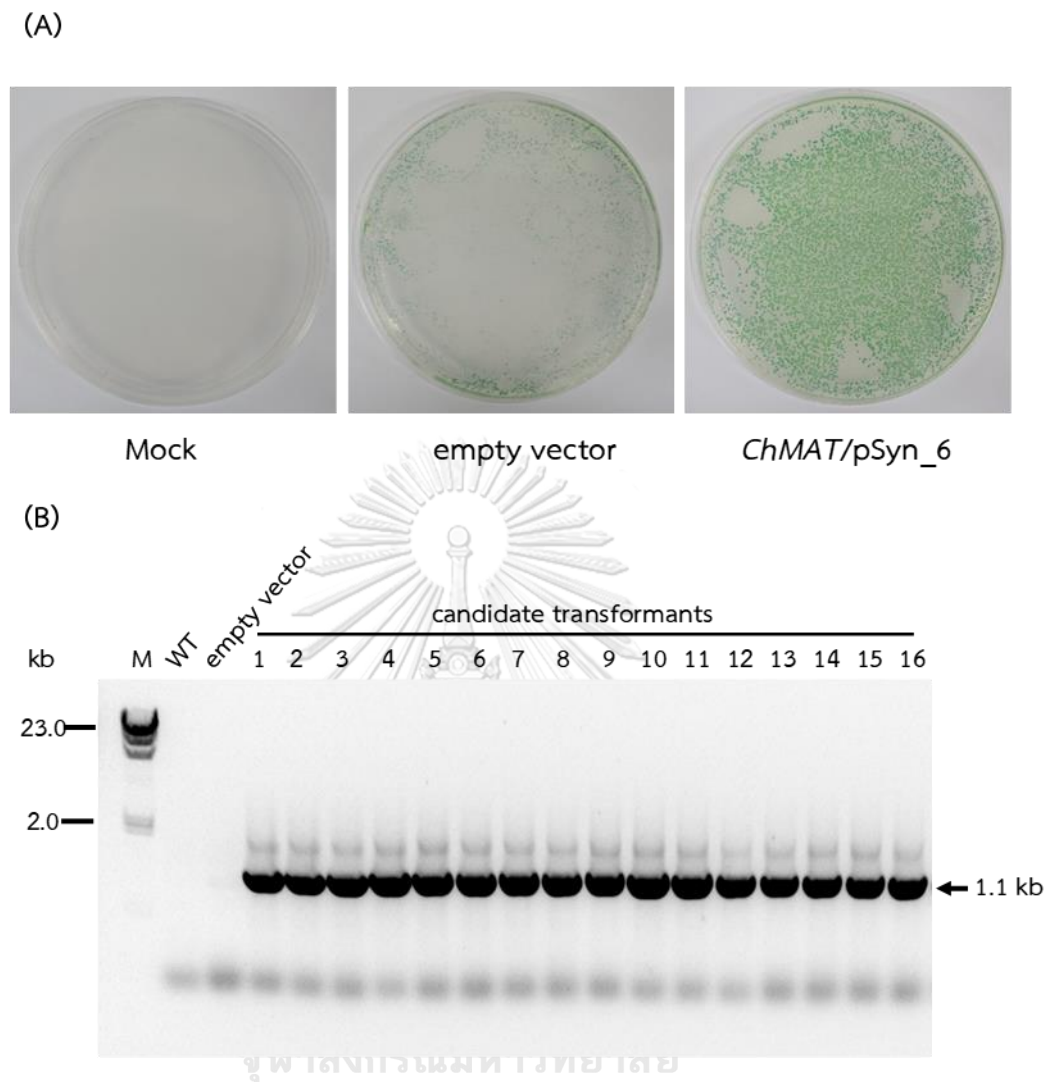


Figure 21 Natural transformation of *ChMAT/pSyn_6* in a fresh water cyanobacterium *S. elongatus* PCC 7942 on BG-11 agar plate (supplemented with 10 $\mu\text{g/ml}$ spectinomycin) plate (A). BG11 agar plates were incubated under continuous light ($50 \mu\text{mol m}^{-2}\text{s}^{-1}$) at $26 \pm 1 \text{ }^\circ\text{C}$ for 2 weeks. Colony PCR of 16 candidate transformants *ChMAT/pSyn_6* in *S. elongatus* PCC 7942 (B). A single colony of each candidate was picked up and used as template in PCR reaction. The PCR products were analyzed by gel electrophoresis on 1.2% (w/v) agarose gel precasted with SYBR[®] safe and imaged by GelDocTM. Lane M: DNA ladder, and Lane 1-16: candidate transformants of *ChMAT/7942*.

4.5 Construction of expression plasmid harboring *SynMAT*

4.5.1 Construction of cloning vector harboring *SynMAT* gene

To construct *SynMAT*/pBSK+II plasmid, gDNA was prepared from *S. elongatus* PCC 7942 by using the same protocol as described in section 3.12.1. Genomic DNA (gDNA) was analyzed for its quality by using gel electrophoresis (Figure 22A). The extracted gDNA was used as template for amplification of *SynMAT* by PCR. The KOD-Plus-Neo was used as DNA polymerase. Figure 22B showed the intact band of amplified product on agarose gel. The PCR product was purified and ligated into pBSK⁺II cloning vector. The constructed vector was then transformed into *E. coli* DH5 α for propagation. Colony PCR was performed to confirm the presence of *SynMAT* in the vector. Figure 22C showed five candidate transformants of *SynMAT*/pBSK⁺II/DH5 α . Only the transformant number one that showed negative result on colony PCR which indicated the false positive of transformation. To obtain the *SynMAT*/pBSK⁺II vector, the plasmid extraction was done as described in section 3.11.2.2. The plasmid was then double digested with *Nde*I and *Bam*HI. Two bands were appeared on the agarose gel (Figure 22D). The digested products were run comparing to the empty vector (digested with *Eco*RV) and the undigested plasmid. The upper band (4.0 kb) was the uncomplete digested *SynMAT*/pBSK⁺II and the lower band (0.9 kb) was the target band of *SynMAT* gene.

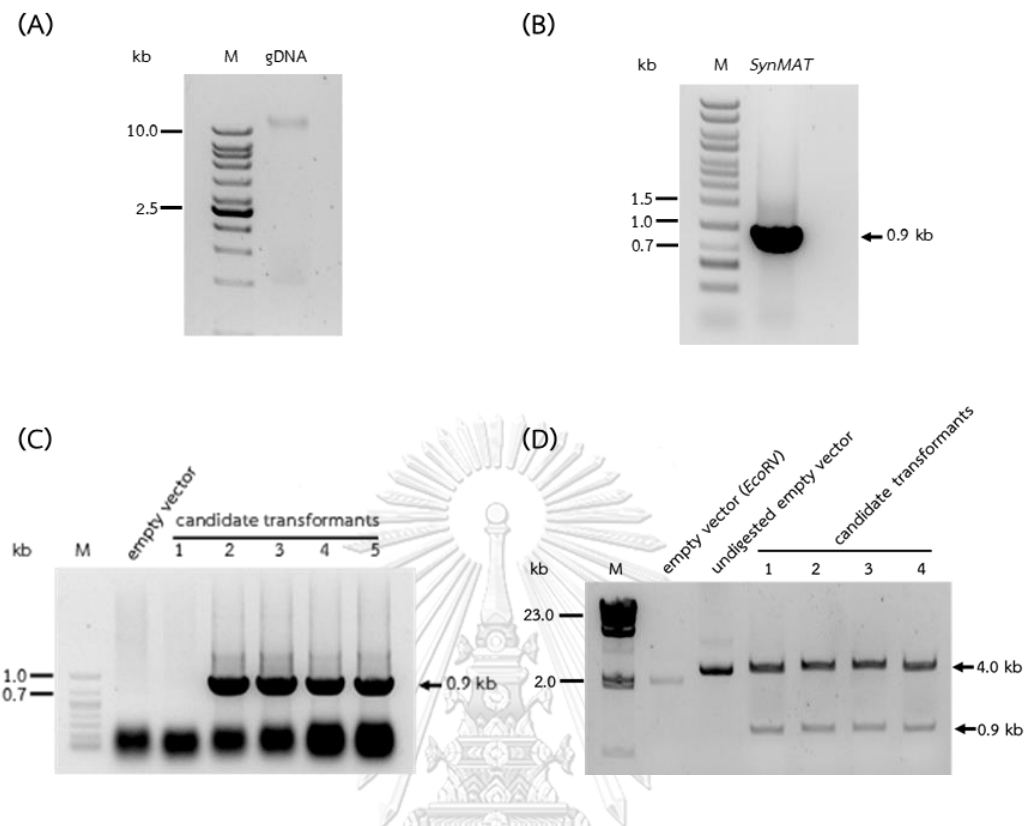
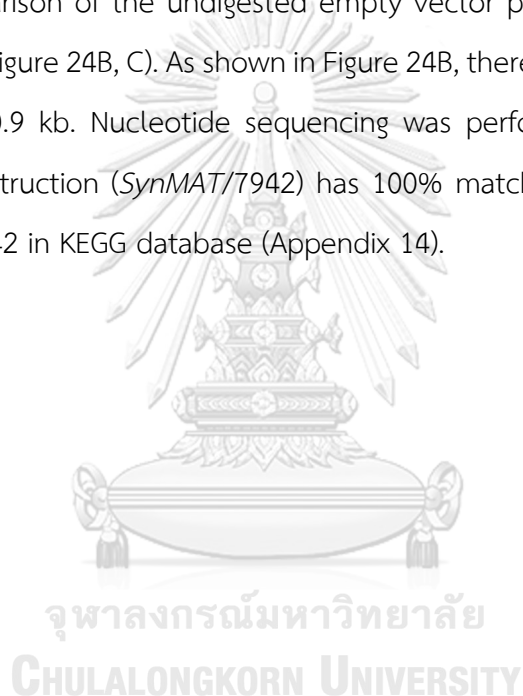


Figure 22 Genomic DNA extracted from *S. elongatus* PCC 7942 (A). *SynMAT* gene amplification (B). PCR reaction was performed using KOD-Neo-Plus as DNA polymerase and using gDNA as template. Colony PCR of the candidate transformants *SynMAT* in *E. coli* DH5 α (C). A single colony of the candidate transformants was picked and used as template in PCR reaction. Lane M: DNA ladder, and Lane 1-5: candidate transformants of *SynMAT*. Restriction enzyme analysis of *SynMAT* in cloning vector, pBSK+II (D). The vector harboring *SynMAT* was prepared and double digested with *Nde*I and *Bam*HI. Lane M: DNA ladder, and Lane 1-4: double digestion of *SynMAT*/pSyn_6 vector extracted from candidates transformants.

4.5.2 Construction of expression vector of *SynMAT*/pSyn_6

To construct the expressing vector of *SynMAT*/pSyn_6, the pBSK⁺II that harbored *SynMAT* was double digested with *Nde*I and *Bam*HI. Fragments were purified and were ligated into pSyn_6 vector. Colony PCR was carried out to confirm the existing of the gene in the transformants. Figure 23 showed 14 candidate transformants of *SynMAT*/pSyn_6/DH5 α . Then, the plasmid was extracted from five candidates and confirmed by double digestion with *Nde*I and *Bam*HI. The digested products were checked in comparison of the undigested empty vector pSyn_6 and the undigested *SynMAT*/pSyn_6 (Figure 24B, C). As shown in Figure 24B, there were the correct insertion with the size of 0.9 kb. Nucleotide sequencing was performed to confirm. Results revealed our construction (*SynMAT*/7942) has 100% matching to putative MAT in *S. elongatus* PCC 7942 in KEGG database (Appendix 14).



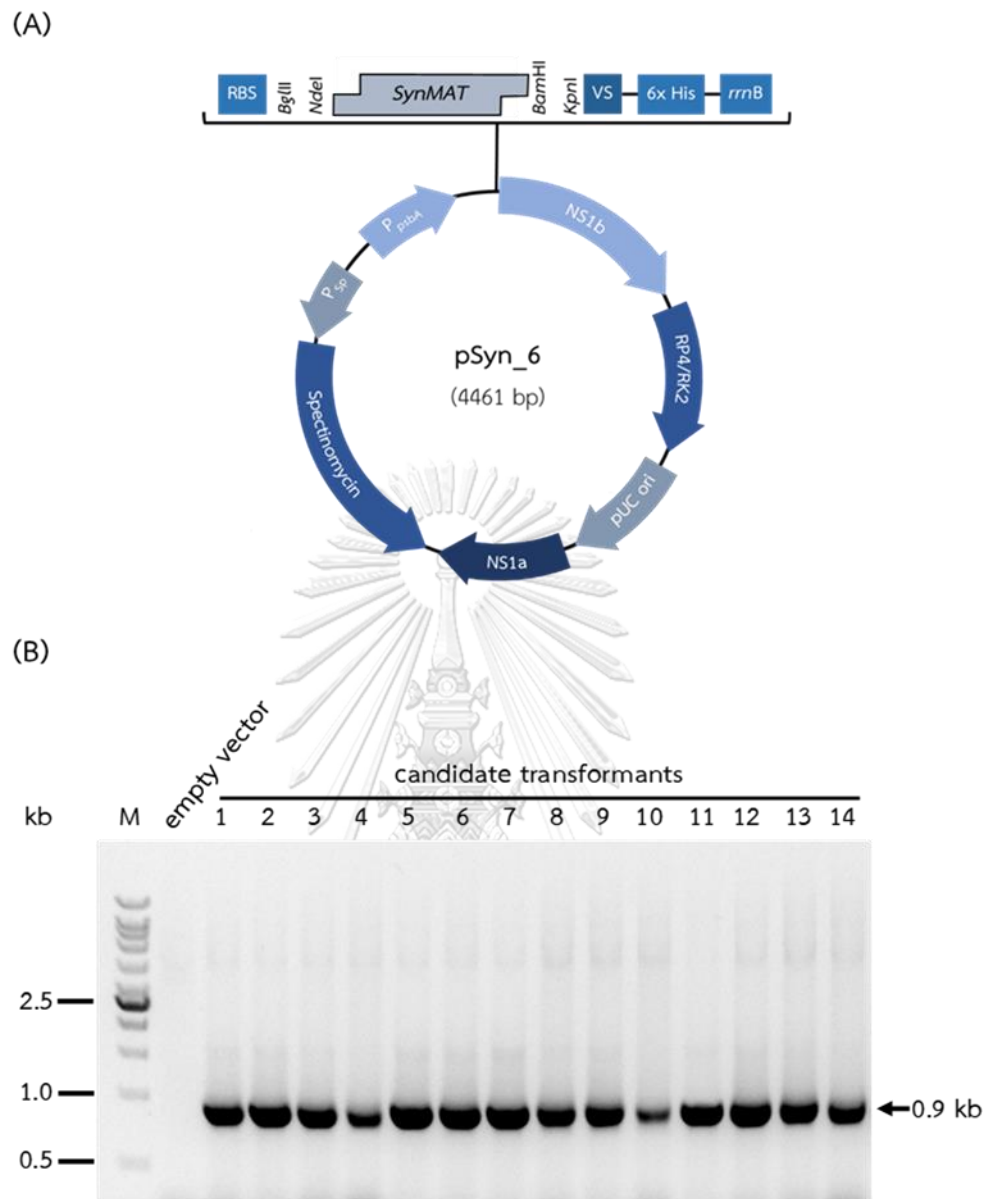
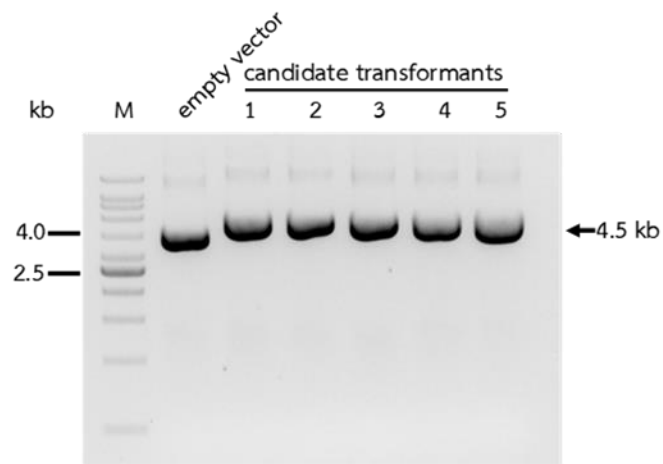


Figure 23 Plasmid of *SynMAT*/pSyn₆ (A). The grey box represents as *SynMAT* gene inserted between *NdeI* and *BamHI* site. Colony PCR of the candidate transformants *SynMAT*/pSyn₆ in *E. coli* DH5 α (B). A single colony of the candidate transformants was picked and used as template in PCR reaction. The PCR products were analyzed by gel electrophoresis on 1.2% (w/v) agarose gel precasted with SYBR[®] safe and imaged by GelDoc[™]. Lane M: DNA ladder, and Lane 1-14: candidate transformants of *SynMAT*/pSyn₆.

(A)



(B)

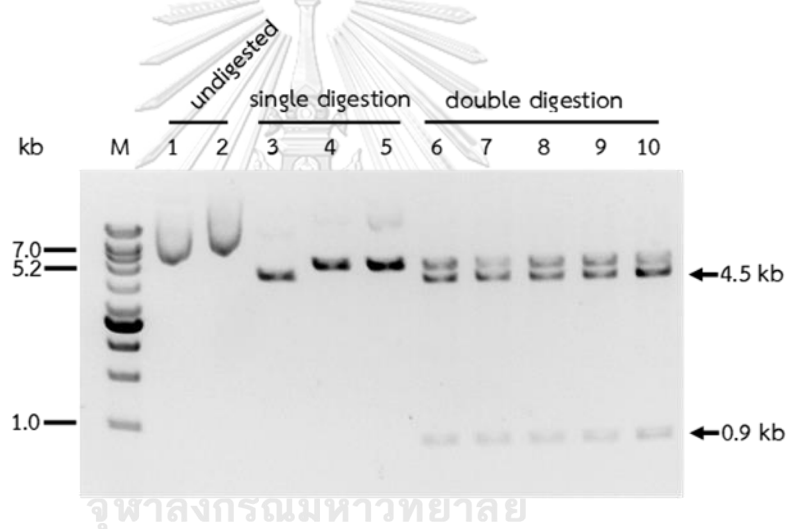
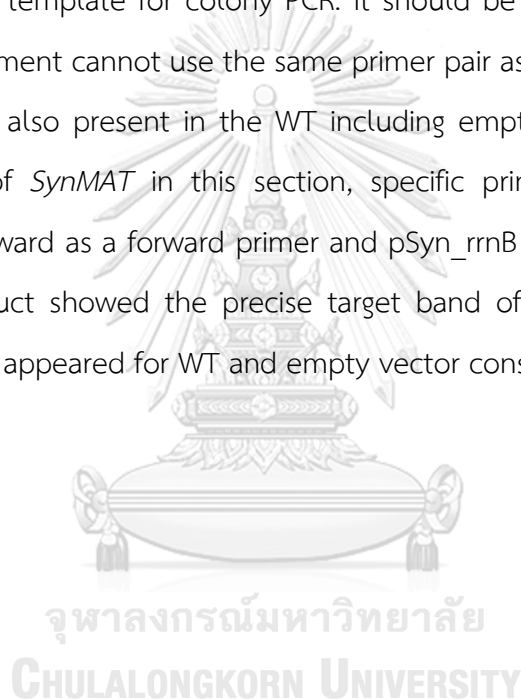


Figure 24 *SynMAT/pSyn_6* extraction (A). The *pSyn_6* vector harboring *SynMAT* gene was extracted as described in section 3.11.2.2. Lane M: DNA ladder, and Lane 1-5: *SynMAT/pSyn_6* vector extracted from candidates transformants. Restriction enzyme analysis of *SynMAT/pSyn_6* (B). The *SynMAT/pSyn_6* vector was prepared and double digested with *Nde*I and *Bam*HI. Lane M: DNA ladder, Lane 1: undigested empty vector *pSyn_6*, Lane 2: undigested *SynMAT/pSyn_6*, and Lane 3: single digestion of *pSyn_6* with *Bam*HI, Lane 4-5: single digestion of *SynMAT/pSyn_6* with *Bam*HI, and Lane 6-10: double digestion of *SynMAT/pSyn_6* vector extracted from candidate transformants.

4.5.3 Transformation of *SynMAT/pSyn_6* into *S. elongatus* PCC 7942

SynMAT/pSyn_6 vector was natural transformed into *S. elongatus* PCC 7942. The transformants were over layered onto the BG11 agar plates and selected by spectinomycin as the same as 4.4.3. Figure 25 showed that no single colony on the mock plate while the empty vector and the transformants plates showed several independent colonies. To confirm the existing of *SynMAT* gene in the transformants, the colonies of empty vector and *SynMAT/7942* were randomly picked up and were directly used as a template for colony PCR. It should be noted that amplifying the gene in this experiment cannot use the same primer pair as section 3.12.2. Because of the *SynMAT* gene also present in the WT including empty vector strain. Hence, to confirm existing of *SynMAT* in this section, specific primer pair was changed to *SynMAT_NdeI_Forward* as a forward primer and *pSyn_rrnB* as a reverse primer (Table 3). The PCR product showed the precise target band of *SynMAT* which is 0.9 kb. Whereas, no band appeared for WT and empty vector constructs (Figure 25B).



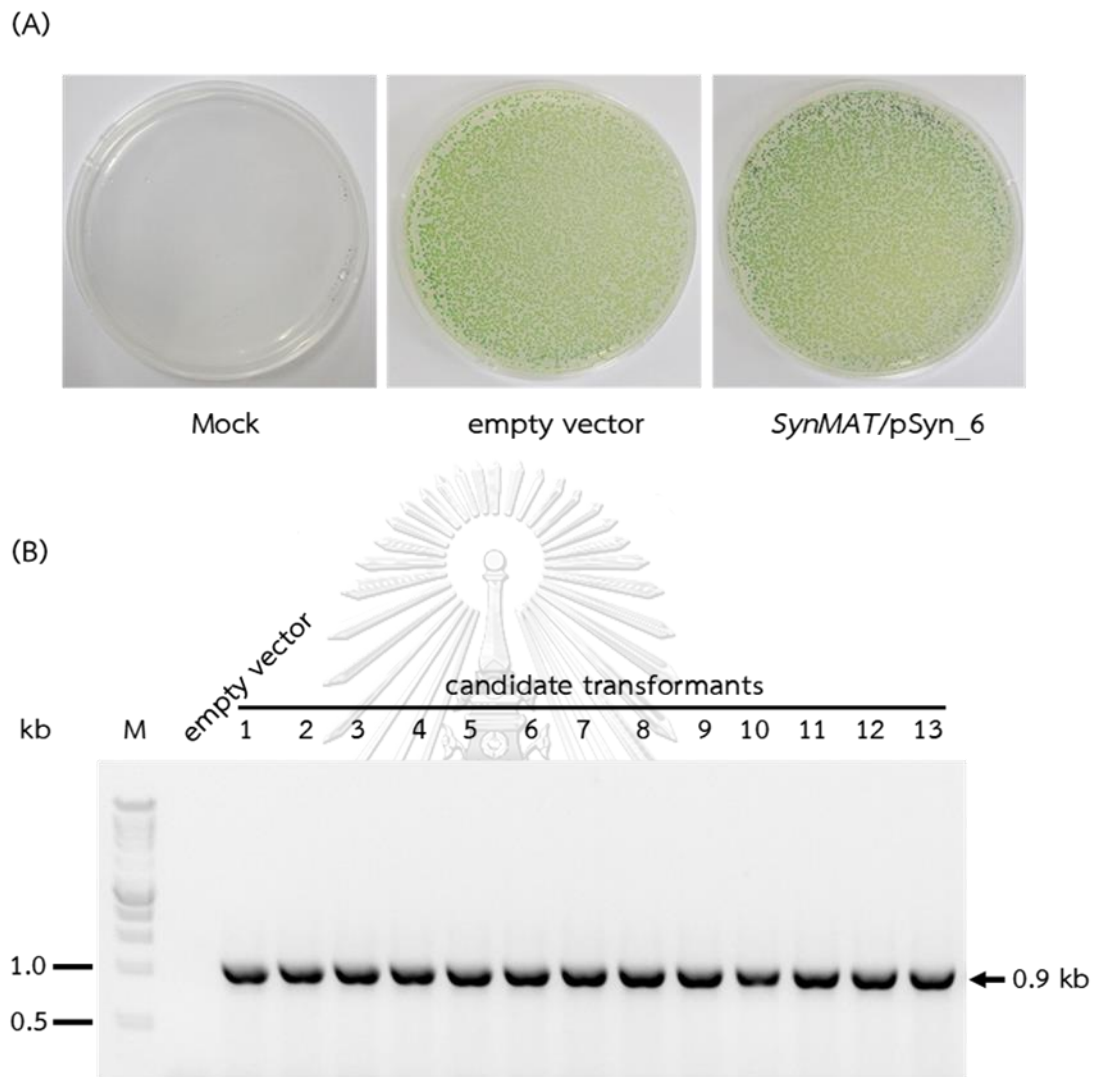


Figure 25 Natural transformation of *SynMAT/pSyn_6* in a fresh water cyanobacterium *S. elongatus* PCC 7942 on BG-11 agar plate (supplemented with 10 $\mu\text{g/ml}$ spectinomycin) plate (A). BG11 agar plates were incubated under continuous light ($50 \mu\text{mol m}^{-2}\text{s}^{-1}$) at $26 \pm 1 \text{ }^\circ\text{C}$ for 2 weeks. Colony PCR of 16 candidate transformants *SynMAT/pSyn_6* in *S. elongatus* PCC 7942 (B). A single colony of each candidate was picked up and used as template in PCR reaction. The PCR products were analyzed by gel electrophoresis on 1.2% (w/v) agarose gel precasted with SYBR[®] safe and imaged by GelDoc[™]. Lane M: DNA ladder, and Lane 1-13: candidate transformants of *SynMAT/7942*.

4.6 Analysis of expressing cells harboring *ChMAT* and *SynMAT*

4.6.1 Morphology of expressing cells

In accordance to the fact that FA is a precursor for phospholipid formation. The overexpression of genes associated with FA synthesis might affect cyanobacterial cell morphology, cell size in particular. We observed the cells of WT, empty vector, *ChMAT/7942*, and *SynMAT/7942* at exponential growth phase under light microscope. The average cell length of WT *S. elongatus* PCC 7942 was approximately 2-5 μm . There were no obviously different among WT, empty vector, and transformants (Figure 26). Nile red staining did not perform due to the cell sizes were too small to observe.

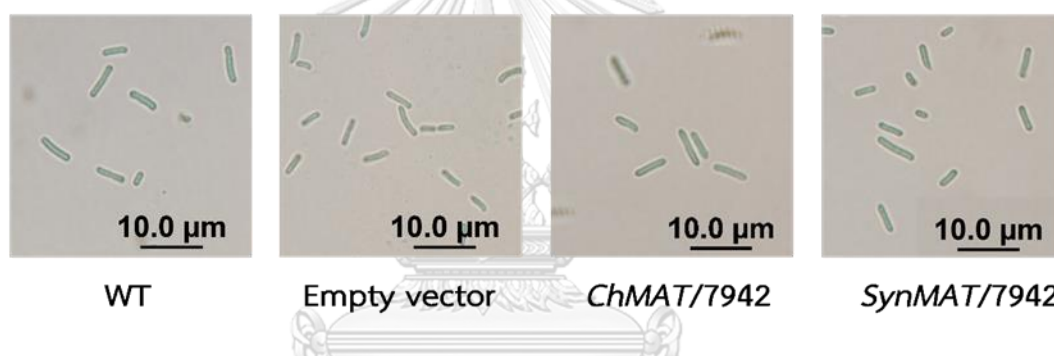


Figure 26 Morphology of *S. elongatus* PCC 7942 cells under light microscope. The cultures of wild type (WT) *S. elongatus* PCC 7942, empty vector, and the transformants of *ChMAT/7942* and *SynMAT/7942* were dropped on the glass slide and was observed under light microscope. The images were taken by DPController software.

4.6.2 Screening and comparing transformants harboring *ChMAT* and *SynMAT*

4.6.2.1 Expression analysis

We successfully transformed and confirmed the presence of *ChMAT* or *SynMAT* in *S. elongatus* PCC 7942. In this study, before detail analyses in molecular and cellular levels, we used three independent clones harboring *ChMAT* or *SynMAT* (that showed positive results in section 4.4.3 and 4.5.3). As pSyn_6 was used in constructs, the ChMAT and SynMAT proteins are fused in-frame with 6x His-tag; thus, allowing the analysis by western blotting. For ChMAT, western blotting was negative (no cross-reacting bands) (Figure 27A). One of plausible reasons may be from codon bias between *C. reinhardtii* (137c) and *S. elongatus* PCC 7942. On the other hand, the expression of SynMAT protein (from three independent clones) was clearly detected by western blot analysis, indicating the same expression level (Figure 27B). Next step, we therefore chose only one clone for analysis.

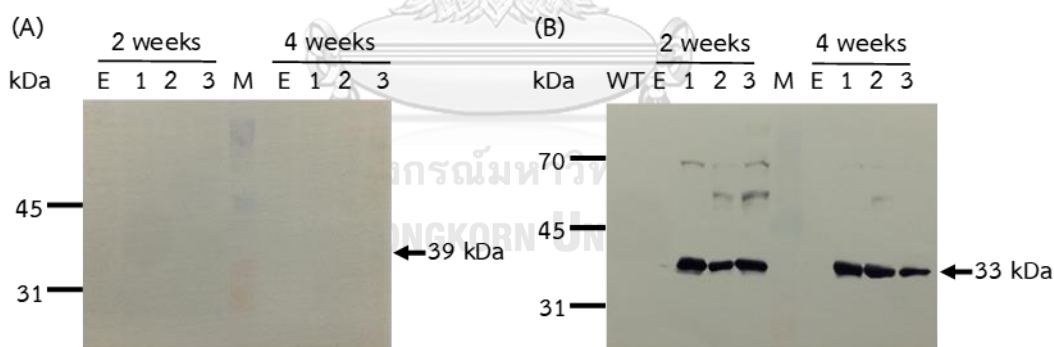


Figure 27 Western blot analysis of *ChMAT* (A) and *SynMAT* (B) expressing cells. Equal amount of crude extracted protein (20 μ g) was applied for all lanes. Blotting was done by using PVDF membrane. Antibody raised against 6x His-tag and anti-mouse IgG-HRP conjugated were used as primary and secondary antibodies, respectively. The membranes were developed by using Horseradish Peroxidase Conjugate Substrate kit.

4.6.2.2 Transcriptional analysis

4.6.2.2.1 Growth phase

Independent clones of empty vector, *ChMAT/7942*, and *SynMAT/7942* were cultured in BG11 (supplemented with spectinomycin) for 2 and 4 weeks which are exponential and stationary growth phases, respectively. Transcriptional level was analyzed by semiquantitative RT-PCR as described in section 3.13.3. Equal amount of cDNA template was confirmed by using *mpB* (Figure 28). *SynMAT* was found to be significantly up-regulated at stationary growth phase in empty vector (control transformant) which accounted for 3.37 ± 0.48 folds compared to the exponential phase. The expression level of *SynLACS* was not statistically different between exponential and stationary phase. For *ChMAT/7942*, both *SynMAT* and *SynLACS* regulation were modulated in the different growth phase.

The expression of *ChMAT* in *S. elongatus* PCC 7942 was clearly detected by RT-PCR. This confirmed that the transformation of *ChMAT* into *S. elongatus* PCC 7942 was achieved. Nonetheless, the expression of *SynMAT* at stationary phase in *SynMAT/7942* was found to be down-regulated compared to the exponential one while the expression of *SynLACS* remain unchanged. Figure 28 also demonstrated the accomplishment of *SynMAT* overexpression in *S. elongatus* PCC 7942. The expression level of this gene in *SynMAT/7942* was 8.12 ± 0.10 folds compared to control ones.

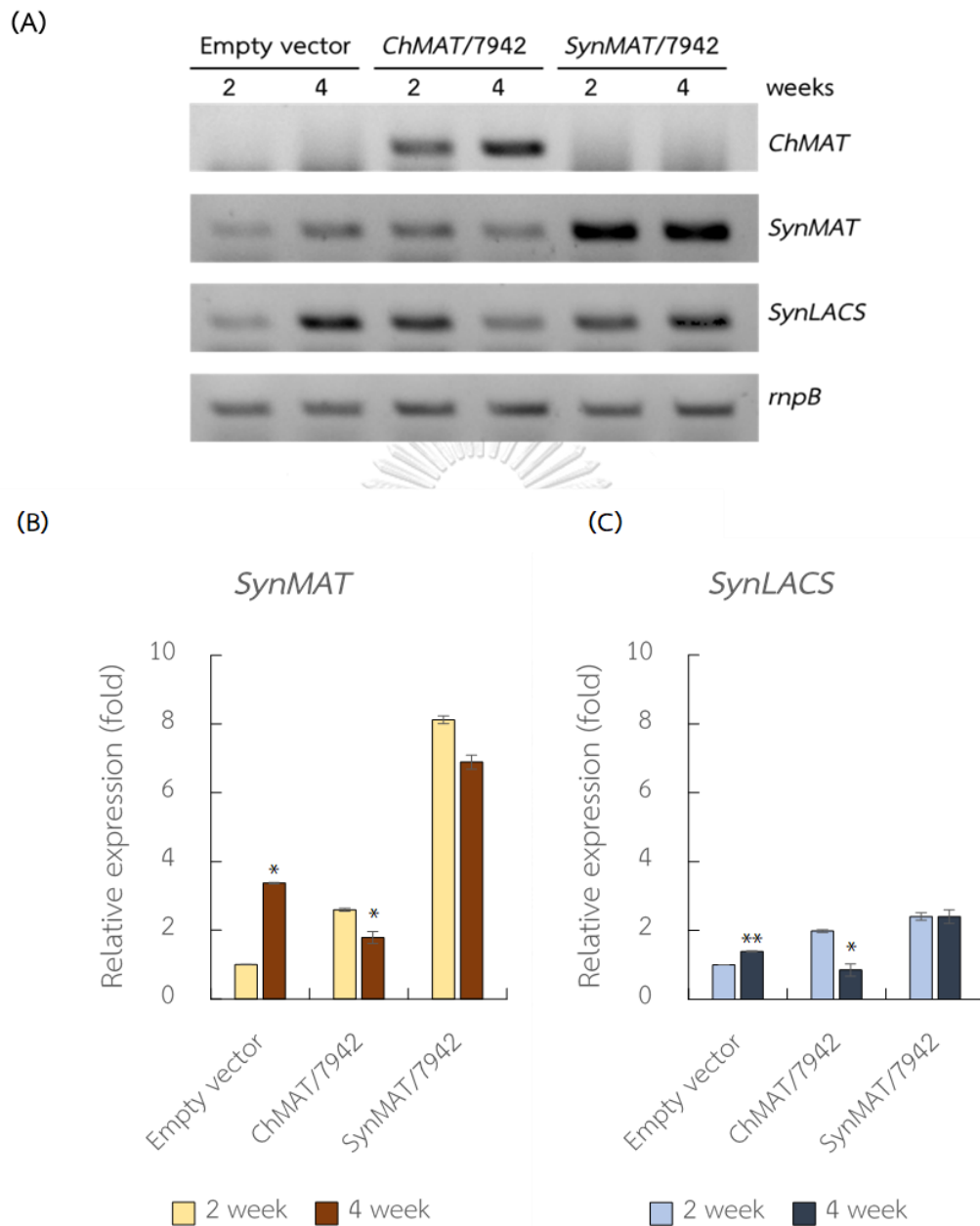


Figure 28 Semiquantitative RT-PCR analysis of two candidate transformants (A). Equality of total RNA concentrations were confirmed by an internal control *rnpB* expression. PCR products were analyzed by 1.2% (w/v) gel electrophoresis precasted with SYBR[®] safe. Relative expression analysis of stressed cells quantitated by Image Lab program (B) (* $p < 0.05$ and ** $p < 0.01$ by paired student t-test).

4.6.2.2.2 Salt stress

The WT, empty vector, and *SynMAT/7942* were cultured under salt stress (300 mM NaCl) for 0, 6, and 12 hours, respectively. To confirm the equality of total RNA, *mpB* was used as internal control. Figure 29 demonstrated that the total RNA in each condition was equal. Semiquantitative RT-PCR was performed to analyze genes expression. The results showed that the expression of *SynMAT* in the engineered strain was highly induced compared to the WT and empty vector. However, the expression seemed to be down-regulated when the cells were treated with NaCl for 6 and 12 hours. For *SynLACS*, the result showed the similar trend as *SynMAT* expression. The expression level seemed to be decreased when the cells were cultured under NaCl stress. However, the bands intensity cannot be measured due to the low intensity of the bands even in 50 cycles of PCR.

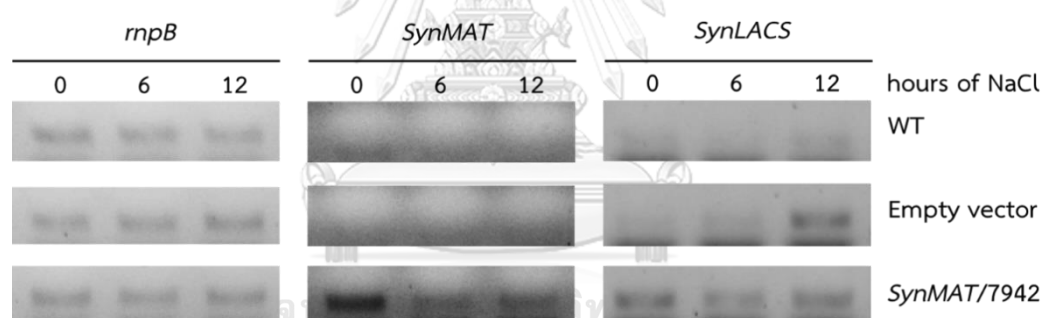


Figure 29 Semiquantitative RT-PCR analysis of two candidate transformants. Equality of total RNA concentrations were confirmed by an internal control *mpB* expression. PCR products were analyzed by 1.2% (w/v) gel electrophoresis precasted with SYBR[®] safe. WT; wild type

4.6.2.3 Protein expression analysis

Protein expression analysis was divided into two experiments. The first was the effect of different growth phase. The second was the effect of salt stress. It should be noted that, due to the protein expression of *ChMAT/7942* cannot be detected (Figure 27), this clone was therefore excluded from these experiments.

4.6.2.3.1 Growth phase

SynMAT/7942 expressing cells were cultured until the growth reached to exponential (2 weeks) and stationary growth phases (4 weeks). Crude proteins were extracted from the cells and analyzed by western blotting. Equal amount of protein was loaded into 10% acrylamide gel (Appendix 14). Figure 30 revealed that protein expression in either exponential or stationary growth phase was very similar. This result suggested that growth phase did not impact on protein expression.

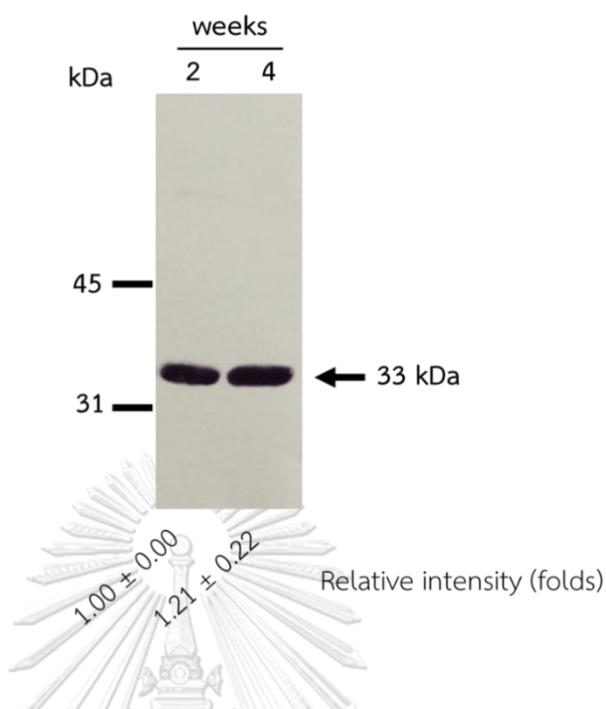


Figure 30 Western blot analysis of *SynMAT* expressing cells in different growth phase. Equal amount of crude extracted protein (20 μ g) was applied on all lanes. Blotting was done by using PVDF membrane. Antibody raised against 6x His-tag and anti-mouse IgG-HRP conjugated were used as primary and secondary antibody, respectively. The membranes were developed by using Horseradish Peroxidase Conjugate Substrate kit. The band intensity was analyzed by using ImageJ software. The data represent as mean \pm SE.

4.6.2.3.2 Salt stress

SynMAT expression in *S. elongatus* PCC 7942 that was up-shocked in 300 mM NaCl was investigated at 0, 24, and 48 hours, respectively (Figure 31). The protein was extracted and was analyzed by western blotting on PVDF membrane. The result revealed that the expression of SynMAT was moderately induced at the first 24 hours of salt stress in both candidate transformants. The expression was observed to be merely down-regulated in 48 hours of stress. This suggested that at the first 24 hours of stress, the cells might adapt themselves to tolerate in high salt concentration environment. After 24 hours, cells might synthesis another necessary enzyme for living in the harsh condition.

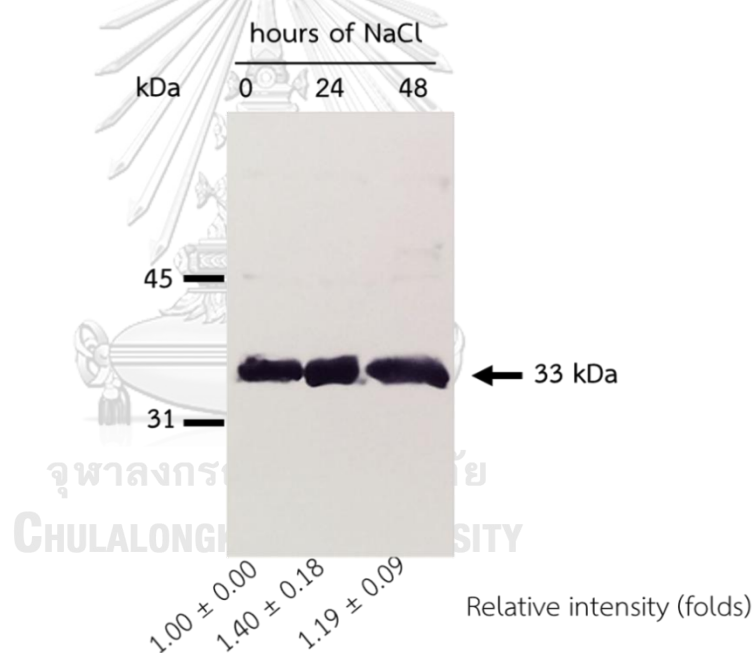


Figure 31 Western blot analysis of *SynMAT* expressing cells under 300 mM NaCl stress. Equal amount of crude extracted protein (20 μ g) was applied on all lanes. Blotting was done by using PVDF membrane. Antibody raised against 6x His-tag and anti-mouse IgG-HRP conjugated were used as primary and secondary antibody respectively. The membranes were developed by using Horseradish Peroxidase Conjugate Substrate kit. The band intensity was analyzed by using ImageJ software. The data represent as mean \pm SE.

4.6.3 FAMES analysis of *ChMAT* and *SynMAT* expressing cells

4.6.3.1 Growth phase

Two independent transformant cells of *ChMAT/7942* (1 and 3) and *SynMAT/7942* (1 and 2) were collected at the exponential growth phase ($OD_{730} \sim 0.8-1.0$). The cells were extracted for lipid as described in section 3.2.2.2. The lipid was analyzed for FA profile and lipid content by FAMES analysis. Table 5 represented that the expression of heterologous *ChMAT* and homologous *SynMAT* in *S. elongatus* PCC 7942 were not significantly changed their lipid profiles. The total FA of *SynMAT* transformants was merely increased but not significant (statistic significant = 0.05 by one-way ANOVA test).

Although heterologous expression of *ChMAT* observed in transcriptional level but not translational level (Figure 27). We could not have the plausible reason(s) to explain these results. Thus, the constant lipid content and profile in *ChMAT/7942* may not alter since protein expression seems to be low (or not succeed). In *SynMAT/7942*, transcriptional level was highly up-regulated. The translational level was considerably high (Figure 27). Table 5 showed the overexpression of *SynMAT* increased in the level of palmitic acid (C16:0) and stearic acid (C18:0). A slight decrease in palmitoleic acid (C16:1) and oleic acid (C18:1) was observed. Thus, these results impact only for C16 and C18. Very recently, overexpression of putative *fabD* (*SynMAT*) under the regulation of *trc* promotor in *S. elongatus* PCC 7942 led in the alteration of lipid composition. The increasing of myristic acid (C14:0) and palmitoleic acid (C16:1) were detected, while the level of palmitic acid (C16:0), stearic acid (C18:0), and oleic acid (C18:1) were decreased (Santos-Merino *et al.*, 2018). Although the same gene was used in this study and as reporting by Santos-Merino *et al* (2018), promotor in our case is *psbA* promotor (constitutively expressed). Thus, obtained results were different. In *E. coli*, the overexpression of *MAT* under regulation of *trc* promotor showed significantly increasing in total FA. Myristic acid (C14:0) and palmitoleic acid (C16:1) were increased whereas palmitic acid (C16:0) was unchanged (Zhang *et al.*, 2012). However, when

MAT was regulated under *lac* promoter in *E. coli*, oleic acid (C18:1) was detected to be increased while palmitoleic acid (C16:1) was decreased (Magnuson *et al.*, 1992). This inferred that the different promoter usage led to the different result in lipid profile.



Table 5 Lipid profile of *ChMAT/7942* and *SynMAT/7942* cells at the exponential growth phase. *ChMAT/7942* and *SynMAT/7942* were collected and extracted lipid as described in Materials and Methods. (ND; not detected)

Fatty acid	Empty vector	<i>ChMAT/7942</i>	<i>SynMAT/7942</i>
SATURATED FATTY ACIDS (SFAs)			
Caprylic acid (C8:0)	0.07	0.10	0.07
Capric acid (C10:0)	ND	ND	ND
Lauric acid (C12:0)	ND	ND	ND
Myristic acid (C14:0)	2.07	2.12	2.09
Palmitic acid (C16:0)	42.93	43.52	48.74
Stearic acid (C18:0)	0.36	0.30	1.12
Arachidic acid (C20:0)	ND	ND	ND
Behenic acid (C22:0)	ND	ND	ND
Lignoceric acid (C24:0)	ND	ND	ND
Total SFA	45.43	46.03	52.00
MONO-UNSATURATED FATTY ACIDS (MUFAs)			
Palmitoleic acid (C16:1)	49.38	49.42	43.91
Oleic acid (C18:1)	4.99	4.41	3.80
Erucic acid (C22:1)	ND	ND	ND
Total MUFA	54.37	53.83	47.71
POLY-UNSATURATED FATTY ACIDS (PUFAs)			
Linoleic acid (C18:2)	0.20	0.15	0.29
Linolenic acid (C18:3)	ND	ND	ND
Total PUFA	0.20	0.15	0.29
Total FA (% dry weight)	6.68	6.09	7.56

4.6.3.2 Salt stress

SynMAT/7942 transformant was subjected into NaCl stress for 0, 48, and 72 hours, respectively. Lipid profile was analyzed by FAMES analysis. At 0 hour of stress, palmitoleic acid (C16:1) showed to be the major component FA in empty vector (55.23% of total FA), followed by palmitic acid (C16:0) (38.21% of total FA). Total MUFA was 60.04% of total FA and total SFA was 39.52% of total FA. However, total PUFA was found to be extremely low. Total FA was measured to be 4.33% of DCW. In the overexpressor, *SynMAT/7942*, lipid profile was negligible different (at 0 hour of NaCl stress) comparing to the empty vector. Palmitic acid (C16:0) was no changed while palmitoleic acid (C16:1) was found to be decreased statistically. Trace amount of myristic acid (C14:0), stearic acid (C18:0), and linoleic acid (C18:2) were also detected. Under salt stress, *SynMAT/7942* exhibited the significant decreasing of palmitoleic acid (C16:1) content at 48 and 72 hours compared with the empty vector.

When the cyanobacteria were treated with salt stress, lipid profile was modulated. In empty vector, total SFA decreased at 72 hours of salt stress. This result seems to be because the low level of palmitic acid (C16:0), which is the major component of SFA. A slight increase of MUFA, especially palmitoleic acid (C16:1), was showed under 72 hours of NaCl stress. Similar as empty vector, lipid profile of transformant was altered due to NaCl. Palmitic acid (C16:0) was declined when *SynMAT/7942* was cultured under 300 mM NaCl for 48 and 72 hours. This result caused the obvious decreasing of total SFA content in *SynMAT/7942*. Palmitoleic acid (C16:1) and oleic acid (C18:1) showed slightly increased under this stress. Consequently, this resulted in the increasing of total MUFA. For total FA, there were non-statistically significant difference in all tested conditions.

UFAs are crucial for microorganisms to tolerate under stress condition particularly salinity and temperature (Lari *et al.*, 2016). Under cold stress, UFA contributes in maintaining of membrane permeability. Under salt stress; nonetheless, UFA plays an important role in protecting photosynthetic machinery (Allakhverdiev *et*

al., 2001). Overexpression of desaturase gene (*desA*) induced UFA production in *Synechocystis* sp. PCC 6803. When the transformant strain was cultured under salt stress (0.5 M NaCl), UFA was found to be increased with the tolerance of oxygen-evolving machinery (Allakhverdiev *et al.*, 1999).

In summary, FA profile observing in *SynMAT* expressing cells increased FA content, C16 and C18 in particular. As mentioned in section 4.2.2., MCFA is considered to be important in biodiesel production. Hence, overexpression of *SynMAT* might be one of an interesting alternative approach for fourth generation biofuels production.



Table 6 Lipid profile of *SynMAT/7942* cells under 300 mM NaCl stress. Empty vector and *SynMAT/7942* cells were collected and extracted lipid as described in Materials and Methods. (ND; not detected)

Fatty acid	Empty vector			<i>SynMAT/7942</i>		
	0 hour	48 hours	72 hours	0 hour	48 hours	72 hours
STATURATED FATTY ACIDS (SFAs)						
Caprylic acid (C8:0)	ND	ND	ND	ND	ND	ND
Capric acid (C10:0)	ND	ND	ND	ND	ND	ND
Lauric acid (C12:0)	ND	ND	ND	ND	ND	ND
Myristic acid (C14:0)	0.73	1.61	1.08	1.56	0.93	1.12
Palmitic acid (C16:0)	38.21	37.56	36.99	43.16	41.37	41.78
Stearic acid (C18:0)	0.58	0.53	0.44	1.57	1.26	1.20
Arachidic acid (C20:0)	ND	0.24	0.23	ND	ND	ND
Behenic acid (C22:0)	ND	ND	ND	ND	ND	ND
Lignoceric acid (C24:0)	ND	ND	ND	ND	ND	ND
Total SFA	39.52	39.94	38.74	46.29	43.56	44.10
MONO-UNSATURATED FATTY ACIDS (MUFAs)						
Palmitoleic acid (C16:1)	55.23	54.60	55.84	46.44	48.44	47.95
Oleic acid (C18:1)	4.81	4.97	4.93	6.91	7.47	7.54
Erucic acid (C22:1)	ND	ND	ND	ND	ND	ND
Total MUFA	60.04	59.57	60.77	53.35	55.91	55.49
POLY-UNSATURATED FATTY ACIDS (PUFAs)						
Linoleic acid (C18:2)	0.44	0.50	0.47	0.37	0.54	0.42
Linolenic acid (C18:3)	ND	ND	ND	ND	ND	ND
Total PUFA	0.44	0.50	0.47	0.37	0.54	0.42
Total FA (% DCW)	4.33	4.14	4.22	5.01	4.99	5.08

CHAPTER V

CONCLUSIONS

- I) Salt stress was recognized to be an attractive lipid inducer. Nile red staining indicated that LiCl was the strongest inducer. It induced lipid signal to the highest at 3.27 ± 0.16 folds compared with control condition. For NaCl and KCl, the relative intensity was peaked at 2.01 ± 0.2 and 2.22 ± 0.11 folds, respectively.
- II) FAMES analysis revealed that salt stress modified lipid composition in the green microalga. The same trend was observed in all salt stresses. Total SFA was found to be significantly increased while PUFA was dramatically decreased. For MUFA, the total content remained unchanged during cultivation time.
- III) Genes involved in FA biosynthesis were up-regulated under NaCl stress while genes associated in TAG biosynthesis were dramatically down-regulated.
- IV) Transformation of *ChMAT* or *SynMAT* into *S. elongatus* PCC 7942 was achieved. However, protein expression of ChMAT cannot be detected by western blotting while SynMAT was obviously observed.
- V) Transcriptional analysis showed high up-regulation of *SynMAT* in *SynMAT/7942* comparing with the empty vector. The expression levels were 8.12 ± 0.10 folds at exponential phase and 6.89 ± 0.74 folds at stationary phase. However, protein expression was not distinct between these phases.
- VI) Salt stress likely to affected to genes expression level in *SynMAT/7942*. *SynMAT* and *SynLACS* were found to be down-regulated. Nevertheless, protein expression was not statistically different in all time-course.
- VII) Total MUFA was observed to be slightly increased with the cultivation time under salt stress in the transformant cells.

REFERENCES

- Ajjawi, I., Verruto, J., Aqai, M., Soriaga, L. B., Coppersmith, J., Kwok, K., Peach, L., Orchard, E., Kalb, R., & Xu, W. (2017). Lipid production in *Nannochloropsis gaditana* is doubled by decreasing expression of a single transcriptional regulator. *Nature biotechnology*, *35*, 647-656.
- Allakhverdiev, S. I., Nishiyama, Y., Suzuki, I., Tasaka, Y., & Murata, N. (1999). Genetic engineering of the unsaturation of fatty acids in membrane lipids alters the tolerance of *Synechocystis* to salt stress. *Proceedings of the national academy of sciences*, *96*, 5862-5867.
- Allakhverdiev, S. I., Kinoshita, M., Inaba, M., Suzuki, I., & Murata, N. (2001). Unsaturated fatty acids in membrane lipids protect the photosynthetic machinery against salt-induced damage in *Synechococcus*. *Plant physiology*, *125*, 1842-1853.
- Alvarez, H., & Steinbüchel, A. (2002). Triacylglycerols in prokaryotic microorganisms. *Applied microbiology and biotechnology*, *60*, 367-376.
- Ambrozova, J. V., Misurcova, L., Vicha, R., Machu, L., Samek, D., Baron, M., Mlcek, J., Sochor, J., & Jurikova, T. (2014). Influence of extractive solvents on lipid and fatty acids content of edible freshwater algal and seaweed products, the green microalga *Chlorella kessleri* and the cyanobacterium *Spirulina platensis*. *Molecules*, *19*, 2344-2360.
- Amiar, S., MacRae, J. I., Callahan, D. L., Dubois, D., Van Dooren, G. G., Shears, M. J., Cesbron-Delauw, M. F., Maréchal, E., McConville, M. J., & McFadden, G. I. (2016). Apicoplast-localized lysophosphatidic acid precursor assembly is required for bulk phospholipid synthesis in *Toxoplasma gondii* and relies on an algal/plant-like glycerol 3-phosphate acyltransferase. *PLoS pathogens*, *12*, e1005765.
- Aro, E. M. (2016). From first generation biofuels to advanced solar biofuels. *Ambio*, *45*, 24-31.
- Avidan, O., Brandis, A., Rogachev, I., & Pick, U. (2015). Enhanced acetyl-CoA production is associated with increased triglyceride accumulation in the green alga *Chlorella desiccata*. *Journal of experimental botany*, *66*, 3725-3735.

- Avidan, O., & Pick, U. (2015). Acetyl-CoA synthetase is activated as part of the PDH-bypass in the oleaginous green alga *Chlorella desiccata*. *Journal of experimental botany*, *66*, 7287-7298.
- Bajhaiya, A. K., Moreira, J. Z., & Pittman, J. K. (2017). Transcriptional engineering of microalgae: prospects for high-value chemicals. *Trends in biotechnology*, *35*, 95-99.
- Bellou, S., Baeshen, M. N., Elazzazy, A. M., Aggeli, D., Sayegh, F., & Aggelis, G. (2014). Microalgal lipids biochemistry and biotechnological perspectives. *Biotechnology advances*, *32*, 1476-1493.
- Bellou, S., Triantaphyllidou, I. E., Aggeli, D., Elazzazy, A. M., Baeshen, M. N., & Aggelis, G. (2016). Microbial oils as food additives: recent approaches for improving microbial oil production and its polyunsaturated fatty acid content. *Current opinion in biotechnology*, *37*, 24-35.
- BenMoussa-Dahmen, I., Chtourou, H., Rezgui, F., Sayadi, S., & Dhouib, A. (2016). Salinity stress increases lipid, secondary metabolites and enzyme activity in *Amphora subtropica* and *Dunaliella* sp. for biodiesel production. *Bioresource technology*, *218*, 816-825.
- Bharathiraja, B., Sridharan, S., Sowmya, V., Yuvaraj, D., & Praveenkumar, R. (2017). Microbial oil—a plausible alternate resource for food and fuel application. *Bioresource technology*, *233*, 423-432.
- Brennan, L., & Owende, P. (2010). Biofuels from microalgae—a review of technologies for production, processing, and extractions of biofuels and co-products. *Renewable and sustainable energy reviews*, *14*, 557-577.
- Çakmak, Z. E., Ölmez, T. T., Çakmak, T., Menemen, Y., & Tekinay, T. (2014). Induction of triacylglycerol production in *Chlamydomonas reinhardtii*: comparative analysis of different element regimes. *Bioresource technology*, *155*, 379-387.
- Campenni, L., Nobre, B. P., Santos, C. A., Oliveira, A., Aires-Barros, M., Palavra, A., & Gouveia, L. (2013). Carotenoid and lipid production by the autotrophic microalga *Chlorella protothecoides* under nutritional, salinity, and luminosity stress conditions. *Applied microbiology and biotechnology*, *97*, 1383-1393.

- Chen, C. Y., Kao, A. L., Tsai, Z. C., Chow, T. J., Chang, H. Y., Zhao, X. Q., Chen, P. T., Su, H. Y., & Chang, J. S. (2016). Expression of type 2 diacylglycerol acyltransferase gene DGTT1 from *Chlamydomonas reinhardtii* enhances lipid production in *Scenedesmus obliquus*. *Biotechnology journal*, *11*, 336-344.
- Chen, J. E., & Smith, A. G. (2012). A look at diacylglycerol acyltransferases (DGATs) in algae. *Journal of biotechnology*, *162*, 28-39.
- Chen, X., Hu, G., & Liu, L. (2018). Hacking an algal transcription factor for lipid biosynthesis. *Trends in plant science*, *23*, 181-184.
- De Bhowmick, G., Koduru, L., & Sen, R. (2015). Metabolic pathway engineering towards enhancing microalgal lipid biosynthesis for biofuel application—a review. *Renewable and sustainable energy reviews*, *50*, 1239-1253.
- Demirbas, A., & Demirbas, M. F. (2011). Importance of algae oil as a source of biodiesel. *Energy conversion and management*, *52*, 163-170.
- Douglass, A., Fioletov, V., Godin-Beekmann, S., Müller, R., Stolarski, R., Webb, A., Arola, A., Burkholder, J., Burrows, J., & Chipperfield, M. (2011). Stratospheric ozone and surface ultraviolet radiation *Global ozone research and monitoring project—report No. 52* (pp. 1-59): World meteorological organization.
- Ducat, D. C., Way, J. C., & Silver, P. A. (2011). Engineering cyanobacteria to generate high-value products. *Trends in biotechnology*, *29*, 95-103.
- Fan, X., Burton, R., & Zhou, Y. (2010). Glycerol (byproduct of biodiesel production) as a source for fuels and chemicals mini review. *The open fuels & energy science journal*, *3*, 17-22.
- Gambelli, D., Alberti, F., Solfanelli, F., Vairo, D., & Zanolli, R. (2017). Third generation algae biofuels in Italy by 2030: a scenario analysis using bayesian networks. *Energy policy*, *103*, 165-178.
- Gammone, M. A., Riccioni, G., & D'Orazio, N. (2015). Marine carotenoids against oxidative stress: effects on human health. *Marine drugs*, *13*, 6226-6246.
- Gim, G. H., Ryu, J., Kim, M. J., Kim, P. I., & Kim, S. W. (2016). Effects of carbon source and light intensity on the growth and total lipid production of three microalgae under different culture conditions. *Journal of industrial microbiology & biotechnology*, *43*, 605-616.

- Griffiths, M. J., & Harrison, S. T. (2009). Lipid productivity as a key characteristic for choosing algal species for biodiesel production. *Journal of applied phycology*, *21*, 493-507.
- Harwati, T. U., Willke, T., & Vorlop, K. D. (2012). Characterization of the lipid accumulation in a tropical freshwater microalgae *Chlorococcum* sp. *Bioresource technology*, *121*, 54-60.
- Higgins, B. T., Gennity, I., Samra, S., Kind, T., Fiehn, O., & VanderGheynst, J. S. (2016). Cofactor symbiosis for enhanced algal growth, biofuel production, and wastewater treatment. *Algal research*, *17*, 308-315.
- Ho, S. H., Nakanishi, A., Ye, X., Chang, J. S., Hara, K., Hasunuma, T., & Kondo, A. (2014). Optimizing biodiesel production in marine *Chlamydomonas* sp. JSC4 through metabolic profiling and an innovative salinity-gradient strategy. *Biotechnology for biofuels*, *7*, 97-113.
- Ho, S. H., Nakanishi, A., Ye, X., Chang, J. S., Chen, C.-Y., Hasunuma, T., & Kondo, A. (2015). Dynamic metabolic profiling of the marine microalga *Chlamydomonas* sp. JSC4 and enhancing its oil production by optimizing light intensity. *Biotechnology for biofuels*, *8*, 48-65.
- Ho, S. H., Nakanishi, A., Kato, Y., Yamasaki, H., Chang, J. S., Misawa, N., Hirose, Y., Minagawa, J., Hasunuma, T., & Kondo, A. (2017). Dynamic metabolic profiling together with transcription analysis reveals salinity-induced starch-to-lipid biosynthesis in alga *Chlamydomonas* sp. JSC4. *Scientific reports*, *7*, 45471.
- Hockin, N. L., Mock, T., Mulholland, F., Kopriva, S., & Malin, G. (2012). The response of diatom central carbon metabolism to nitrogen starvation is different from that of green algae and higher plants. *Plant physiology*, *158*, 299-312.
- Janßen, H. J., & Steinbüchel, A. (2014). Fatty acid synthesis in *Escherichia coli* and its applications towards the production of fatty acid based biofuels. *Biotechnology for biofuels*, *7*, 7-33.
- Jüppner, J., Mubeen, U., Leisse, A., Caldana, C., Brust, H., Steup, M., Herrmann, M., Steinhauser, D., & Giavalisco, P. (2017). Dynamics of lipids and metabolites during the cell cycle of *Chlamydomonas reinhardtii*. *The plant journal*, *92*, 331-343.
- Karatay, S. E., & Dönmez, G. (2011). Microbial oil production from thermophile cyanobacteria for biodiesel production. *Applied energy*, *88*, 3632-3635.

- Kato, Y., Ho, S. H., Vavricka, C. J., Chang, J. S., Hasunuma, T., & Kondo, A. (2017). Evolutionary engineering of salt-resistant *Chlamydomonas* sp. strains reveals salinity stress-activated starch-to-lipid biosynthesis switching. *Bioresource technology*, *245*, 1484-1490.
- Khona, D. K., Shirolikar, S. M., Gawde, K. K., Hom, E., Deodhar, M. A., & D'Souza, J. S. (2016). Characterization of salt stress-induced palmelloids in the green alga, *Chlamydomonas reinhardtii*. *Algal research*, *16*, 434-448.
- Kitchener, R. L., & Grunden, A. M. (2018). Methods for enhancing cyanobacterial stress tolerance to enable improved production of biofuels and industrially relevant chemicals. *Applied microbiology and biotechnology*, *102*, 1617-1628.
- Klok, A., Lamers, P., Martens, D., Draaisma, R., & Wijffels, R. (2014). Edible oils from microalgae: insights in TAG accumulation. *Trends in biotechnology*, *32*, 521-528.
- Kreimer, G., Overländer, C., Sineshchekov, O. A., Stolzis, H., Nultsch, W., & Melkonian, M. (1992). Functional analysis of the eyespot in *Chlamydomonas reinhardtii* mutant ey 627, mt⁻. *Planta*, *188*, 513-521.
- Laemmli, U. K. (1970). Cleavage of structural proteins during the assembly of the head of bacteriophage T4. *Nature*, *227*, 680-685.
- Lari, Z., Moradi-kheibari, N., Ahmadzadeh, H., Abrishamchi, P., Moheimani, N. R., & Murry, M. A. (2016). Bioprocess engineering of microalgae to optimize lipid production through nutrient management. *Journal of applied phycology*, *28*, 3235-3250.
- Li, Y., Han, D., Hu, G., Sommerfeld, M., & Hu, Q. (2010). Inhibition of starch synthesis results in overproduction of lipids in *Chlamydomonas reinhardtii*. *Biotechnology and bioengineering*, *107*, 258-268.
- Liang, M. H., & Jiang, J. G. (2013). Advancing oleaginous microorganisms to produce lipid via metabolic engineering technology. *Progress in lipid research*, *52*, 395-408.
- Liang, M. H., & Jiang, J. G. (2016). Characterization and nitrogen deficiency response of ATP-citrate lyase from unicellular alga *Dunaliella tertiolecta*. *Algal research*, *20*, 77-86.
- Liu, X., Sheng, J., & Curtiss III, R. (2011). Fatty acid production in genetically modified cyanobacteria. *Proceedings of the national academy of sciences* 1-6.

- Lü, J., Sheahan, C., & Fu, P. (2011). Metabolic engineering of algae for fourth generation biofuels production. *Energy and environmental science*, 4, 2451-2466.
- Lurling, M., & Beekman, W. (2006). Palmelloids formation in *Chlamydomonas reinhardtii*: defence against rotifer predators? *Annales de limnologie-international journal of limnology*, 42, 65-72.
- Ma, X., Yao, L., Yang, B., Lee, Y. K., Chen, F., & Liu, J. (2017). RNAi-mediated silencing of a pyruvate dehydrogenase kinase enhances triacylglycerol biosynthesis in the oleaginous marine alga *Nannochloropsis salina*. *Scientific reports*, 7, 11485.
- Ma, Y. H., Wang, X., Niu, Y. F., Yang, Z. K., Zhang, M. H., Wang, Z. M., Yang, W. D., Liu, J. S., & Li, H. Y. (2014). Antisense knockdown of pyruvate dehydrogenase kinase promotes the neutral lipid accumulation in the diatom *Phaeodactylum tricornutum*. *Microbial cell factories*, 13, 100-109.
- Machado, I. M., & Atsumi, S. (2012). Cyanobacterial biofuel production. *Journal of biotechnology*, 162, 50-56.
- Magnuson, K., Oh, W., Larson, T. J., & Cronan, J. E. (1992). Cloning and nucleotide sequence of the *fabD* gene encoding malonyl coenzyme A-acyl carrier protein transacylase of *Escherichia coli*. *FEBS letters*, 299, 262-266.
- Mata, T. M., Martins, A. A., & Caetano, N. S. (2010). Microalgae for biodiesel production and other applications: a review. *Renewable and sustainable energy reviews*, 14, 217-232.
- Michalak, I., & Chojnacka, K. (2015). Algae as production systems of bioactive compounds. *Engineering in life sciences*, 15, 160-176.
- Milano, J., Ong, H. C., Masjuki, H., Chong, W., Lam, M. K., Loh, P. K., & Vellayan, V. (2016). Microalgae biofuels as an alternative to fossil fuel for power generation. *Renewable and sustainable energy reviews*, 58, 180-197.
- Minhas, A. K., Hodgson, P., Barrow, C. J., & Adholeya, A. (2016). A review on the assessment of stress conditions for simultaneous production of microalgal lipids and carotenoids. *Frontiers in microbiology*, 7, 546-565.

- Moellering, E. R., Miller, R., & Benning, C. (2009). Molecular genetics of lipid metabolism in the model green alga *Chlamydomonas reinhardtii* *Lipids in photosynthesis* (Vol. 30, pp. 139-155). Illinois, USA: Springer.
- Mohan, S. V., Rohit, M., Chiranjeevi, P., Chandra, R., & Navaneeth, B. (2015). Heterotrophic microalgae cultivation to synergize biodiesel production with waste remediation: progress and perspectives. *Bioresource technology*, *184*, 169-178.
- Moon, M., Kim, C. W., Park, W. K., Yoo, G., Choi, Y.-E., & Yang, J. W. (2013). Mixotrophic growth with acetate or volatile fatty acids maximizes growth and lipid production in *Chlamydomonas reinhardtii*. *Algal research*, *2*, 352-357.
- Mühlroth, A., Li, K., Røkke, G., Winge, P., Olsen, Y., Hohmann-Marriott, M. F., Vadstein, O., & Bones, A. M. (2013). Pathways of lipid metabolism in marine algae, co-expression network, bottlenecks and candidate genes for enhanced production of EPA and DHA in species of *Chromista*. *Marine drugs*, *11*, 4662-4697.
- Najafabadi, H. A., Malekzadeh, M., Jalilian, F., Vossoughi, M., & Pazuki, G. (2015). Effect of various carbon sources on biomass and lipid production of *Chlorella vulgaris* during nutrient sufficient and nitrogen starvation conditions. *Bioresource technology*, *180*, 311-317.
- Nakanishi, A., Aikawa, S., Ho, S. H., Chen, C. Y., Chang, J. S., Hasunuma, T., & Kondo, A. (2014). Development of lipid productivities under different CO₂ conditions of marine microalgae *Chlamydomonas* sp. JSC4. *Bioresource technology*, *152*, 247-252.
- Nascimento, I. A., Marques, S. S. I., Cabanelas, I. T. D., Pereira, S. A., Druzian, J. I., de Souza, C. O., Vich, D. V., de Carvalho, G. C., & Nascimento, M. A. (2013). Screening microalgae strains for biodiesel production: lipid productivity and estimation of fuel quality based on fatty acids profiles as selective criteria. *Bioenergy research*, *6*, 1-13.
- Niu, Y. F., Wang, X., Hu, D. X., Balamurugan, S., Li, D. W., Yang, W. D., Liu, J. S., & Li, H. Y. (2016). Molecular characterization of a glycerol-3-phosphate acyltransferase reveals key features essential for triacylglycerol production in *Phaeodactylum tricorutum*. *Biotechnology for biofuels*, *9*, 60-71.

- Noraini, M., Ong, H. C., Badrul, M. J., & Chong, W. (2014). A review on potential enzymatic reaction for biofuel production from algae. *Renewable and sustainable energy reviews, 39*, 24-34.
- Nozzi, N. E., Oliver, J. W., & Atsumi, S. (2013). Cyanobacteria as a platform for biofuel production. *Frontiers in bioengineering and biotechnology, 1*, 7-13.
- Oliver, N. J., Rabinovitch-Deere, C. A., Carroll, A. L., Nozzi, N. E., Case, A. E., & Atsumi, S. (2016). Cyanobacterial metabolic engineering for biofuel and chemical production. *Current opinion in chemical biology, 35*, 43-50.
- Pancha, I., Chokshi, K., & Mishra, S. (2015). Enhanced biofuel production potential with nutritional stress amelioration through optimization of carbon source and light intensity in *Scenedesmus* sp. CCNM 1077. *Bioresource technology, 179*, 565-572.
- Patel, M. S., Nemeria, N. S., Furey, W., & Jordan, F. (2014). The pyruvate dehydrogenase complexes, structure-based function and regulation. *Journal of biological chemistry* 1-19.
- Peramuna, A., & Summers, M. L. (2014). Composition and occurrence of lipid droplets in the cyanobacterium *Nostoc punctiforme*. *Archives of microbiology, 196*, 881-890.
- Quintana, N., Van der Kooy, F., Van de Rhee, M. D., Voshol, G. P., & Verpoorte, R. (2011). Renewable energy from cyanobacteria: Energy production optimization by metabolic pathway engineering. *Applied microbiology and biotechnology, 91*, 471-490.
- Radakovits, R., Jinkerson, R. E., Darzins, A., & Posewitz, M. C. (2010). Genetic engineering of algae for enhanced biofuel production. *Eukaryotic cell, 9*, 486-501.
- Radakovits, R., Jinkerson, R. E., Fuerstenberg, S. I., Tae, H., Settlage, R. E., Boore, J. L., & Posewitz, M. C. (2012). Draft genome sequence and genetic transformation of the oleaginous alga *Nannochloropsis gaditana*. *Nature communications, 3*, 686-697.
- Ramanan, R., Kim, B. H., Cho, D. H., Ko, S. R., Oh, H. M., & Kim, H. S. (2013). Lipid droplet synthesis is limited by acetate availability in starchless mutant of *Chlamydomonas reinhardtii*. *FEBS letters, 587*, 370-377.
- Reig, M., Casas, S., Aladjem, C., Valderrama, C., Gibert, O., Valero, F., Centeno, C. M., Larrotcha, E., & Cortina, J. L. (2014). Concentration of NaCl from seawater reverse

- osmosis brines for the chlor-alkali industry by electrodialysis. *Desalination*, *342*, 107-117.
- Rismani-Yazdi, H., Haznedaroglu, B. Z., Bibby, K., & Peccia, J. (2011). Transcriptome sequencing and annotation of the microalgae *Dunaliella tertiolecta*: pathway description and gene discovery for production of next-generation biofuels. *Biomed central*, *12*, 148-165.
- Rittmann, B. E. (2008). Opportunities for renewable bioenergy using microorganisms. *Biotechnology and bioengineering*, *100*, 203-212.
- Ruenwai, R., Cheevadhanarak, S., & Laoteng, K. (2009). Overexpression of acetyl-CoA carboxylase gene of *Mucor rouxii* enhanced fatty acid content in *Hansenula polymorpha*. *Molecular biotechnology*, *42*, 327-332.
- Ruffing, A. M., & Jones, H. D. (2012). Physiological effects of free fatty acid production in genetically engineered *Synechococcus elongatus* PCC 7942. *Biotechnology and bioengineering*, *109*, 2190-2199.
- Ruffing, A. M. (2014). Improved free fatty acid production in cyanobacteria with *Synechococcus* sp. PCC 7002 as host. *Frontiers in bioengineering and biotechnology*, *2*, 17-27.
- Ryall, K., Harper, J. T., & Keeling, P. J. (2003). Plastid-derived Type II fatty acid biosynthetic enzymes in chromists. *Gene*, *313*, 139-148.
- Salama, E. S., Kim, H. C., Abou-Shanab, R. A., Ji, M. K., Oh, Y. K., Kim, S. H., & Jeon, B. H. (2013). Biomass, lipid content, and fatty acid composition of freshwater *Chlamydomonas mexicana* and *Scenedesmus obliquus* grown under salt stress. *Bioprocess and biosystems engineering*, *36*, 827-833.
- Santos-Merino, M., Garcillán-Barcia, M. P., & de la Cruz, F. (2018). Engineering the fatty acid synthesis pathway in *Synechococcus elongatus* PCC 7942 improves omega-3 fatty acid production. *Biotechnology for biofuels*, *11*, 239-252.
- Sarsekeyeva, F., Zayadan, B. K., Usserbaeva, A., Bedbenov, V. S., Sinetova, M. A., & Los, D. A. (2015). Cyanofuels: biofuels from cyanobacteria. Reality and perspectives. *Photosynthesis research*, *125*, 329-340.

- Sato, N., Tsuzuki, M., Matsuda, Y., Ehara, T., Osafune, T., & Kawaguchi, A. (1995). Isolation and characterization of mutants affected in lipid metabolism of *Chlamydomonas reinhardtii*. *European journal of biochemistry*, *230*, 987-993.
- Savakis, P., & Hellingwerf, K. J. (2015). Engineering cyanobacteria for direct biofuel production from CO₂. *Current opinion in biotechnology*, *33*, 8-14.
- Shtaida, N., Khozin-Goldberg, I., Solovchenko, A., Chekanov, K., Didi-Cohen, S., Leu, S., Cohen, Z., & Boussiba, S. (2014). Downregulation of a putative plastid PDC E1 α subunit impairs photosynthetic activity and triacylglycerol accumulation in nitrogen-starved photoautotrophic *Chlamydomonas reinhardtii*. *Journal of experimental botany*, *65*, 6563-6576.
- Shtaida, N., Khozin-Goldberg, I., & Boussiba, S. (2015). The role of pyruvate hub enzymes in supplying carbon precursors for fatty acid synthesis in photosynthetic microalgae. *Photosynthesis research*, *125*, 407-422.
- Shukla, M., Tabassum, R., Singh, R., & Dhar, D. W. (2016). Influence of light intensity, temperature and CO₂ concentration on growth and lipids in green algae and cyanobacteria. *Indian journal of experimental biology* *54*, 482-487.
- Siaut, M., Cuiné, S., Cagnon, C., Fessler, B., Nguyen, M., Carrier, P., Beyly, A., Beisson, F., Triantaphylidès, C., & Li-Beisson, Y. (2011). Oil accumulation in the model green alga *Chlamydomonas reinhardtii*: characterization, variability between common laboratory strains and relationship with starch reserves. *BMC biotechnology*, *11*, 7-22.
- Silva, C. S. P., Silva-Stenico, M. E., Fiore, M. F., de Castro, H. F., & Da Rós, P. C. M. (2014). Optimization of the cultivation conditions for *Synechococcus* sp. PCC7942 (cyanobacterium) to be used as feedstock for biodiesel production. *Algal research*, *3*, 1-7.
- Sirikhachornkit, A., Vuttipongchaikij, S., Suttangkakul, A., Yokthongwattana, K., Juntawong, P., Pokethitiyook, P., Kangvansaichol, K., & Meetam, M. (2016). Increasing the triacylglycerol content in *Dunaliella tertiolecta* through isolation of starch-deficient mutants. *Journal of microbiology and biotechnology*, *28*, 854-866.

- Spolaore, P., Joannis-Cassan, C., Duran, E., & Isambert, A. (2006). Commercial applications of microalgae. *Journal of bioscience and bioengineering*, *101*, 87-96.
- Sutendra, G., & Michelakis, E. D. (2013). Pyruvate dehydrogenase kinase as a novel therapeutic target in oncology. *Frontiers in oncology*, *3-14*, 38-49.
- Sutendra, G., Kinnaird, A., Dromparis, P., Paulin, R., Stenson, T. H., Haromy, A., Hashimoto, K., Zhang, N., Flaim, E., & Michelakis, E. D. (2014). A nuclear pyruvate dehydrogenase complex is important for the generation of acetyl-CoA and histone acetylation. *Cell*, *158*, 84-97.
- Taghavi, N., & Robinson, G. (2016). Improving the optimum yield and growth of *Chlamydomonas reinhardtii* CC125 and CW15 using various carbon sources and growth regimes. *African journal of biotechnology*, *15*, 1083-1100.
- Tan, H., Aziz, A. A., & Aroua, M. (2013). Glycerol production and its applications as a raw material: a review. *Renewable and sustainable energy reviews*, *27*, 118-127.
- Timmons, T. M., & Dunbar, B. S. (1990). Protein blotting and immunodetection *Methods in enzymology* (Vol. 182, pp. 679-688). California, USA: Elsevier.
- Úbeda-Mínguez, P., García-Maroto, F., & Alonso, D. L. (2017). Heterologous expression of *DGAT* genes in the marine microalga *Tetraselmis chui* leads to an increase in TAG content. *Journal of applied phycology*, *29*, 1913-1926.
- van Eerden, F. J., de Jong, D. H., de Vries, A. H., Wassenaar, T. A., & Marrink, S. J. (2015). Characterization of thylakoid lipid membranes from cyanobacteria and higher plants by molecular dynamics simulations. *Biochimica et biophysica acta*, *1848*, 1319-1330.
- Vargas, M., Rodriguez, H., Moreno, J., Olivares, H., Campo, J. d., Rivas, J., & Guerrero, M. (1998). Biochemical composition and fatty acid content of filamentous nitrogen-fixing cyanobacteria. *Journal of phycology*, *34*, 812-817.
- Vigani, M., Parisi, C., Rodríguez-Cerezo, E., Barbosa, M. J., Sijtsma, L., Ploeg, M., & Enzing, C. (2015). Food and feed products from micro-algae: market opportunities and challenges for the EU. *Trends in food science and technology*, *42*, 81-92.
- Wagner, M., Hoppe, K., Czabany, T., Heilmann, M., Daum, G., Feussner, I., & Fulda, M. (2010). Identification and characterization of an acyl-CoA: diacylglycerol

- acyltransferase 2 (*DGAT2*) gene from the microalga *O. tauri*. *Plant physiology and biochemistry*, 48, 407-416.
- Wang, H. M. D., Chen, C. c., Huynh, P., & Chang, J. S. (2015). Exploring the potential of using algae in cosmetics. *Bioresource technology*, 184, 355-362.
- Wang, T., Ge, H., Liu, T., Tian, X., Wang, Z., Guo, M., Chu, J., & Zhuang, Y. (2016). Salt stress induced lipid accumulation in heterotrophic culture cells of *Chlorella protothecoides*: mechanisms based on the multi-level analysis of oxidative response, key enzyme activity and biochemical alteration. *Journal of biotechnology*, 228, 18-27.
- Xiao, Y., Zhang, J., Cui, J., Yao, X., Sun, Z., Feng, Y., & Cui, Q. (2015). Simultaneous accumulation of neutral lipids and biomass in *Nannochloropsis oceanica* IMET1 under high light intensity and nitrogen replete conditions. *Algal research*, 11, 55-62.
- Xue, J., Niu, Y. F., Huang, T., Yang, W. D., Liu, J. S., & Li, H. Y. (2015). Genetic improvement of the microalga *Phaeodactylum tricornutum* for boosting neutral lipid accumulation. *Metabolic engineering*, 27, 1-9.
- Yao, L., Shen, H., Wang, N., Tatlay, J., Li, L., Tan, T. W., & Lee, Y. K. (2017). Elevated acetyl-CoA by amino acid recycling fuels microalgal neutral lipid accumulation in exponential growth phase for biofuel production. *Plant biotechnology journal*, 15, 497-509.
- Yu, A. Q., Juwono, P., Kurniasih, N., Leong, S. S. J., & Chang, M. W. (2014). Production of fatty acid-derived valuable chemicals in synthetic microbes. *Frontiers in bioengineering and biotechnology*, 2, 78-90.
- Zalutskaya, Z., Kharatyan, N., Forchhammer, K., & Ermilova, E. (2015). Reduction of PII signaling protein enhances lipid body production in *Chlamydomonas reinhardtii*. *Plant science*, 240, 1-9.
- Zhang, L., Pei, H., Chen, S., Jiang, L., Hou, Q., Yang, Z., & Yu, Z. (2018). Salinity-induced cellular cross-talk in carbon partitioning reveals starch-to-lipid biosynthesis switching in low-starch freshwater algae. *Bioresource technology*, 250, 449-456.

- Zhang, X., Agrawal, A., & San, K. Y. (2012). Improving fatty acid production in *Escherichia coli* through the overexpression of malonyl CoA-acyl carrier protein transacylase. *Biotechnology progress*, 28, 60-65.
- Zienkiewicz, K., Du, Z. Y., Ma, W., Vollheyde, K., & Benning, C. (2016). Stress-induced neutral lipid biosynthesis in microalgae-molecular, cellular and physiological insights. *Biochimica et biophysica acta*, 1861, 1269-1281.



Online references

Life science. Global warming: news, facts, causes & effects [online]. 2018. Available from: <https://www.livescience.com/topics/global-warming> [10 September 2018]

NASA. June 2018 ties for third-warmest June on record [online]. 2018. Available from: <https://climate.nasa.gov/news/2766/june-2018-ties-for-third-warmest-june-on-record/> [10 September 2018]

NASA. Carbon dioxide [online]. 2018. Available from: <https://climate.nasa.gov/> [10 September 2018]

United states environmental protection agency. Overview of Greenhouse Gases [online]. 2017. Available from: <https://www.epa.gov/ghgemissions/overview-greenhouse-gases> [10 September 2018]

Thesis references

Atikij, T. (2015). *Expression level analysis of genes involved in lipid synthesis in green microalga Chlamydomonas reinhardtii (137c) under salt stress*. Bachelor's degree, Department of microbiology, Faculty of science, Chulalongkorn university. (written in Thai)

Miller, R. E. (2015). *Triacylglycerol biosynthesis in Chlamydomonas reinhardtii*. Doctor of philosophy, Department of cell and molecular biology, Faculty of biomedical physical sciences, Michigan state university.



APPENDICES

จุฬาลงกรณ์มหาวิทยาลัย
CHULALONGKORN UNIVERSITY

Appendix 1

Amino acid sequence

1. Microalgae and plants

1.1. *Chlamydomonas reinhardtii* (Accession number: XP_001689862)

MVAVRGRRALAVRASGDDAFANYKPTIAALFPGQGAQSVGMAKDLVATVPKAKEMFDKASEILGYD
LLKVCVEGPKEKLDSTAVSQPAIYVASLAAVEKLRADGQVRVLGFEGPGYARACDWWLGGASVRH
AAVATHNRPALPPLCAPPPSARAHLSLCSHTILPPFAATEQVGQDKPVQIANYLCPGNYAVSGSKE
GCDAVEKLGKSFGARMTVRLAVAGAFHTSYMSPAVDKLKAALAQVRGRGGGRVGGGEAGGGRPHS
DPAVIKDILSRQVTSPVLWENTIKSLQEKGLTKSYEVPKVIAGIVKRMDKGANIVNITA

1.2. *Volvox carteri f. nagariensis* (Accession number: XP_002949800)

MALLSSAQRICALQGRVNAFKPCAPALSIRGRKAVAVRAASDDAFAAYKPTTAALFPGQGAQSVGM
AKDLVAEVPAAKELFDKASEILGYDLLKLCVEGPKDKLDSTAISQPAIYVASLAAVEKLRATEGQAAID
AIDVAAGLSLGEYTALAFAGAMSFEDGLRLVKLRGESMQAAADAQPSSMVSIGLDSGKVAELCKA
ATAQVGEDKPKIANFLCPGNYAVSGSKEGCDAVEKLGKSFGARMTVRLAVAGAFHTEYMSPAVAK
LREALAATTLVTPRIPVSNVDAQPHSDPATIKDILSRQVTSPVLWENTIKTLQEKGLTKSYEIGPGKVI
AGIVKRMDKGANIVNITA

1.3. *Gonium pectorale* (Accession number: KXZ48432)

MALLSSAQRICALKGRAAAFQPCAPALAGRGRRALAVRAAADDASFASYKPTVAALFPGQGAQSVGM
AKDLVSVPAKELFDKAADILGYDLYKLCVEGPKDKLDSTAISQPAIYVASLAAVEKLRATEGQAAIDSI
DVAAGLSLGEYTALAFAGAMSFEDGLRLVALRGASMQAADAQPSSMVSIGLDSAKVAELCKAAT
AEAGEDKPKIANFLCPGNYAVSGSKEGCDAVEKLGKSFGARMTVRLAVAGAFHTEYMSPAVGKLR
EALAATTISTPRIPVSNVDAAPHSDPEVIKDILSRQVTSPVLWENTVKILMEKGMTKSYEIGPGKVIAG
IVKRIDKAHNIINITA

1.4. *Haematococcus lacustris* (Accession number: AEF13163)

MRIARGAASSHRAASYCARARKVSVRAVAAPAVWHAPSDTKFDDYKPSVAFFPGQGVQSVGMAK
DLVAEVPAAKAMFDKASEILGYDLLQLCVEGPKEKLDSTVYSQPAIYVASLAAVEKLRATEGQAAVD
AIDVACGLSLGEHTALAFAGAFSFEDGLRLVKLXGESMQAAADASPSGMVSVGLDSSKVAELCAA
ATAEVGEDKAVKIANYLCPGNYAVSGSKEGCAAVEKLGKSFKARMTVRLAVAGAFHTEYVQPAVAKL
LTALDATDLRIPRIPVISNVDAQPHSDPGTIRQILAQQVTSPVLWENSLKTLFDKGLGKSYEIGPGKVIA
GIVKRINKEHAITNVTA

1.5. *Coccomyxa subellipsoidea* C-169 (Accession number: XP_005651334)

MALKASPMSVNLRSVLGTRKFRSRTSVAKPTRSQTVRPKATASVAEKTSDTKFAQYTPGTAFLFPGQ
GAQTVGMAKDVVEEVPAAKDLFDRASEILGYDLLKLCVEGPKERLDSTVISQPAIYVASLAAVEKLRRL
TEGEEAVQAADVAAGLSLGEYTALTFAGALKFEDGVRLVKIRGESMQAAADARPSAMVSVIGLAADK
VEELCEANKEVGADEGVRIANFLCNGNYAVSGGLPGCEAVEKLAJSFKARMTVRLAVAGAFHTAY
MQPAEEKLREALASTEIVPRIPVSNVDAQPHSDPDVIKDILARQLTSPVQWEKSMQTMLEKGLER
SFEIGPNKVIAGILKRIDKKHSVTNIQV

1.6. *Chlorella variabilis* (Accession number: XP_005848556)

MKAGTLPCPGRTAEELKRQRDAAELKKGKEQRRARVAADAAAAAGPATPAAKPAAPATPIAFLFP
GQGSQAVGMLKESKDLPAVRKMLDTAQAVLGYDLLALCLEGPKEKLDDTVYAQPALFVAGLAAVE
RLRSQNPAAVDGCACAGLSLGEYTALVFAGALSFEDGLKVVKVRAESMSAAAKQGKPHGMLSV
GLGDADLEGVCAAVRAARPDVAVCQLANFLFPOGRVVS GHKDALEEVQRQATAKGALKAVPVAVSG
AFHTPLMQPARDALTQVLSSVSIREPRIPIYSNVTGEPFQGAADIAALLPRQLVEPVQWEGTIRKLV
AGKNQMHELPGGQIQIKAMVKRVDNAAWAALKNTAA

1.7. *Oryza sativa japonica* (Accession number: XP_015628213)

MLRCPPRRRLCLRLGSPVSTMASTLAFLRPSAPAPLAASRGAARGVPAAVRVPCRSRVSAAGVSLGS
EVAVGSDALFADYKPTTAFLFPGQGAQTVGMGAEAVNVPAAAKLFDKANDILGYDLLDFCTNGPK
KLDSTVISQPAIYVTSLAAVEVLRSDGGQONVIDSDVTCGLSLGEYTALAFAGAFSFEDGLKLVKLRG
EAMQDASDAASSAMVSVIGLDSEKVQQLCDAANEEVDEKERVQIANFLCPGNYAVSGGVKIEAVE

AKAKSFKARMTVRLAVAGAFHTSFMQPAVSRLSALAETEIKTPRIPVISNVDASPHSDPDTIKKILAR
QVTSPVQWESTVKTLMGKGLEKSYELGPGKVIAGILKRIDKGASIEENIGA

1.8. *Linum usitatissimum* (Accession number: AGD95011)

MASSLAFPAPSPRSLFSAIDGCSRNGARGFGVKSFARSRVSMSVSLGSQTVVDDSLFADYKPTSAFL
FPGQGAQAVGMGKEAQSVAAAELYKKANDILGYDLLELCLAGPKEKLDSTVISQPAIYVTSAAVE
MLRARDGGQIIDSVDVTCGLSLGEYALAFSGAFSFDGLKLVKLRGEAMQEASDAAKSAMVSIIGL
DSDKVQQLCDAANQEVDEAEKVQIANFLCTGNYAVSGGVKIEAVEAKAKSFKARMTVRLAVAGAF
HTSFMQPAVSRLSALAETEIRSPRIPVISNVDQAQPHADPATIKKILARQVTSPVQWETTUKTLGKGL
KKSYLELGPVGIAGIVKRMDRGAELENISA

1.9. *Theobroma cacao* (Accession number: XP_007016988)

MHTLLHLRLASSANSHYSLFAMSAASLALPSSLSL RANGAAPPFCFRLHNPSRVRVMSVSVGSQ
AVVDDALFADYKPTSAFLFPGQGAQAVGMGKEAQSVAAAELYKKANDILGFDLLDVCINGPKEKL
DSTVISQPAIYVTSAAVELLRTRDGGQIIDSVDVTCGLSLGEYALAFAGAFSFEGLKLVKLRGEA
MQEAADAAMVSVIGLDSEKVQQLCDAANQEVDEADKVQIANFLCPGNYAVSGGVKIEAVEA
KAKSFKARMTVRLAVAGAFHTSFMQPAVSRLSALAATEQVTRIPRIPVISNVDQAQPHADSETIKKILAR
QVTSPVQWETTUKTLTKGLKKSYLELGPVGIAGIVKRMMDKGAEIENIGA

1.10. *Triticum urartu* (Accession number: EMS56914)

MLLRPPRLPRLSPRRLRSDSPMASTLALLRPSAPSPATNLRAPFRSRVSTRVSVGSAVAAGADTLFA
DYKPTTAFLFPGQGAQAVGMGKEALNVRAAAELFDKANDILGYDLLNLCIDGPKEKLNSTVISQPAIY
VTSAAVEVLRAREEQSVINSVDVTCGLSLGEYALAFAGAFSFDGLKLVKLRGEAMQDASDAAN
SAMVSVIGLDSEKVQQLCDAANEDVDEKERVQIANFLCPGNYAVSGGVKIEAVEAKAKSFKARMTV
RLAVAGAFHTSFMQPAVSRLSALAATEIRSPRIPVISNVDQAQPHSDPETIKKILAQQVTSPVHWETT
VTLLGRGLEKSYELGPGKVIAGIIRINKGASIEENIGA

1.11. *Capsicum annuum* (Accession number: NP_001311562)

MLFSAFTINTTESTCSSTTMSCSSTLILPSVVTKNGFRFRSSKQQLDKSRVFMSTISVGSRAAASAVV
DDALFADYKPTNAFLFPGQGAQAVGMGVEAQKVPAAAELYKRANEIMGFDLLDICINGPKEKLDST

VLSQPAIYVTSAAVEMLRAREGGQLIIDSVDVTCGLSLGEY TALAFAGAFS FEDGLKLVKLRGEAMQ
 DAADAAKSAMVSIIGLDSDKVQQLCDAANEEVDEANKVQIANFLCPGNYAVSGGVKIEAVEAKAKS
 FKARMTVRLAVAGAFHTSFMNPAVSRLETALGATEIRTPRIPVISNVDAQPHADPDTIKKILASQVTSP
 VQWETTITLLTKGLKKS YELGPGKVIAGIVKRMDRGAEIENIGA

2. Bacteria and cyanobacteria

2.1 *Synechococcus elongatus* PCC 7942 (Accession number: ABB57486)

MAKTWVWVFPQGGSQATGMGVDLQDWPEAQRLAEAEALLGWSVLERCQADLETLSQTINTQPC
 LYVLEAILS DRLKQOGEQPD AVAGHSLGEYSALYTAGVFN FATGLQLVQKRAELMQAASGGKMAA
 LIGFDAEALAAAIANTEGVWLANDNSAAQVVISGTPAAVDAILAAVKS KRAVPLTVSGAFHSPFMAEA
 ATTF AATLAAVDFQDAQVPVLSNVSATPSTDAAVLKQNLLQQMTG SVRWRETCLAIEALGVEELVE
 VGP GKVLTGLMKRTCPAIGLRNVGTAADLTV

2.2. *Synechococcus elongatus* PCC6301 (Accession number: BAD78291)

MAKTWVWVFPQGGSQATGMGVDLQDWPEAQRLAEAEALLGWSVLERCQADLETLSQTINTQPC
 LYVLEAILS DRLKQOGEQPD AVAGHSLGEYSALYTAGVFN FATGLQLVQKRAELMQAASGGKMAA
 LIGFDAEALAAAIANTEGVWLANDNSAAQVVISGTPAAVDAILAAVKS KRAVPLTVSGAFHSPFMAEA
 ATTF AATLAAVDFQDAQVPVLSNVSATPSTDAAVLKQNLLQQMTG SVRWRETCLAIEALGVEELVE
 VGP GKVLTGLMKRTCPAIGLRNVGTAADLTV

2.3. *Geitlerinema* sp. PCC 7407 (Accession number: AFY66884)

MTKTAWVWVFPQGGSQATGMGADLV DLPVGQAKLAI AEDILGWSVSEVCSSDDAQLSRTLYTQPCLY
 VIESILVDLLREKGHQPALVAGHSLGEYVALYTAGVFSFEAGRLVQRR AELMDSTSDGKMAALIGFD
 REALDQQLQQTPGVWLANDNNAGQVVISGTP EAVAHIMATVKAKRAVPLNVSGAFHSPLMAPAAT
 EFQQVLD SVTFQDAQVPVLSNVEPLPATDGSVLRDRLSRQMTG SVRWRELSLQLAAEGVDRVIEVG
 PGK VLTGLIKRTCGDIALENISSAAEIPA

2.4. *Arthrospira platensis* (Accession number: WP_006617508)

MTKTAWVFPQGGSQAVGMGADLFDSPDAQPKLNKAADILGWSLPDLCQGEADKLSRTLYTQPCL
 YVVESLLVDALKKQKTPDLVAGHSLGEYVALYAAGVDFEAGLRLVKHRAELMDKAAGGQMAALI
 GFNAEQLNQLEQSENVVLANDNSSAQVVISGTPEAVDNLLSKIKVKRAVKLVNVSFHFHSPHMAEA
 ATQFQQVLDLVNFQQATVPVLSNVDPTPATDGEILKERLVKQMTGSRWREICLQLSEQGIQKVIEW
 GPGQVLTGLIKRTCSGLTLENCDRILPS

2.5. *Synechocystis* sp. PCC 6803 (Accession number: BAA17269)

MKTAWVFPQGGSQAVGMGVDLLSTAIKEKYQQAEEILGWSVVEKCGDEASLALTQNTQPCLYV
 IEAILADLLRDKGFQPDYVAGHSLGEYSALYAAGVDFATGLQLVKQRSEVMASASGGMMAALMKF
 DQTQLQQALTDNTEVVLANDNSPEQVVISGTVAGVEAILANVKARRAVPLKVSGAFHSSFMAQPSQ
 SFAQTLTACHFNATVPVLSNVDPSPTQNGDRLKEKLIQOMTGSRWRETMVNLGEIGATDYWEV
 GPGKVLTLGLCKRTCPDLNLKNIGQLDDLNSL

2.6. *Halothece* sp. PCC 7418 (Accession number: AFZ45530)

MTKLAFVFPQGGSQTIGMEADLVETSLGKEKFEKAEIILGWSVLETCRQDEANLSRTLYTQPCLYV
 ESILIDLLLDKAGYLPQYVAGHSLGEYSALYAARVFSFEAGLRLVQORAKLMDTAAGGKMVALMKID
 RAQLDSALDKNNDWVLANDNSPQQVVISGTPEAVDSILSEVKAKRAVPLNVSGAFHSPHMASVAQD
 YKQLLDEVSFGEAIVPVLSNVNPTPTIDATELKTRELMEQMTGTVRWRETLKLAEEEDVSQLEIVGPG
 NVLTGLCKRTCPMELQNISRAAECQL

2.7. *Oscillatoria acuminata* (Accession number: AFY84397)

MTKTAWVFPQGGSQALGMGVDVANLPIAQEKYAAAETILGWSVLDICTNAEDKLTSSLYTQPSLYV
 VESILVDLMRDRHQQPDLVAGHSLGEYVALYAAGVDFFAAGLQLVKYRAELMNTVAGGQMTALIG
 FNREQLDAQISATPDWVLANDNSDGQVVISGTPEAVESVIAAIKVKRAVKLVNVSFHFHSPHMAEA
 EFQKALDAVPFTDAIVPVLSTNDPTPETKAEALKQRLSRQMTGSRWREIMLQLPQEGIESVIEIGPG
 KVLANLIKRAVSDLAVTNVSTAADLPA

2.8. *Nostoc punctiforme* (Accession number: ACC78901)

MTKTAWVFPQGGSQTLGMGIDLLDIPFAKDKFAQAEIILGWSVTKICQNEEAKLSQTLTYTQPSLYVI
 ESILADLLQERGQQPDLVAGHSLGEYSALYVAGVFEWSAGLYLVKRRRAELMDNAVGGMMAALMNF
 DREQLEK VIAHTPDVVLANDNSSAQVVISGTTEAVQAVMTQVKAKRAIPLKVSGAFHSHLIAPAAAEF
 QNILESVEFQPATVPVLSNVEPIPSIDAEILKQRLNKQMTGSVRWREISLQLPANGIORWVEVGPVKVL
 TGLIKRSSPDLILENIQSGADLALG

2.9. *Escherichia coli* BL21 (DE3) (Accession number: ACT42983)

MTQFAFVFPQGGSQTVGMLADMAASYPIVEETFAEASAALGYDLWALTQQGPAEELNKTWQTQP
 ALLTASVALYRWWQQGGKAPAMMAGHSLGEYSALVCAGVIDFADAVRLVEMRGKFMQEAVPEG
 TGAMAAIIGLDDASIAKACEEAAEGQVSPVNFNSPGQVVIAGHKEAVERAGAACKAAGAKRALPLP
 VSVPSHCALMKPAADKLAVELAKITFNAPTVPVNNVDVKCETNGDAIRDALVRQLYNPVQWTKSV
 EYMAAQGVEHLYEVGPVKVL TGLTKRIVDTLTASALNEPSAMAAALEL



Appendix 2

TAP medium

Composition per 1 liter

Tris base	2.42	g
TAP salt	25	ml
Phosphate solution	375	μ l
Hutner's trace element	1	ml
Acetic acid	1	ml

Dissolve all compositions with distilled water to 1 liter. Sterilize by autoclaving at 121 °C, 15 lb/in² pressurized for 15 minutes. Add 13 g/L Bacto® agar for solidified media.

TAP salt

NH ₄ Cl	15	g
MgSO ₄ ·7H ₂ O	4	g
CaCl ₂ ·2H ₂ O	2	g

Dissolve all compositions with distilled water to 1 liter. Sterilize by autoclaving at 121 °C, 15 lb/in² pressurized for 15 minutes.

Phosphate solution

K_2HPO_4	144	g
KH_2PO_4	72	g

Dissolve all compositions with distilled water to 1 liter. Sterilize by autoclaving at 121 °C, 15 lb/in² pressurized for 15 minutes.

Hutner's trace element

$Na_2EDTA \cdot 2H_2O$	5	g
$ZnSO_4 \cdot 7H_2O$	2.20	g
H_3BO_3	1.14	g
$MnCl_2 \cdot 4H_2O$	0.50	g
$CoCl_2 \cdot 6H_2O$	0.16	g
$CuSO_4 \cdot 5H_2O$	0.16	g
$(NH_4)_6Mo_7O_{24} \cdot 4H_2O$	0.11	g
$FeSO_4 \cdot 7H_2O$	4.99	g

First dissolve $Na_2EDTA \cdot 2H_2O$ in 100 mL distilled water by heating at 60 °C, then adjust pH with KOH to 5.0. Add all trace elements separately and check the pH value constantly. Let the solution stand at 4 °C. When the color changes from orange to red or purple, filter the solution and store at 4 °C in polycarbonate containers. Adjust pH by adding acetic acid to 7.0.

Appendix 3

Blue-Green 11 (BG 11) medium

BG 11 solution

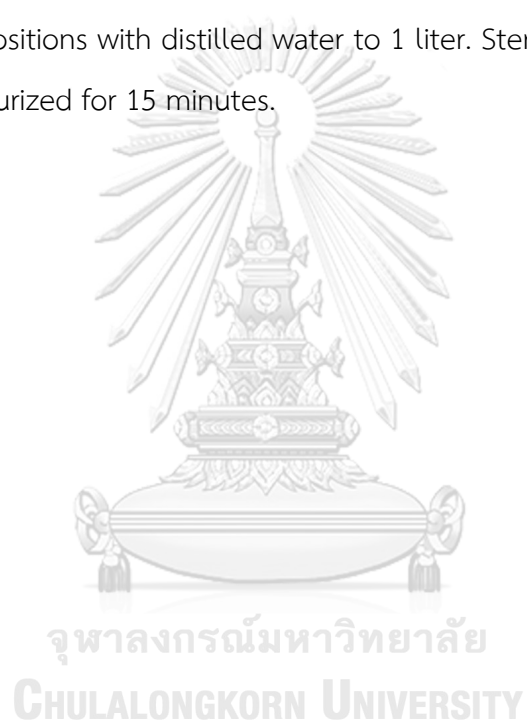
NaNO ₃	1.5	g
K ₂ HPO ₄	40	mg
MgSO ₄ ·7H ₂ O	75	mg
CaCl ₂ ·H ₂ O	36	mg
Na ₂ CO ₃	200	mg
Na ₂ EDTA·2H ₂ O	1	mg
Citric acid	6	mg
Ferric ammonium nitrate	6	mg
Trace element	1	mg

Dissolve all compositions with distilled water to 1 liter. Sterilize by autoclaving at 121 °C, 15 lb/in² pressurized for 15 minutes. Add 15 g/L Bacto[®] agar for solidified media.

Trace element solution

H_3BO_3	2.8	g
$\text{MnCl}_2 \cdot 4\text{H}_2\text{O}$	1.81	g
$\text{ZnSO}_4 \cdot 7\text{H}_2\text{O}$	0.22	g
$\text{CuSO}_4 \cdot 5\text{H}_2\text{O}$	0.079	g
$\text{Co}(\text{NO}_3)_2 \cdot 6\text{H}_2\text{O}$	0.049	g

Dissolve all compositions with distilled water to 1 liter. Sterilize by autoclaving at 121 °C, 15 lb/in² pressurized for 15 minutes.



Appendix 4

Luria-Bertani (LB) medium

Bacto® Tryptone	10	g
Yeast extract	5	g
NaCl	10	g

Dissolve all compositions with distilled water to 1 liter, adjust pH to 7.0 with NaOH and HCl. Sterilize by autoclaving at 121 °C, 15 lb/in² pressurized for 15 minutes. Add 15 g/L Bacto® agar for solidified media.



Appendix 5

Nile red solution

Nile red 250 mg

Adjust volume to 1 milliliter with acetone and kept in a lightproof container.



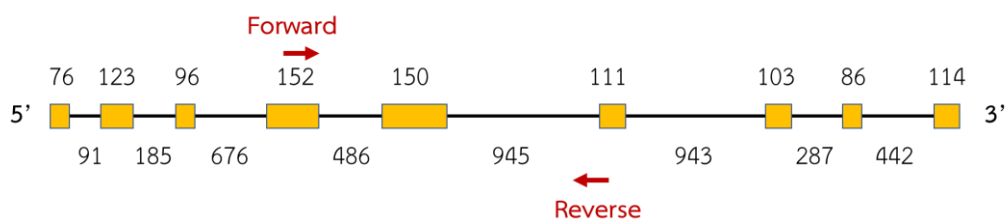
Appendix 6

Nucleotide sequence, primer design, and gene organization

1. *PDH2*: 1011 nucleotides (Accession number: CHLREDRAFT_190446)

ATGCTCGCTTCTCGCAACATGCGCGCCAGCGGCGCCCGTGTGGCCGCGGCTCCCGCCCAGCGC
 GCCATCCTGGCTGCTCGCTCCGGCCGCGCGCCTCGGTCGCCGCTAAGGCCCAGAAGAAGGAG
 ATTATGATGTGGGAGGCTCTGCGCGAGGCCATTGACGAGGAGATGGAGCGCGACCCACCGTC
 TCGTGATGGGCGAGGACGTTGGCCACTACGGTGGCTCCTACAAGTGCACGCTGGGCCTGTAC
 AAGAAGTATGGCGACATGCGCGTGCTGGACACGCCCATTTGCGAGAACGGCTTCATGGGCATG
 GGTGTGGGCGCCGCCATGACCGGCCTGCGC**CCCATTGTGGAGGGC**ATGAACATGGGCTTCCTG
 CTGCTGGCCTTCAACCAGATCTCCAACAACCTGCGGCATGCTGCACTACACCTCGGGAGGACAGT
 TCAAGACCCCTGGTCATCCGCGGCCCGCGGCGGTGGGTGCCAGCTGGGCGCCGAGCACT
 CGCAGCGCCTGGAGTCGTA

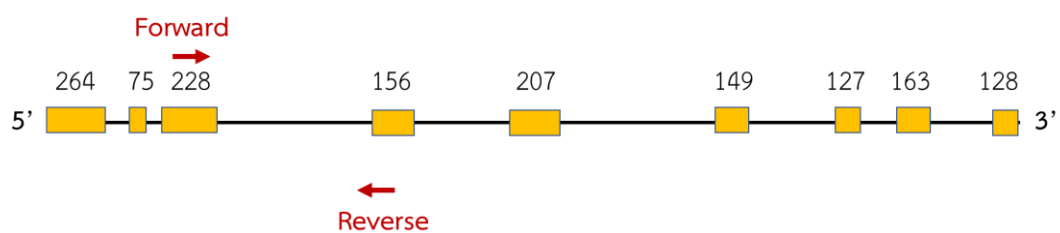
Forward Primer	Pos	Len	Tm	Reverse Primer	Pos	Len	Tm	Amp	dG
5'-CCCATTGTGGAGGGC-3'	345	15	56.31	5'-ACAGCAGAACGTGCT-3'	645	15	55.32	300	-6.67



2. ACCase: 1497 nucleotides (Accession number: CHLREDRAFT_184945)

ATGCAGGTCCTCAAGAGCAAGACTCTGGTTAGCGATGCTGCTGCGGCACCGCGCTGCTCAG
CGTGCCACTGTGGCCCGACCGAGCGTTAAGGTGCAAGCGGCACCCCGACTGCCCCGGACACG
CCTAAGGAGCGCGAGGGAGGCCGCGAGTGGCTGGGCACTATCCTGTCTCGCTTTGGGCCGGTG
AAGGACAAGGCGCAGAACACCACGACGCTTGAGTTTGAGAAGCCTCTGCTGGAGCTGGATAAG
CGCATCAAGGAGGTGCGCAAGGTCGCCGAGGAGAACGGCGTGGATGTGAGCGCCTCCATTGCT
GAGCTGGAGGGCCGCGCAAGCAGCTGCGGAAGGAGACTTACAGCCGGCTGACGCCCCGTCCAG
CGTCTGCAAGTCGCTCGCCACCCCAATCGCCCTACCTGCCTGGACATCATCCTGAACATCACCG
ATAAGTTCGTGGAGCTGCACGGTGACCGCGCGGGTCTCGACGACCCCGCCATCGTGTGCGGTA
TCGGCAGCATCAATGGCACGCCGTTTCATGATGATCGGCCACCAGAAGGGCCGGAACACAAAGG
AGAACATTCGCCGCAACTTCGGCATGCCCCAGCCCAACGGCTACCGCAAGGCGCTGCGCTTCAT
GCGCCACGCCGACAAGTTTGGTCTGCCCATCATCACCTTCGTGGACACGCCCCGGAGCCTATGCC
GGCAAGACCGCGGAGGAGCTGGGCCAGGGCGAGGCCATTGCCGTGAACCTGCGTGAGATGTTT
GGCCTGCGTGTGCCCATCATCTCGGTGGTTCATTGGCGAGGGCGGCTCGGGCGGCGCGCTGGCC
ATTGGCTGCGCCAACCGCAACCTGATCATGGAGAACGCGGTCTACTACGTGGCCTCGCCCGAG
GCCTGCGCCGCCATCCTGTGGAAGAGCCGCTCTGCCGCCGGCGAGGCCACTGAGGCCCTGCGC
ATCACCTCGGCCGAGCTGGTGAAGTTCGGCGTCATGGACCACATCGTGCCGGAGCCGCTGGGC
GGCGCGCACAGCGACCCGCTGGCGGCCTTCCCCATGATCAAGGAGAGCATCCTCAACGTCTACT
CCGAGTACGCCGTGATGAGCGAGGAGGAGATCAAGCTGGACCGCTACGCCAAGTTCCGCAAGC
TGGGCCAGTTCCAAGAGTTTGTGGTCAAGGGCGGTGACTGGCGCACCGCCCTGGCGGAGCGCG
CGGCAACCTCCGGCACCACCACCAAGACCGGCGCCTGGGCCGCCACTGAGGCCGAGGCCGCGCT
ACATCGAGCAGCTGGTGGACGCGGACGAGAAGTGGGAGAAGCTCATGGCGGAGGGCGCCGAGT
GGCTCAACAAGCCCGTGCAGCCCGGGCCTGGGCCGGTCAGGCATCATGGACGTGGCGGTGT
CTATGGTGGAGGCGGCGGCGGAAGCAGCAGCGGGCCAGGTGCACAAGTCGGCACCCCG
CCCCGCCAGCAGCAACGGCGCCGTCGTCAACGCCCGCCGCTTAA

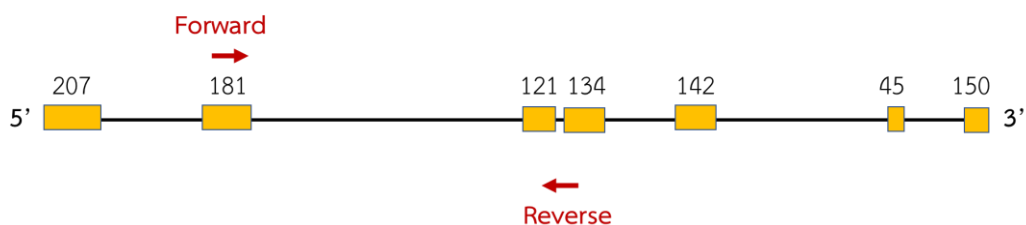
Forward Primer	Pos	Len	Tm	Reverse Primer	Pos	Len	Tm	Amp	dG
5'-TCTGCAAGTCGCTCG-3'	380	15	56.11	5'-CGTGTCCACGAAGGT-3'	680	15	55.48	300	-0.39



3. MAT: 981 nucleotides (Accession number: CHLREDRAFT_101671)

ATGGTCGCTGTCCGTGGTCGCCGCGCCCTGGCCGTCCGCGCCTCGGGCGACGACGCGTTCCGCC
 AACTACAAGCCCACTATCGCGGCATTGTTCCCCGGCCAGGGTGCGCAGAGCGTCGGCATGGCC
 AAGGACCTTGTGGCGACCGTGCCGAAGGCCAAGGAGATGTTGACAAGGCGTCTGAGATCCTG
 GGCTACGACCTGCTGAAGGTGTGCGTGGAGGGCCCCAAGGAGAAGCTGGACAGCACCG **CCGTG**
AGTCAGCCCCGCTATCTACGTGGCCTCGCTGGCCGCCGTGGAGAAGCTGCGCGCGGACGAGGGC
 CAGGTGCGTGTTCTAGGGTTTGAGGGTCCAGGGTACGCTCGTGCCTGCGATGTGTGGCTGGGT
 GGTGCGTCTGTGCGCCATGCAGCAGTGGCCACACACAACCCGCGTCCTGCCCTGCCGCCGCTC
 TGTGCACCCCCGCCAGTGCACGCGCGCACCTCATTTCCTTGTGCTCTCACACAATCCTTCCCC
 CCTTTGCCGCCACGGAGCAGGTGGGTCA **GGACAAGCCGGTCCA**GATCGCCAACTACCTGTGCC
 CCGGCAACTACGCCGTGTCGGGCTCCAAGGAGGGCTGCGACGCTGTGGAGAAGCTGGGCAAGA
 GCTTCGGCGCGCGCATGACTGTGCGCCTGGCTGTGGCCGGCGCCTTCCACACCTCCTACATGTC
 CCCCGCCGTGGACAAGCTCAAGGCCGCCCTGGCGCAGGTGCGGGGGCGGGGGGGGGGAGGG
 TTGGAGGGGGGAGGCAGGCGGAGGGAGGCCGCACTCCGACCCCGCCGTCATCAAGGACATCC
 TGTCGCGCCAGGTGACCTCCCCCGTGCTGTGGGAGAACACCATTAAGTCGCTGCAGGAGAAGG
 GCCTGACCAAGTCCTACGAGGTCGGCCCCGGCAAGGTCATCGCTGGCATCGTTAAGCGCATGG
 ACAAGGGCGCGAACATCGTCAACATCACCGCTTAA

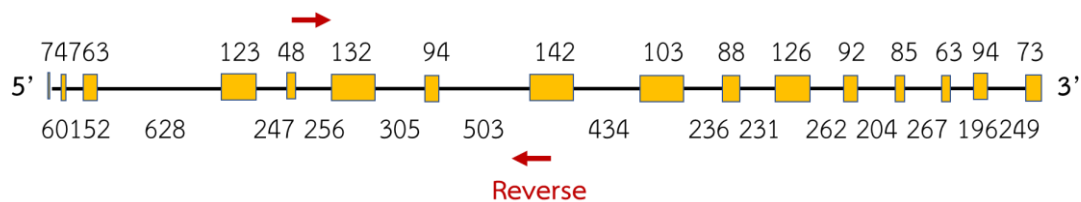
Forward Primer	Pos	Len	Tm	Reverse Primer	Pos	Len	Tm	Amp	dG
5'-CCGTGAGTCAGCCCCG-3'	247	15	59.31	5'-TGGACCGGCTTGTC-3'	547	15	58.23	300	-6.80



4. KAS2: 1380 nucleotides (Accession number: CHLREDRAFT_139619)

ATGCTGGGCTCACAAAGTTTCCTCGGCAAGCGGCAAGCTTCCGAGTGAAAGCTACCCGGGC
GGGCGGATGCCAAACGGTCCGCGTCTCCGCGGCCGTGCACGACATTTCCAAGACTGAGAAGG
CGCCACGCCGTGTGGTGGTGACGGGCATGGGTCTGGTGTCTGCCTGGGCCATGACCACGACG
AGTTCTACAACAACCTGCTGGCCGGAAGTCCGGAATCACAAACATCGAGGGCTTCCCCTGCGC
GGACTACACGACGCGCTTCGCTGGCGAAATCAAGTCTCTTACTGCACCGGCTATGTCACCAAG
AAGTTTGAGAAGCGCGTGGACGCTGTAATCAAGTATATCTTGGTGGCTGGCAAGAAGGCGCTAG
GGGACGCGGGCCTGGCGTGGGACGGGACAGGAGATCAAGGACCTGGACCGCATGCGCTGTGGCA
CGCTGGTGGGCACGGCCATGGGCGGCATGACCTCATTGCGCAACGCCGTGGAGGCGCTGGAGA
CGTCGGGCTACCGCAAGATGAACCCCTTCTGCATTCCCTTCGCCATCACCAACATGGGCGGGCGC
CATGCTGGCCATGGACATCGGCTTCATGGGACCCAACTACTCCATCTCCACAGCCTGCGCAACC
GGCAACTACTGTATCATGAACTCGGCAGAGCACATCCGGCGCGGTGACGCGGACCTGATGCTG
GCGGGTGCGGGTGACGCCGAATCATCCCCTCCGGCATTGGCGGCTTCATTGCGTGCAAGGCC
CTGTCCAAGCGCAACGATGACCCCGCCGCGCTCGCGGCCTTGGGACACGGACCGTGATGGC
TTCGTTATGGGCGAGGGCGCGGGTGTGCTGGTGGTGGAGGAGTATGAGCACGCCAAGGCGCGT
GGCGCCCGCATCTACGCCGAGTACGTGGGCGGGGCGGTACCTGCGACGCCACCACATGACG
GAGCCGAGCCAGAGGGCAAGGTGTGATCATGTGCCTGCAGCGCGCTGGCGTCTACGGGT
CTGTCCGCTCTGACGTCAACTACGTGAACGCGCACGCCACGTCCACACAGGCTGGCGACATGG
CTGAGTACCGGGCGATCAACACGGTGTCAACCATTGCGACCTGCGCATCAACGCCACCAAGTC
CATGATCGGCCATCTGTTGGGCGGCGCTAGCGCAGTAGAGGCGGTAGCGACCATCAAGGCCAT
CCAGACGGGTTGGCTCCACCCGAGCATCAACCTGCACACCCCGAGGCGGGCGTGACCTGGT
GCGCGTGGTGGCGGGCGCCAAGCAGCACCACCCCATCAAGGTGGCGCTCTGAACTCGTTCGG
CTTCGGCGGCCACAACAGCTGCGTGATGTTCAAGCCGCCCCCGCAGTAA

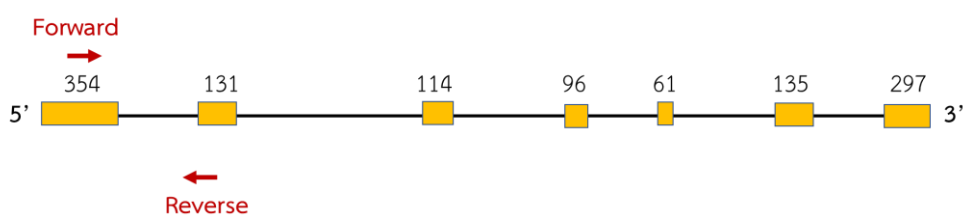
Forward Primer	Pos	Len	Tm	Reverse Primer	Pos	Len	Tm	Amp	dG
5'-CGCGGACTACACGAC-3'	251	15	56.74	5'-GGCGAAGGGAATGCA-3'	551	15	56.35	300	-2.52



5. **FAT1: 1188 nucleotides** (Accession number: CHLREDRAFT_196283)

ATGCGTCGCTTTGCGACGTTGAACGAGCAGGCACAGTCCACTGCGTCAACTTCGTCGTCGACCC
 GGTCCTGTGTGCACGGATATGCAGCAATAGGCGTCGTGCATCAATTCAGCCGTTAGGCACTGT
 CGCCCTTGCCGTCGCAGCGGCGTCGCTTGCCGCTCAGGAGTCGCGGTGCAAGCAGCGGCGGT
 GGTTACAGGAGGAGTATGACGTTGTTATTCCCAAGTTCAGCCCCAGCAGCTGGCGCGTTCCTG
 CCGGATAAGCGCTCGTTCCTGAGGAGCACAGGATCCGCGGCTACGAGGTCAGCCCGGACCAG
 CGTGCCACCATCGTTACTGTCGCCAACCTATTGCAGGAGGTCGCTGGCAACCACGCCGTGGGCA
 TGTGGGGCCGCACTGACGAGGGGTTTGCCAGCCTGCCAGCATGAAGGACCTGCTGTTCGTCA
 TGACACGCCTGCAAGTGCATGTACGAGTACCCCAAGTGGGGCGACGTGGTTGCTGTGGAGA
 CGTACTTCACGGAGGAGGGGCGGCTGGCGTTCGGCGTGAGTGGAAGCTCATGGACGTGGCCA
 CCGGCAAGCTGCTGGGCGCGGGCACCAGCACCTGGGTACCATCAACACGGCCACTCGCCGGC
 TGTGCAAGCTGCCGAGGACGTGCGCAAGCGCTTCTGCGCTTCGCGCCGCCAGCAGCGTCC
 ACATCCTGCCCCCTGAGGAGACCAAGAAGAAGCTGCAGGACATGGAGCTGCCCGGCCAGGTCC
 AGTCTGCTCAGCAGGTGGCTCGGCGCGGACATGGACATGAACGGCCACATCAACAACGTGA
 CCTACCTGGCCTGGACGCTGGAGAGCCTGCCGGAGCGGGTCATGAGCGGCGGGTACAAGATGC
 AGGAGATTGAGCTGGACTTCAAGGCCGAGTGCACGGCTGGCAACGCCATTGAGGCGCACTGCA
 ACCCCCTGGACGATCACTCCGCGTCTTCGTGGGACCCGCGCCCGCCAACGGCAACGGCAACG
 GCCACGCAGCCGAGCCCCGCCGCGACTCCGCACCGCTGTACTTCCTCAGCATGCTGCAAAAAGT
 GTGACGAGAACGGGTGTACGGAGCTGGTGCGGGCGCGCACGACATGGAGCCGTACGCTGGAGG
 GCGCCAAGCCGGCACCGCCCGCTGTCGGAGCTGTCTGCGGCTCAGTGA

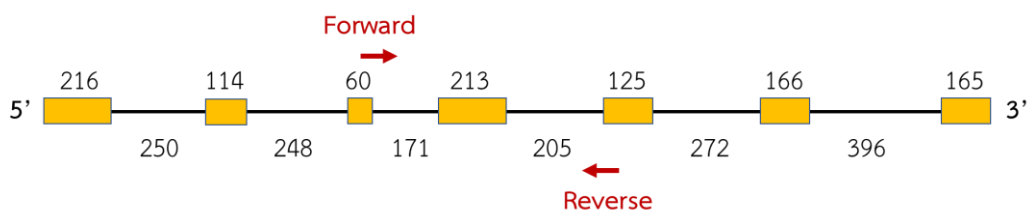
Forward Primer	Pos	Len	Tm	Reverse Primer	Pos	Len	Tm	Amp	dG
5'-TCAGGAGTCGCGGTG-3'	162	15	58.00	5'-GCACTTGCAAGGCGTG-3'	462	15	58.87	300	-2.47



6. *GPD1*: 1059 nucleotides (Accession number: CHLREDRAFT_94229)

ATGCGGTGGTCGAAGGTGTTCAACACGCGTAAGCTCGCGGGGAGCCCCCTTGAAGCCGCAAAG
 AAAATTGTAGTGTTTCGGCGGGGGCTCGTTCGGCACGGCGATGGGCTGCGCCCTCGCACGGCAA
 AAGCCGGACCTGGAGGTGGTGTGCTGGTGCGGGACCCCTACCTGTGCAAGGACATCAACCTG
 CTGCATGAAAACACGCGCTACTTGAAGGGCTTCAAGATGCCGCCAACGTGCGCGCCACCACGC
 ACGCACCGGAGGCCATCGTGGGCGCGCAGTATGCGGTGCACGCCGTGCCCGTCCAGTCATCCC
 GAGCCTTCTGCAGGGCATCAAGGAGTACCTCCCATCCTCGGTGCCCATCATTTGCGTCAGCAA
 AGGCCTTGAGGTGGGCAGTGGGCAGATGATGTCCGAGCTCATTCCCAGCGCGTTGGAACGCAA
 GCAGCCGGCGGTGTTCTGTGTCAGGGCCGTGTTTCGCCAAGGAGGTCATGCAGAACCGGCCAC
 GGGCGTGGTAGCGGCGTGCAAGGACGCCAAGCTGGCGCGGACGGTGCAGGCGTTGTTCCGCCAG
 CCCCACCATGCGGGTCAACACCACAACCGACGTGGTGGGCGTGGAGATCTGCGGCGCGCTGAA
 AAACGTGCTCGCCATTGCGGCGGGCATCGTGGAGGGCATGGACTTGGGGCACAACGCGTTGGC
 AGCGCTCATAGCGCAGGGCTGCTCGGAGATCAGGTGGCTGGCGGAGAAGCTGGGCGCCAAGCC
 CACCACCATGTCGGGGCTGTCGGGCCTGGGCGACATCATGCTCACCTGCTACGGCGACCTGAG
 CCGCAACCGCAGTGTGGGCATGCGCCTGGGGCGCGGCGAGCGGCTGGAGGACATCATTGCGTC
 CAGCTCACAGGTGGCGGAGGGCGTGGGCGACGGCTGGCGTGGTGGTGGGGCTGGCGCGCAAGTA
 CCGCGTGTGCTGCCGGTGTGACGGCGGTGGCGCAGGTGCTGGACAACAACCTCACGGGCGG
 GGAGGCGGTGTTCCACATCATGAACCTGCCGCAGATCGAGGAGGCATAG

Forward Primer	Pos	Len	Tm	Reverse Primer	Pos	Len	Tm	Amp	dG
5'-CAAAGCCTTGAGGT-3'	377	15	52.30	5'-CAAGTCCATGCCCTC-3'	677	15	53.12	300	0



7. *DGTT1*: 996 nucleotides (Accession number: KC788199)

ATGAACCAACTAGAGCTCGTGATGTGTCGATTAGCTGTGTCTTGGTTCCTAATCACAGCTATAA
 GCCAAGCATGGGTGTGGCCTCTGCTCATCGGCACATTGCTTTACGTGCAGAGCACCACGCTCAC
 AATTGCCTTCCTGCTGTACCTCTATTATGTTGTCGTCGGCCCGGGCTCTAAAGATGACGCCAAC
 TGCAAGTGAAGCCGACCTTCCGCAAGTGGCATATCTGGAAGTTATGGCCTCTTACTTCCCCG
 GCGCCCGCCT **GATTAAGACCGCCGA** CCTGGATCCGGCTGGCCGCTATATATTCGTGAGCCACCC
 GCACGGCGTCATCGCCATTTCCGACTGGCTGGCATTTCACACAGAGGCGCTGGGCTTCTCCAAA
 CTGTTCCCAGGCCTGGACCTGCGCTGCGCCACGCTGGCTTCAAACCTTCTGGGTGCCTGGTTTGC
 GTGAGTACATCCTATCGCACGGCATGTGCGGCGTGGGGCGAGACACTCTGGCGCGCGTGTGA
 CAGGAAAGCCGGGCCGTGCGGTTGTGTTGGTGGTGGGCGG **CGCGTCTGAGGCGCT** GTTGGCGG
 CGGAGGGAACCTTATGACCTGGTGTGCGCAACCGCAAGGGCTTTGTGCGCCTGGCGCTGCAGA
 CCGGCGCCAGTCTGGTGCCGGTGTGTCGTACGGTGAGACAGACACCTTCCACACCTACATCCC
 GCCGCCCTGCAGCCGGGCGGCCGCGTTCATGAAGGTGTGAAGCAGGTGTTTGGCTTCTCCAC
 GCCCCTGTGCTGGGGCACCGGACTGTTCCGGGGCTGGGGCATGCTAGCGCTGCAGGTGCCGCT
 CACTGTGGTGGTGGGGGCACCCATACAGGTGGACAAGGTGTCCAGTCCCACGGAGGCTGAGGT
 GCGGGCGCTGCATAAGACCTACACGGAGGCACTGCAGAAGCTGTGGGATGACACAGTGGACAA
 GTACGGCAAGGGTGTCAAGCGGCCGCTGGCCATCGTGCAATGA

Forward Primer	Pos	Len	Tm	Reverse Primer	Pos	Len	Tm	Amp	dG
5'-GATTAAGACCGCCGA-3'	267	15	46.10	5'-AGCGCCTCAGACGCG-3'	567	15	54.30	300	-2.05

8. *DGTT2*: 975 nucleotides (Accession number: CHLREDRAFT_184281)

ATGGCGATTGATAAAGCACCGACAAATGTGCGAATTTGGAGCGATGGCGTCACGGAGAAGGGC
 AAGCAAAGCATCTTCTCATCGCTGGTGGCTATGTTGACGCTCTTCATCTACTGTGGCTGGATGC
 ATGTGCTGCTGGCGCTTGTGATCCTGTCCTTCTGGTACCGCTGGGCGCTGGTGACGGTGCTGCT
 GCTGTACTCCACCCTGCTGCTGCCGCCTAAGCCGGTGCTGTGGGGACCGGTCTGTCGCTCCTGG
 ATCTTCCAGACCTGGCGGGAGTACTTCAAGTTCTCTTACGTGTTTGATGAGGTGCTGGACTCGA
 AGAAGAAGTACATCTTCGCGGAGTTCCCGCACGGTGTCTTCCCATGGGCCACTCATTGGCGC
 CACAGAATGCCAGATCATGTTTCCCGGCTTTGACATCTTCGGGCTGGCGGCGAATGTGGTGTTCA
 ACGGTCCCCTTCTGGCGGCATTTCTGTGGCTGGGCTCCGTGCCGGCCACCACACGCGAC
 TTCAAGCGGGTGCTGAAGCAAGGAAGCGTGGCGGTCATCGTGGGAGGCATCGCAGAGATGTAC
 ATGCAGAGCCCCACGAAGGAGCAGATCATGTTGAAGGACCGCAAGGGCTTTGTTTCGTGTGGCG
 GTGGAGGAGGGCGTGGATGGCGGCATCGTGCCGGTCTACCACTTTGGCAACTCTCAGGTGCTG
 GACTTCGGCCCCCAGGCCATGGCCAGTGTGTCCCGCCGGCTGCGTGCGGCCCTGGGCTTCCTG
 TACGGAGTGGCCTACCTGCCCCTGCCAGGCGCCGCAACATTTACATGGTGTGCGGCAAGCCC
 GTTCCCGTCACGCGCACCGCCCCGCGACGCCCAAGTTTGAGGAGGTGGTTGACGCCACTCAC
 GCCGCTGTGATGGCGGCCCTGCAGGAGGCCTACGACCGCCACAAGACCGAGTACGGCTGGGCC
 GACCGACCGCTGGTCATCAGCTGA

Forward Primer	Pos	Len	Tm	Reverse Primer	Pos	Len	Tm	Amp	dG
5'-TCCTGTCCTTCTGGT-3'	149	15	46.10	5'-CGAATGTGGTGTCA-3'	449	15	51.60	300	0

9. *DGTT3*: 1041 nucleotides (Accession number: KC788201)

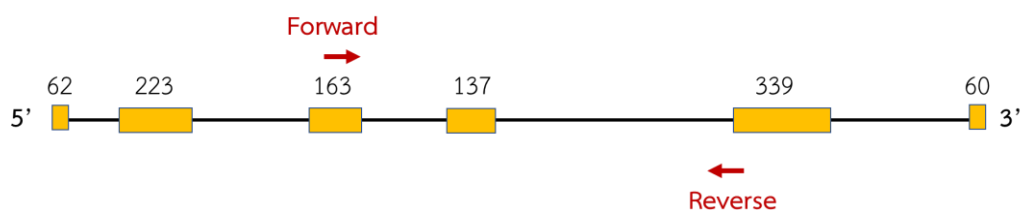
ATGGCAGGTGGAAAGTCAAACGGCACGGGCGGGCGGACGCGCACGTGCGTACCTCGCACTTG
 ACCCTGAAAGCTGGGGAGGACCCGCCCCGAATGTTTCGCATCTACAGTGACGGCATCAAGCCG
 GACGCGCGGCAGAACCTGCTTGTTTCAGATCCTGGCCGGCATCACGATGTCGATTTATGTAGGCT
 TCATGAACTATTTTCATGCTGCTGGTGGTCTCTCTACTGGAGCCGCATCTGCCGCTATGTGGT
 CCTGGCGCTGCTAGGCACACTGGCGCTGCCCTGCAAGCCCGTGCTGTGGCCTGCCTTCAACAA
 GCTGTGGATCTTCAAGACTGGCGTCACTACTTCCACTACAGTTTCCTGATTGAGGAGCCGCTT
 GACCCCAACAAGCGCTACATCTTTGTGAGTTCCCGCACGGCGCGTTCCCCATTGGTCCCATCG
 TGGCGGGCACGCTCATGCAGACTCTGTTCCCGCACATGATGATCTACAGCGTGGCCGCTCCGT
 CGTGTCTACATCCCCTTCTGGCGCCATTTTCATCACGTGGATCGGCTCGGTGCCCGCAACGCCC
 GGCAACTTCAAGCGGCTGCTGAAGAAGGGCAGTGTGGCGGTGGTGGTGGGCGGCATTGCCGAG
 ATGTACATGGGCAACAAGAAGAAGGAGCGCATTAAAGTAGTGGGCCCGCGGGCTTCGCACGC
 ATCGCGCTGGAGGAGCAGGTGGACGGCATTGTGTGCGTGTACTACTTCGGTCAGAGCCAAGTG
 CTGGACTTCGGGCCCTCCTGGCTGGCGGACTTTAGCCGCCGCATGCGCACCAGCTTCGGCTACC
 TCACGGGATGGATGGGGCTGCCGTGCCGCGGCCCATCCCCATCTACATGGTGAATGGGAAGC
 CCATCCCGGTGCCCAAGGTGGCTCGTGACTCGCCCCGAGTTTCGACAAGGAGGTGGATAAGCTGC
 TTGACGCCACCATCACGGAGCTGGGCGAGATGTACAACAGGCACAGAGGCGAGTACGGCTGGG
 GCGACCGCCCGCTGTCCATCGAGTAG

Forward Primer	Pos	Len	Tm	Reverse Primer	Pos	Len	Tm	Amp	dG
5'-TACCTCGCACTTGAC-3'	15	15	46.10	5'-AAGTAGTGACGCCAG-3'	449	315	51.60	300	0

10. *DGTT4*: 984 nucleotides (Accession number: CHLREDRAFT_190539)

ATGCCGCTCGCAAAGCTGCGAAACGTGGTGCTGGAGTACGCGGCCATAGCCATCTACGTCAGC
 GCCATCTACACCTCGGTGGTGCTGCTGCCCTCGGCGCTCGCGCTGTTCTACCTGTTTGGGGCCA
 CCAGCCCCTCGGCCTGGCTGCTGCTAGCCGCCTTCTGGCCCTCACCTTCACGCCGCTGCAGCT
 GACCACCGGTGCGCTGTCGGAGCGGTTTCGTGCAGTTCAGTGTGGCGCGGGCGGCGGCCTACTT
 CCCCACCCGCGTGGTGGTCACGGACCCGGAGGCCTTCCGCACTGACCGCGGCTACTTGTTCGG
 ATTCTGCCCGCACTCGGCTCTGCCCATCGCACTGCCCATCGCCTTCGCCACCACCTCGCCGCTG
 CTGCCAAGGAGCTGCGCGGCCGCACACACGGCTTGGCGTCGTCCGTGTGCTTCAGCGCGCCC
 ATAGTGCGGCAGCTGTACTGGTGGCTGGGCGTGCGGCCCGCCACGCGGCAGAGCATCAGCGGC
 CTGTTGCGGGCGCGCAAGGTGGCGGTGCTGGTGCCGGGGGGCGTGCAGGAGGTGCTCAACATG
 GAGCACGGCAAGGAGGTGGCCTACCTCTCCAGCCGCACCGGCTTCGTGCGACTGGCCGTGCAG
 CACGGCGCGCCGCTGGTGCCAGTGTGGGCGTTCGGCCAGACGCGCGCGTACAGCTGGTTCCGG
 CCGGGGCCGCCGCTCGTGCCACGTGGCTCGTGAGCGCATCTCACGTGCCGCCGGCGCCGTA
 CCCATCGGCATGTTTGGGAGTACGGCACGCCATGCCGCACCGCGAGCCCCTCACCATTGTG
 GTGGGTGCGCCCATCCCGGTGCCGGAGCTGGCGCCGGGCCAGCTCGAGCCCGAGCCCGAGGTG
 CTGGCGGCGCTCCTCAAGCGCTTCACGGACGACCTGCAGGCGCTGTACGACAAGCACAAGGCG
 CAGTTCGGCAAGGGCGAGGAGCTGGTCATAATGTAG

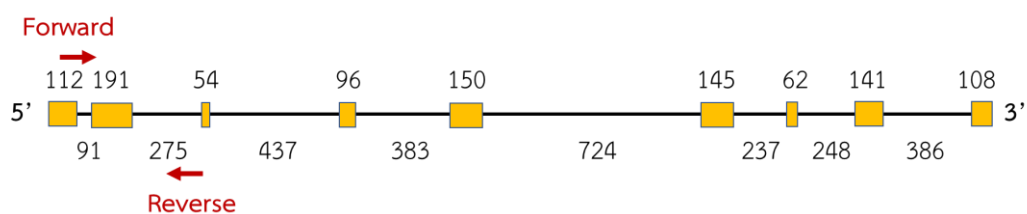
Forward Primer	Pos	Len	Tm	Reverse Primer	Pos	Len	Tm	Amp	dG
5'-GGCTACTTGTTCGGA-3'	304	15	46.10	5'-GCCTACCTCTCCAGC-3'	604	15	51.60	300	-0.28



11. 18s rRNA: 1059 nucleotides (Accession number: CHLREDRAFT_206075)

ATGGGCAAACCAAAGGGCAAGGGCGCCGGAGGAGGCTCAGATGGCGGGCTACGCGTTGCTGGA
 GGAGTGCAGAAGAAGTCTCAGAAGAAGGGGCCCAACACTGGCGTGTCTGGTCTGGAGTTCCAT
 AAAAGCAAGGGCCAGCACATTCTGCGGAACCCGCTGGTCGTGCAAGCCATCGTCGACAAGGCG
 GCGTCAAGTCCACGGACGTGGTGCTAGAAATCGGTCCCGGTACGGGTAAC TTGACGGTGAAG
 CTGCTGGAGAAGGCGAAGAAGGTCATTGCCGTGGAGCTTGACCCACGCATGGTCCTGGAGCTG
 CAGCGGCGTGTGCAGGGCACGCCGTACGCCAACAACCTGCAGATTATCCACGGTGACTTCATGC
 GTGTGGAGCTGCCCTACTTCGACCTGTGTGTGGCCAACATCCCCTACAATATCTCCTCGCCGCT
 CACCTTCAAGCTGCTGGCGCACAGGCCCGCTTCCGCGCTGCGGTGATCATGTACCAGCACGA
 GTTCGCGATGCGGCTGGTGGCCAAGGCGGGCGACAACCTGTACTCGCGCCTGGCGGTCAACAC
 ACAGCTGCTGGCGGAGTCAGCCACCTGCTCAAGGTGGGCAAGAACAACCTCCGGCCCGCCGCC
 CAAGGTGGACTCGTCGGTGGTGCGCATTGAGCCGCGCCACCCGCGCCCGCCGTCAACTTCCT
 CGAGTGGGACGGCCTGGTGC GGCTGTGCTTCAGCCGCAAAAACAAGACGCTGGGCGCCATCTT
 CAAGCAGACCAACACGCTGCAGGCGCTGGAGACCAACTGGCGCACCTACCAGGACGACGCCAT
 GGACGGCGACGACGACAACGACGACGCCATGACGGTGGACGGCGGCGGGTGGCGGGCGCG
 GCGGTGGGCGCGGGCGGCGCAGGGCGGGCGGCAAGGTCAGCCCCGAGTTCAAGGAGCTGGTCA
 TGAAGTTCTGGAGGACAACGGCCTGGACACCAACCGCAGCAGCAAGATGAGCCAGGAGGAGT
 TCCTGCAGCTGCTGGCGCTGTTCAATGCGGCCGGGATACACTTCGCTTAG

Forward Primer	Pos	Len	Tm	Reverse Primer	Pos	Len	Tm	Amp	dG
5'-CGGAACCCGCTGGTC-3'	150	15	56.00	5'-TGAAGGTGAGCGGCG-3'	450	15	53.30	300	-3.80



12. *rnpB*: 312 nucleotides (Accession number: Synpcc7942_R0036)

GAGGAAAGTCCGGGCTCCC AAAAGACCAGACTTGCTGGGTAACGCCAGTGCGGGTGACCGTG
 AGGAGAGTGCCACAGAAACATACCGCCGATGGCCTGCTTGACAGGCACAGGTAAGGGTGCAAGG
 GTGCGGTAAGAGCGCACCAGCAACATCGAGAGGTGTTGGCTCGGTAAACCCCGTTGGGAGCA
 AGGTGGAGGGACAACGGTTGGTCTTTTACCTGTTCCGTTTATGGACCGCTAGAGGTGGCTAGTA
 ATAGCCATCCCAGAGAGATAACTGCCCTCTGTCTTCGACAGAGAACAGAACCCGGCTTA

Forward Primer	Pos	Len	Tm	Reverse Primer	Pos	Len	Tm	Amp	dG
5'-GAGGAAAGTCCGGGCTCCC-3'	1	19	64.80	5'-TAAGCCGGTCTGTCTC-3'	294	19	59.49	312	-2.95

13. 7942MAT or *fabD*: 882 nucleotides (Accession number: Synpcc7942_1456)

ATGGCTAAAACGGTGTGGGTGTTTTCCGGGGCAAGGATCTCAGGCAACGGGAATGGGCGTTGAC
 CTGCAGGATTGGCCAGAAGCTCAACAGCGTTTGGCCGAAGCTGAGGCGCTTCTCGGATGGTCG
 GTGCTGGAGCGCTGCCAAGCCGATTTAGAAACGCTGTCGCAGACGATTAACACGCAGCCCTGT
 CTCTACGTGCTGGAGGCGATTCTGAGTGATCGCTTGAAGCAACAGGGTGAGCAGCCTGATGCT
 GTCGCTGGCCACAGCCTTGGCGAATATT**CAGCCCTCTACACCG**CAGGTGTCTTTAACTTCGCGA
 CGGGGCTGCAACTGGTTCAGAAACGGGCAGAACTGATGCAGGCCGCTTCCGGTGGCAAGATGG
 CCGCTCTAATTGGCTTTGATGCTGAGGCACTAGCGGCAGCGATCGCCAACACCGAAGGCGTAG
 TGCTCGCCAATGACAATAGCGCCGCCAAGTTGTGATTTCTGGAActCCAGCAGCGGTGCAGCG
 GATCTTGGCAGCCGTCAAGAGTAAACGGGCTGTCCCCCTGACAGTCTCCGGGGCATTCCA**CTC**
GCCGTTTATGGCTGAGGCGGCAACGACGTTTGC GGCCACCCTGGCAGCAGTGGATTTTCAGGA
 TGCGCAGGTCCTGTGCTTTCAAATGTCAGCGCGACTCCTAGCACCGATGCTGCTGTGCTCAAG
 CAAAACCTGTTGCAACAGATGACAGGCTCGGTGCGCTGGCGCGAAACCTGTCTGGCGATCGAA
 GCCCTGGGCGTTGAAGAACTGGTTGAAGTTGGTCCCGGTAAAGTCCTGACGGGCTTGATGAAA
 CGGACTTGTCTGCAATCGGATTGCGCAATGTTGGAACAGCAGCAGACCTCACGGTCTAA

Forward Primer	Pos	Len	Tm	Reverse Primer	Pos	Len	Tm	Amp	dG
5'-CAGCCCTCTACACCG-3'	280	15	55.27	5'-GCCATAAACGGCGAG-3'	580	15	54.75	300	-0.01

14. 7942LACS: 1950 nucleotides (Accession number: Synpcc7942_0918)

GTGACTGGAACCGCCCTCGCGCAACCCCGCGCCATTACGCCCCACGAACAGCAGCTTTTGGCC
AAACTGAAAAGCTATCGCGATATCCAAAGCTTGTGCGAAATTTGGGGACGTGCTGCCAGTCAAT
TTGGATCGATGCCGGCTTTGGTTGCACCCCATGCCAAACCAGCGATCACCCCTCAGTTATCAAGA
ATTGGCGATTAGATCCAAGCGTTTGCAGCCGGACTGCTCGCGCTGGGAGTGCCTACCTCCAC
AGCCGATGACTTTCCGCCTCGCTTGGCGCAGTTTGC GGATAACAGCCCCCGCTGGTTGATTGCT
GACCAAGGCACGTTGCTGGCAGGGGCTGCCAATGCGGTGCGCGGCCCAAGCTGAAGTATCG
GAGCTGCTCTACGTCTTAGAGGACAGCGGTTGATCGGCTTGATTGTGGAAGACGCGGCGCTG
CTGAAGAACTACAGCCTGGTTTAGCGTCACTATCGCTGCAGTTTGTGATCGTGCTCAGCGATG
AAGTAGTCGAGATCGACAGCCTGCGCGTCTGGTTTAGTGACGTGCTGGAGATGGGGCGAT
CGCTGCCGGCACCGGAGCCAATTTTGCAGCTCGATCGCTTAGCCACTTTGATCTATACCTCGGG
CACCACAGGCCACCGAAGGGCGTGATGCTTTCTCACGGCAACCTGCTGCACCAAGTCACAAC
ATTAGGTGTGGTTGTGCAGCCGCAACCTGGCGACACCGTGCTGAGTATTTTGCCGACTTGCCAC
TCCTACGAGCGAGCTTGTGAATATTTCTGCTCTCCCAGGGCTGCACACAGGTCTACACGACGC
TGCGCAATGTCAAACAAGACATCCGGCAGTATCGGCCGAGTTCATGGTCAGTGTGCTGCGCCT
CTGGGAATCGATCTACGAGGGCGTG CAGAAGCAGTTTCGCGAGCAACCGGCGAAGAAACGTCG
CTTGATCGATACCTTCTTTGGCTTGTGAGTCAACGCTATGTTTTGGCACGGCGCCGCTGGCAAGGA
CTGGATTTGCTGGCACTGAACCAATCCCCAGCCCAGCGCCTCGCTGAGGGTGTCCGGATGTTG
GCGCTAGCACCGTTGCATAAGCTGGGCGATCGCCTCGTCTACGGCAAAGTACGAGAAGCCACG
GGTGGCCGAATTCGGCAGGTGATCAGTGGCGGTGGCTCACTGGCACTGCACCTCGATACCTTC
TTCGAAATTGTTGGTGTGATTTGCTGGTGGGTTATGGCTTGACAGAAACCTCACCAGTGCTGA
CGGGGCGACGGCCTTGGCACAACCTACGGGGTTCGGCCGGTCAGCCGATTCCAGGTACGGCGA
TTCGGATCGTCGATCCTGAAACGAAGGAAAACCGACCCAGTGGCGATCGCGGCTTGGTGCTGG
CGAAAGGGCCGCAAATCATGCAGGGCTACTTCAATAAACCCGAGGCGACCGCGAAAGCGATCG
ATGCCGAAGGTTGGTTTGTGACACCGGCGACTTAGGCTACATCGTCGGTGAAGGCAACTTGGTGCT
AACGGGGCGCGCTAAGGACACGATCGTGCTGACCAATGGCGAAAACATTGAACCCAGCCGAT
TGAAGATGCCTGCCTACGAAGTTCCTATATCAGCCAAATCATGTTGGTGGGACAAGACCGCAAG
AGTTTGGGGCGTTGATTGTGCCAATCAAGAGGCGATCGCACTCTGGGCCAGCGAACAGGGC
ATCAGCCAAACCGATCTGCAGGGAGTGGTACAGAAGCTGATTCGCGAGGAACTGAACCGCGAA
GTGCGCGATCGCCGGGCTACCGCATCGACGATCGCATTGGACCATTCCGCCTCATCGAAGAA

CCGTTTCAGCATGGAAAATGGCCAGCTAACCCAAACCCTGAAAATCCGTCGCAACGTTGTCGCGG
 AACACTACGCGGCTATGATCGACGGGATGTTTGAATCGGCGAGTTAA

Forward Primer	Pos	Len	Tm	Reverse Primer	Pos	Len	Tm	Amp	dG
5'-TGCTTTCTCACGGCA-3'	661	15	55.30	5'-TCGATCAAGCGACGT-3'	961	15	54.86	300	-2.43



Appendix 7

Preparation of agarose gel electrophoresis

10X TAE buffer (Tris-Acetate-EDTA)

Tris base	48.4	g
EDTA	3.72	g
Acetic acid	11.4	ml

Dissolve all compositions with distilled water to 1 liter. Dilute the solution to 1X with distilled water before use.

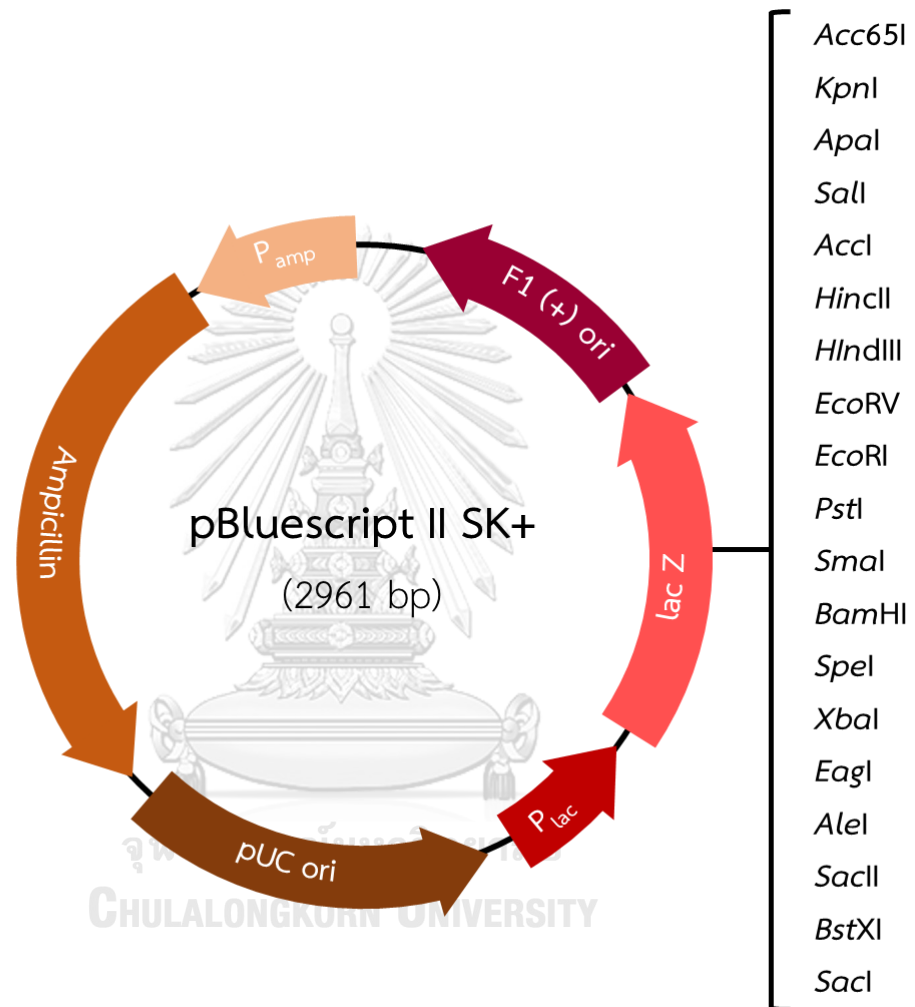
1.2% Agarose gel

Agarose powder	0.48	g
1X TAE buffer	40	ml

Dissolved the agarose powder by warming until it melts. Cool down the solution before adding SYBR® safe DNA gel stain for 4 µl and mix well.

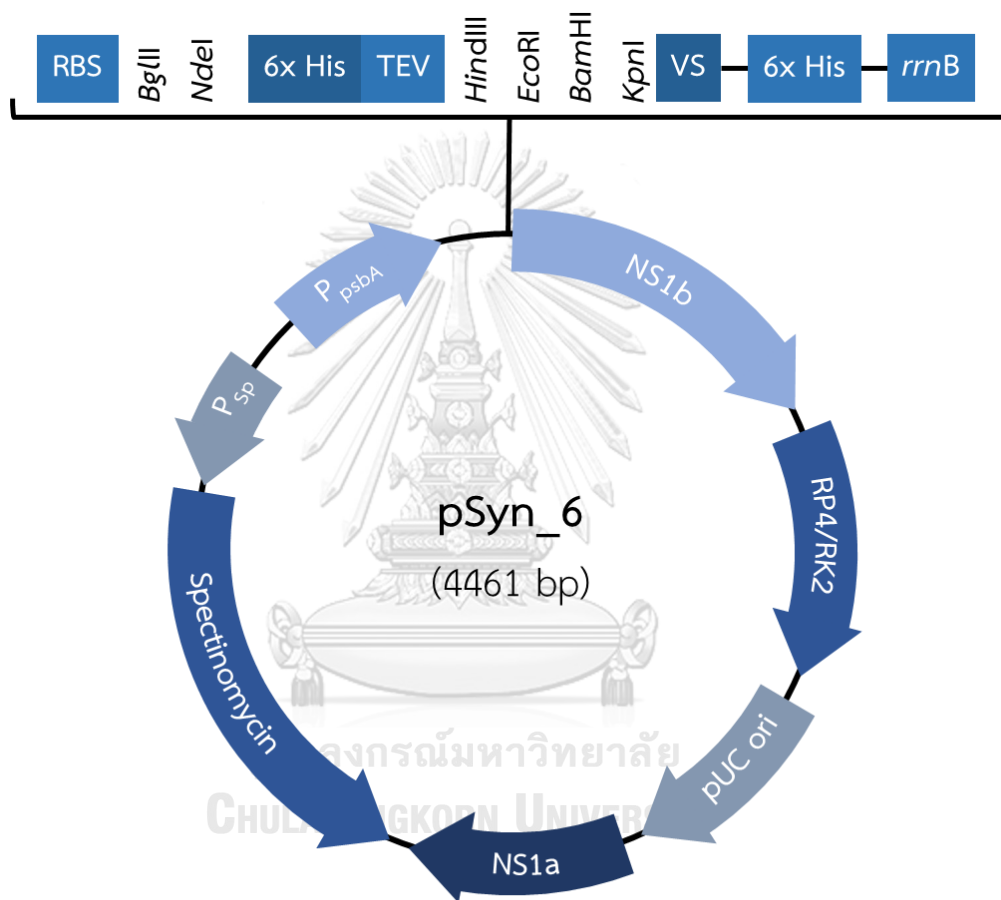
Appendix 8

pBluescript®II SK+ vector (Toyobo, Japan)



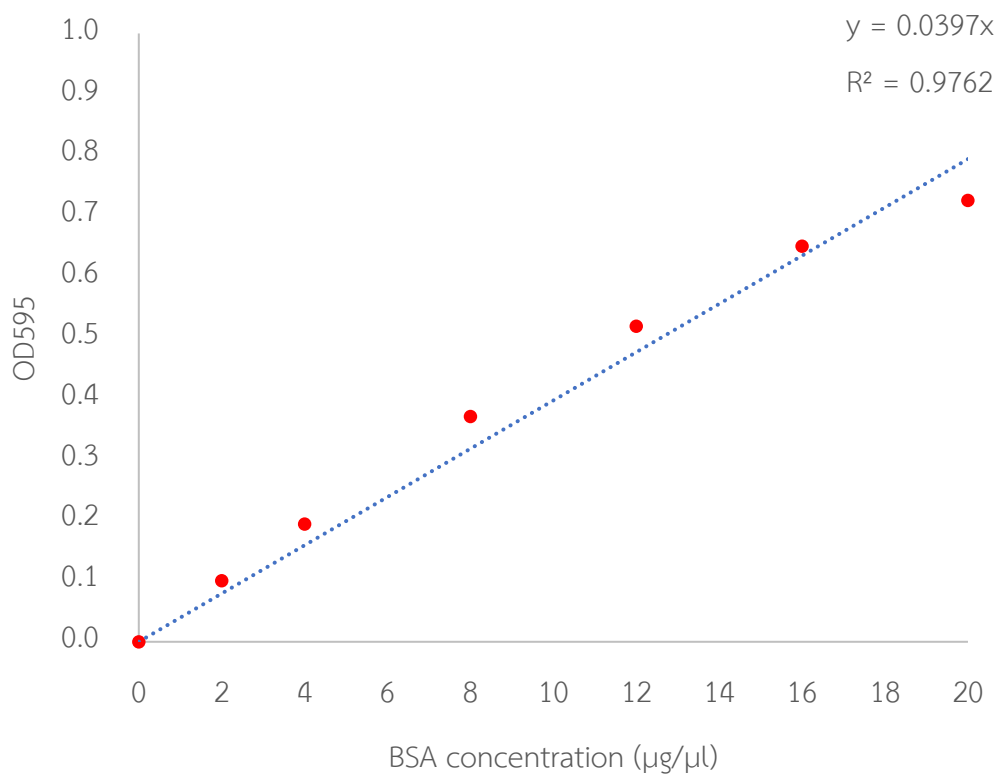
Appendix 9

pSyn_6 vector (Invitrogen, USA)



Appendix 10

Protein standard curve



Appendix 11

Preparation of polyacrylamide gel electrophoresis

1. Stock reagents

1.5 M Tris-Cl pH 8.8

Tris base	8.17	g
-----------	------	---

Dissolve the Tris base with 80 milliliters distilled water and adjust pH to 8.8 with HCl or NaOH then adjust the volume to 100 milliliters.

0.5 M Tris-Cl pH 6.8

Tris base	6.06	g
-----------	------	---

Dissolve the Tris base with 80 milliliters distilled water and adjust pH to 6.8 with HCl or NaOH then adjust the volume to 100 milliliters.

1 M Tris-Cl pH 6.8

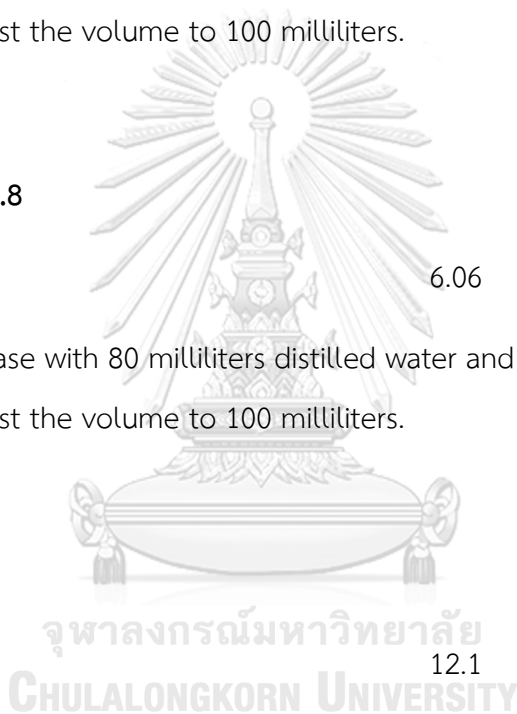
Tris base	12.1	g
-----------	------	---

Dissolve the Tris base with 80 milliliters distilled water and adjust pH to 6.8 with HCl or NaOH then adjust the volume to 100 milliliters.

10% SDS solution

Sodium lauryl sulfate	10	g
-----------------------	----	---

Adjust volume to 100 milliliters.



2. SDS-PAGE

10% separating gel (for 1 gel)

Distilled water	3.56	ml
1.5 M Tris-Cl pH 8.8	2.25	ml
10% SDS solution	90	μl
30% acrylamide/bis solution	3	ml
TEMED	7.5	μl
10% ammonium persulfate	75	μl

5% stacking gel (for 1 gel)

Distilled water	1.4	ml
0.5 M Tris-Cl pH 6.8	0.625	ml
10% SDS solution	25	μl
30% acrylamide/bis solution	0.415	ml
TEMED	2.5	μl
10% ammonium persulfate	25	μl

4x protein loading buffer

1 M Tris-Cl pH 6.8	0.6	ml
10% SDS solution	2.0	ml
1% bromophenol blue	1.0	ml

50% glycerol	5.0	ml
--------------	-----	----

Mix all the components and adjust volume to 10 milliliters with distilled water. Aliquot the solution to 1 milliliter in microcentrifuge tube. Before use, add 2-mercaptoethanol for 50 μ l and mix by vortex

10X running buffer

Tris base	30.3	g
Glycine	144	g
Sodium lauryl sulfate	10	g

Dissolve all compositions with distilled water to 1 liter. Dilute the solution to 1X with distilled water before use.

Coomassie brilliant blue staining solution

Coomassie brilliant blue G-250	1	g
50% methanol	500	ml
10% acetic acid	100	ml
Distilled water	400	ml

Destaining solution

Methanol	200	ml
Acetic acid	70	ml
Distilled water	730	ml

Appendix 12

Preparation of solutions for western blotting

1X PBS buffer (Phosphate buffer saline) pH 7.4

NaCl	8	g
KCl	0.2	g
Na ₂ HPO ₄	1.44	g
KH ₂ PO ₄	0.24	g

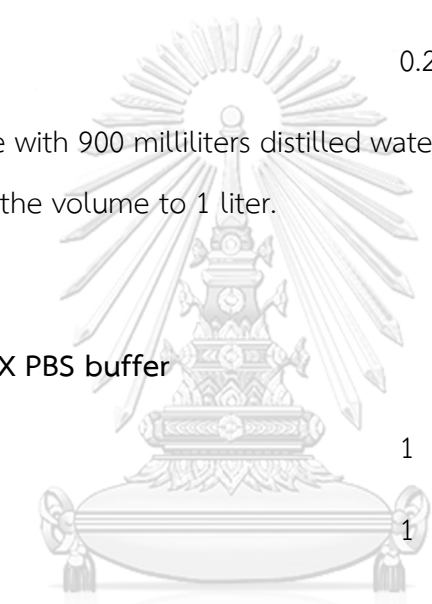
Dissolve the Tris base with 900 milliliters distilled water and adjust pH to 7.4 with HCl or NaOH then adjust the volume to 1 liter.

0.1% Tween 20 in 1X PBS buffer

Tween 20	1	ml
1X PBS buffer	1	l

Blocking solution

Skim milk powder	5	g
0.1% Tween 20 in 1X PBS buffer	100	ml



จุฬาลงกรณ์มหาวิทยาลัย

CHULALONGKORN UNIVERSITY

Western blotting buffer

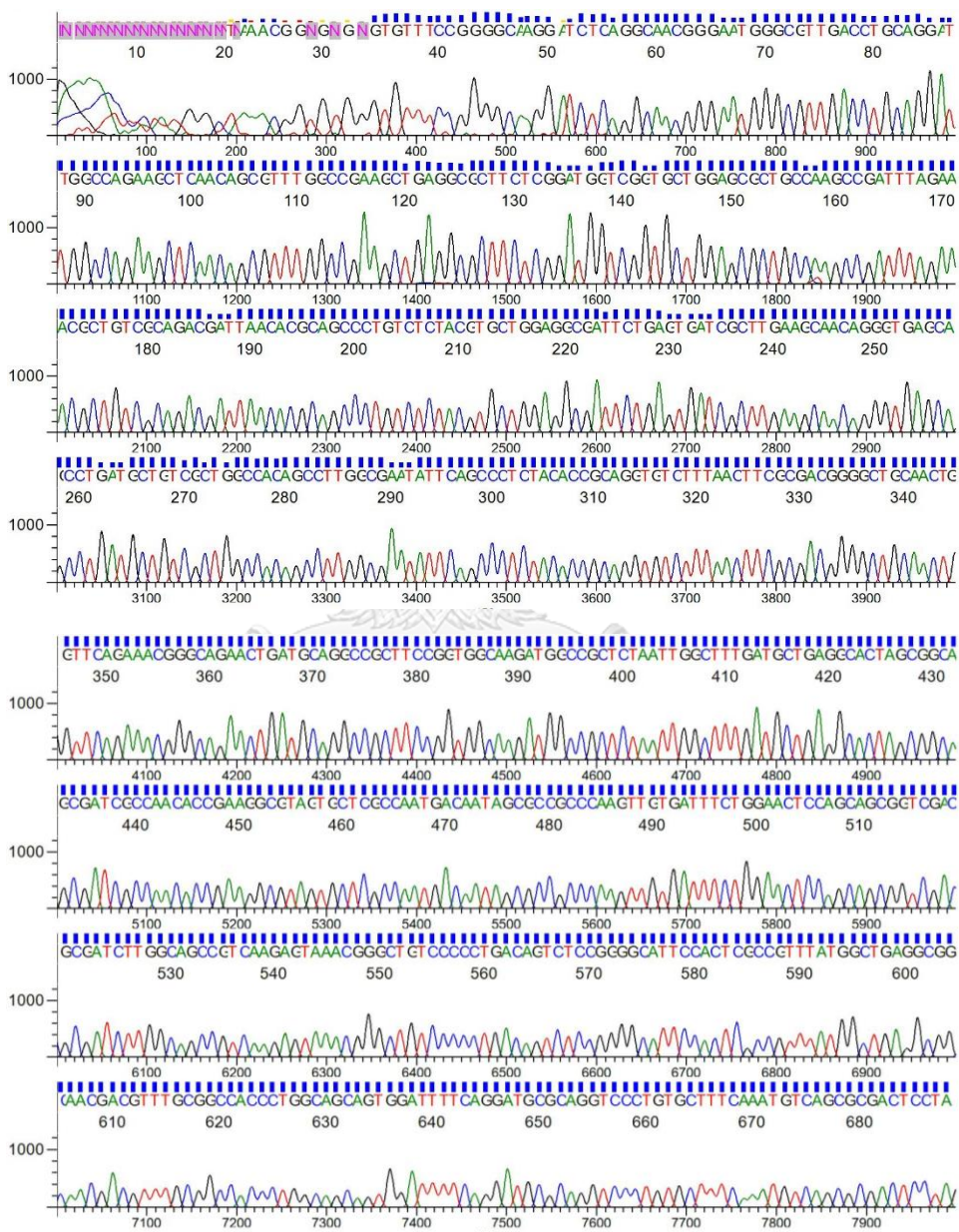
Tris base	3	g
Glycine	14.4	g
Methanol	200	ml
Distilled water	800	ml

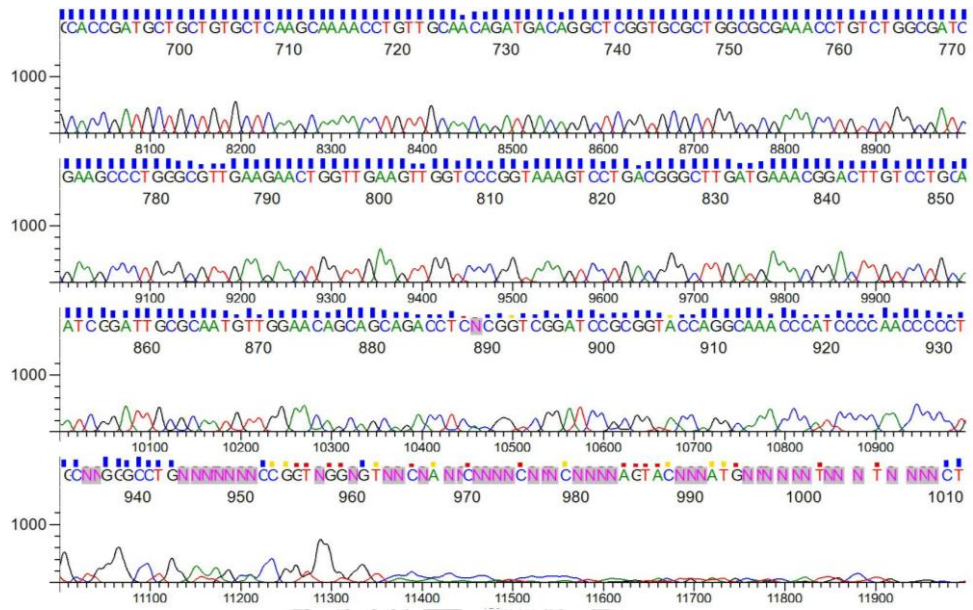


Appendix 13

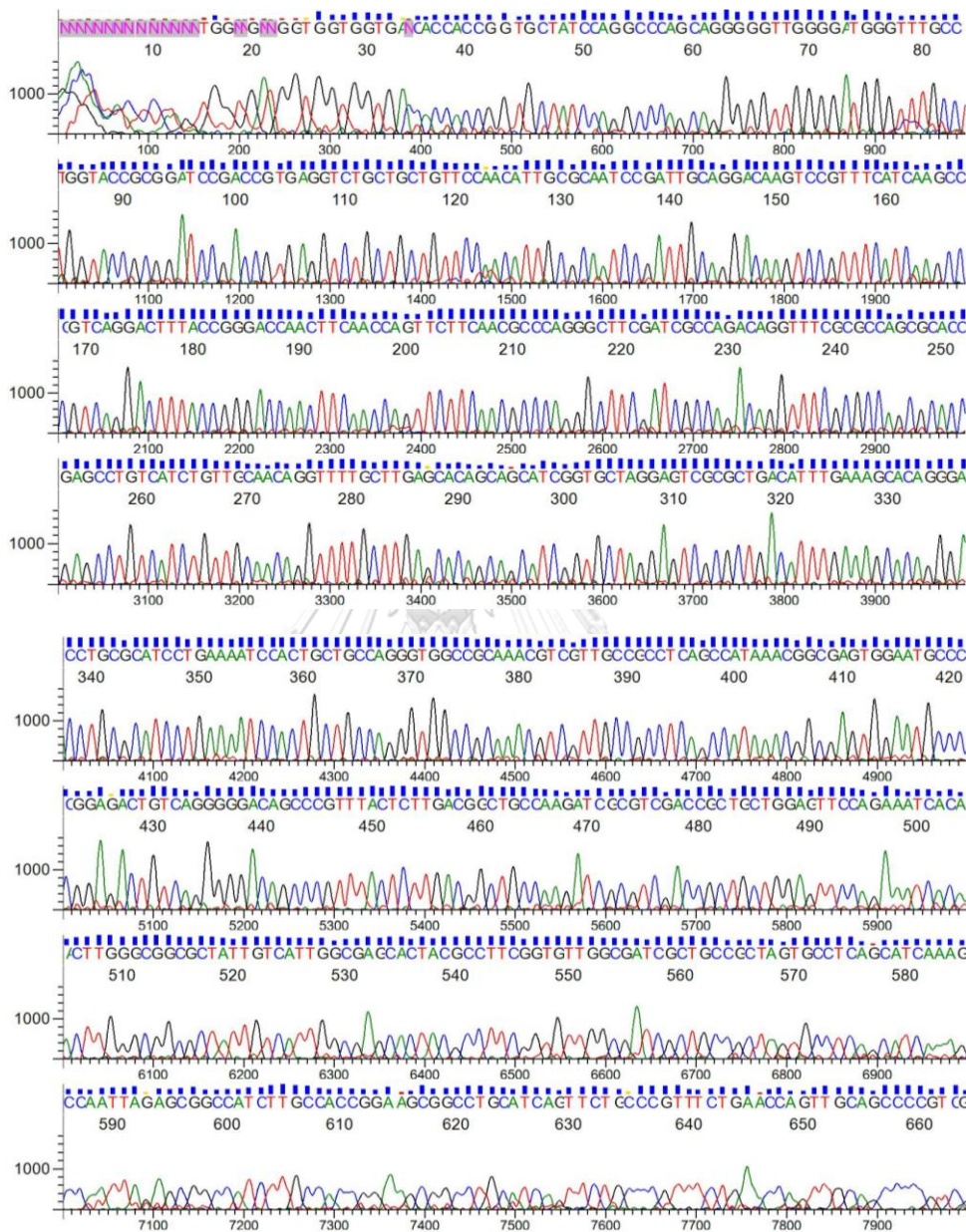
DNA sequencing of *ChMAT*/pBSK⁺II

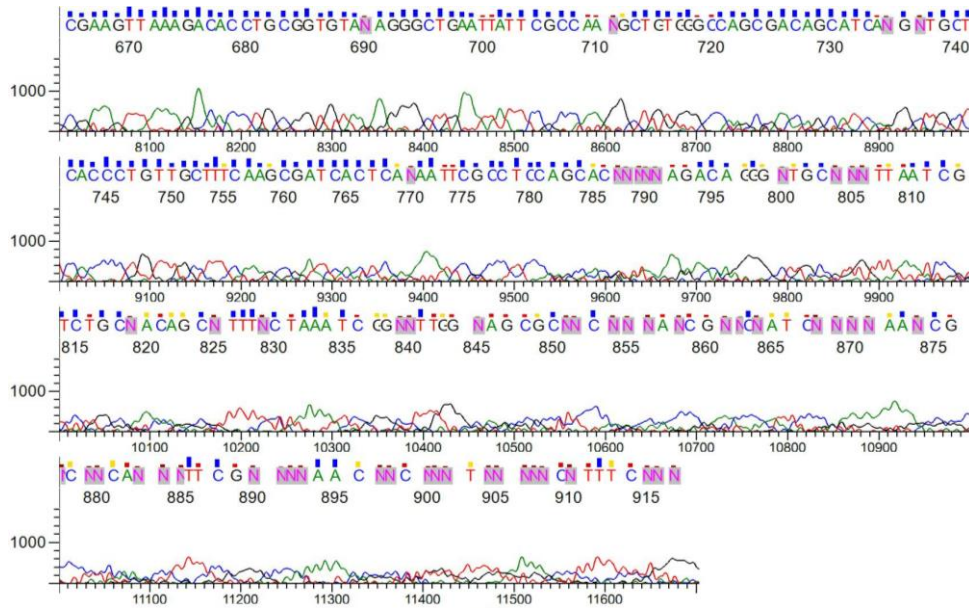
Appendix 14

DNA sequencing of *SynMAT/pSyn_6*1. *SynMAT/pSyn6_psbA*

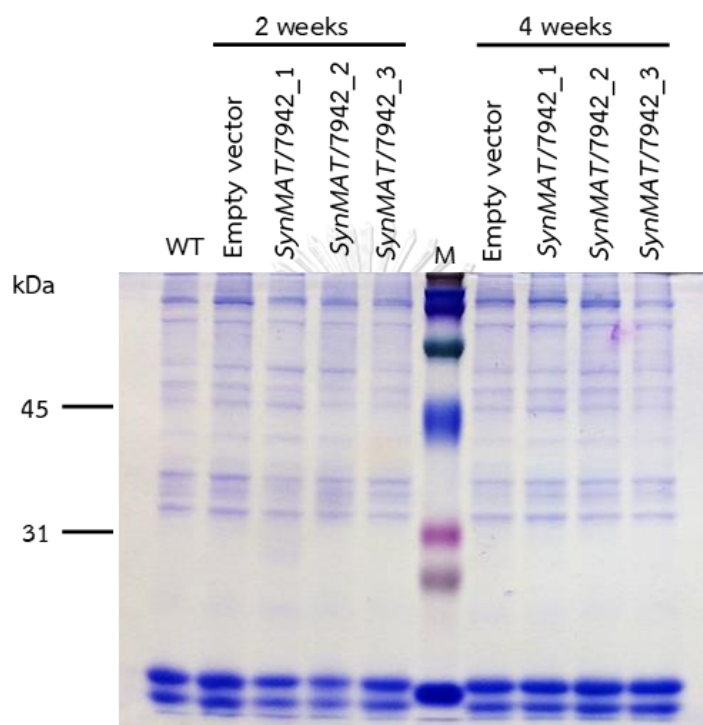


2. SynMAT/pSyn6_rrnB





Appendix 15

SDS-PAGE of *SynMAT/7942*

VITA

NAME	Thanapa Atikij
DATE OF BIRTH	11 June 1993
PLACE OF BIRTH	Bangkok, Thailand
INSTITUTIONS ATTENDED	Department of Microbiology, Faculty of Science, Chulalongkorn university
HOME ADDRESS	42 Soi Borommaratchachonnani 32 Borommaratchachonnani Road Taling Chan Bangkok 10170
AWARD RECEIVED	Best Poster Presentation Awards at TSB 2017 (Session: Bio- energy & Biomass)